공학박사학위논문

Superporous Patterning by Graphite Oxide Printing/ Reduction and its Application to Supercapacitors

그라파이트 옥사이드의 인쇄/ 환원에 의한

다공성 패터닝 및 수퍼 커패시터 응용

2014 년 8 월

서울대학교 융합과학기술대학원

나노 융합학과 나노융합전공

정 한 영

그라파이트 옥사이드의 인쇄/ 환원에 의한 다공성 패터닝 및 수퍼 커패시터 응용

Superporous Patterning by Graphite Oxide Printing/ Reduction and its Application to Supercapacitors

지도교수 이 정 훈

이 논문을 공학박사 학위논문으로 제출함

2014 년 8 월

서울대학교 융합과학기술대학원

나노융합전공

정 한 영

정한영의 박사학위논문을 인준함

2014 년 8 월

위 원 장	김 기 범	인
부 위 원 장	이 정 훈	인
위 원	조 경 재	인
위 원	김 종 휘	인
위 원	정 남 조	인

Abstract

Superporous Patterning by Graphite Oxide Printing/ Reduction and its Application to Supercapacitors

Hanyung Jung

Graduate school of Convergence Science and Technology

Nano Science and Technology

Seoul National University

Graphene is one of the most attractive materials because of many interesting properties such as two dimensional crystalline structure, high electrical and thermal conductivity, optical transparency, and large surface area. Due to benefits and exciting properties of fundamental importance, graphene is frequently used for a wide variety of devices that reveal its enormous potential.

Although graphene has many advantages mentioned above, it is still challenging technically and economically to mass produce and use high quality graphene. Therefore, many researchers produce graphene through the chemical exfoliation of graphite which is cost effective and convenient for applications. Graphite oxide (GO) is chemically exfoliated graphite which is hydrophilic and completely soluble in water unlike graphene. However, GO has electrical property substantially different from that of graphene, e.g., poor conductivity, due to attached functional

groups resulted from an oxidation process. The conductivity, and therefore the electrical property, of GO can be recovered through reduction processes, from which the product is commonly addressed as reduced graphite oxide (rGO).

Solution phase coating of GO has been followed by reduction process which produced useful devices such as sensors, electrical devices, and supercapacitors. Previous approaches for reduction process include laser scribing DVD writer and photo mask patterning methods. However, these patterning methods had limitations in producing GO and rGO patterns directly on a non-flat surface. Although thin film produced by such methods could be transferred to a curved surface, peeling off technique had limitations such as yield, complicated process, and adhesion to a textured surface. A commercial inkjet printer has been put into test in GO patterning, yet with limitations in repeated ejection to meet the total volume requirement and direct printing on an application surface. Direct patterning will enable more freedom in the choice of materials which include non-flat, textured, slanted and curved surfaces, leading a critical step to realize many modern applications, e.g., wearable and flexible devices.

Herein, we first show the use of a liquid dispenser to enable the direct printing of a GO solution into designed patterns on a slanted substrate. We discovered that there are key parameters to optimize the printing process such as choice of substrate and multiple dispensing. We also show that it is crucial to adjust and optimize the photo-thermal light energy for suitable GO reduction process. Owing to the hydrophilic property of the GO particles, GO could be completely dispersed in

deionized water and used as an “ink” with a liquid dispenser. The amount of GO droplet and printing method were essential to the production of GO patterns.

Substrate material was chosen based on the effective GO reduction and adhesion of rGO. Contact angle between substrate material and GO droplet should meet the condition for patterning GO via multiple dispensing printing method which increased pattern resolution. Among various electrical insulating materials, PET film substrate showed the best result in the GO flash reduction owing to its moderate surface contact angle of 80°~ 90° suitable for adhesion. We demonstrated the GO printing on not only a flat surface but also a slanted surface with satisfactory resolution and reduction characteristics.

There were variety of reduction methods that were available to produce rGO: a thermal reduction at high temperature, a chemical reduction using reducing agent like hydrazine, and a photo-thermal reduction. The photo-thermal reduction of xenon flash lamp was used to deliver photo-thermal light energy without destroying GO pattern structures. By taking advantage of the flash reduction method, printed GO was allowed to carry out the patterning of rGO. Our approach offered a simple, rapid and CMOS-compatible (Complementary metal–oxide–semiconductor) fabrication process to produce a conducting pattern which did not require high temperature and chemical treatment.

GO photo-thermal reduction was verified by Raman spectroscopy and XPS measurement. Sharpness of the D peak and G peak was increased and the remarkable increase of 2D peak was observed, indicating better graphitization

resulted from restoration of sp^2 hybridized C-C bonds. The increase of intensity of the D peak was commonly observed after photo-thermal reduction. This indicated the removal of the oxygen-containing functional groups in GO that induces defects on the hexagonal structure without repair process. The total amount of oxygen was detected by XPS measurements. C-O and C=O bonding in rGO were significantly decreased after photo-thermal reduction. The intensity of sp^2 carbon also increased two times. This also indicated that oxygen-containing functional groups in GO were comparably removed after the reduction process.

By exploiting the nature of GO and rGO, we fabricated supercapacitors through the direct printing of GO solution, followed by reduction treatment. The testing of a supercapacitor made with interdigitated electrodes showed competitive performance which indicated in key parameters such as energy and power densities of volume and mass by cyclic voltammetry and galvanostatic charging/discharging test. Various electrolytes were tested such as aqueous electrolyte, organic electrolytes with propylene carbonate solvent and acetonitrile solvent, and ionic liquid electrolytes. The best possible performance of energy densities were 1.06, 0.87, and 0.09 mWh/cm^3 and power densities were 0.63, 0.82, and 0.70 W/cm^3 in ionic, organic, and aqueous electrolytes, respectively.

The Ragone plot with volume density shows energy and power densities of aqueous, organic, and ionic electrolyte supercapacitor, The Ragone plot with mass density shows the same result performance of volume density. The energy density of a supercapacitor with organic and ionic electrolytes was as high as that of a commercial activated carbon supercapacitor without the use of current collector,

separator, and chemical binder. Additional folding test showed a supercapacitor was made to bend at different angles. It shows that the repeated operation performance was sustained in completely folded structure. A retention test was performed to check the stability of a supercapacitor, which has over 10,000 cycle stability

Keywords: Supercapacitor, Printing, Graphene, Graphene oxide, Graphite, Reduction

Student Number: 2009-31185

Contents

List of Figures

List of Tables

1 Introduction

1.1 Graphene

1.1.1 Carbon

Carbon word is from the Latin carbo, coal and charcoal in 1789 by Antonie L. de Lavoisier. Carbon is the chemical element of atomic number six and the 15th most abundant element in the crust of earth. It is tetravalent of having four electrons to form covalent chemical bonds.

Carbon has several allotropes of graphite, diamond, amorphous carbon, carbon nanotube (Figure 1) and graphene known as potential material of many application lately. All carbon allotropes have a different characteristic. For example, graphene has the highest thermal conductivities of all known materials while diamond has a low electrical conductivity.

The amorphous allotropes form is a non-crystalline and irregular state, which is basically graphite but not in a crystalline structure. In graphite, coal, soot and activated carbon are normally consisted of powder of the amorphous allotropes. In normal pressure, carbon exist as graphite in which each sheet is combined in a plane with loose van der Waals forces. This make graphite cleaving properties and low bulk electrical conductivity.

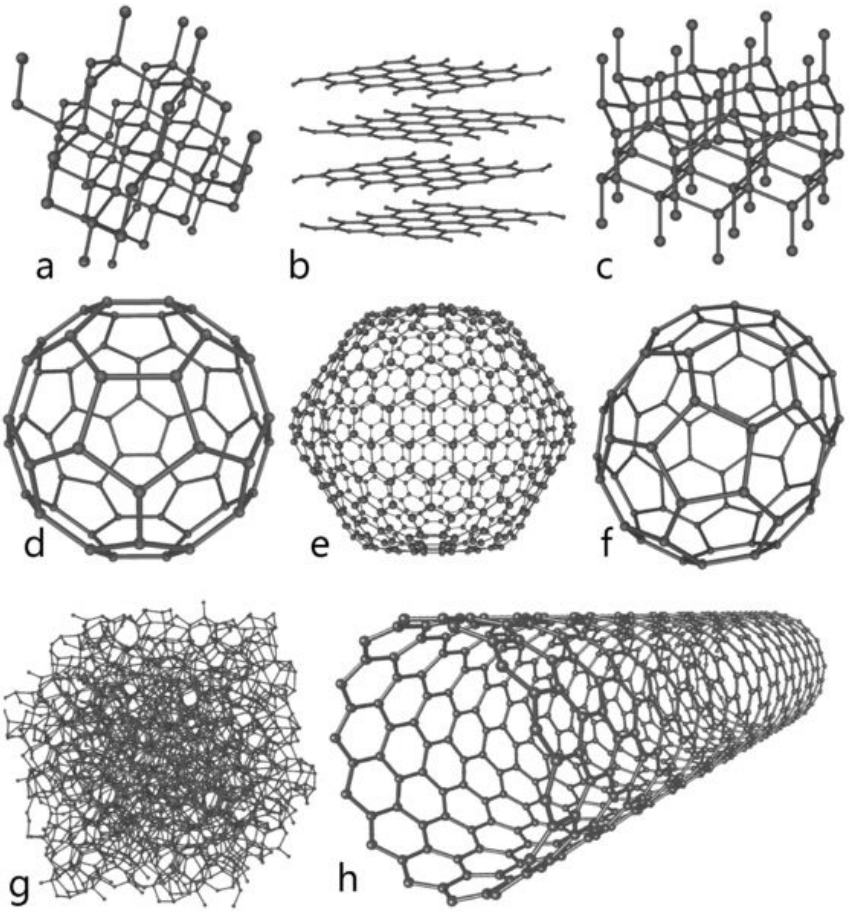

Figure 1. Some allotropes of carbon (a) diamond (b) graphite (c) lonsdaleite (d-f) Fullerenes (g) amorphous carbon (h) carbon nanotube [1]

1.1.2 Introduction of graphene

Graphene word was basically from a combination of graphite and suffix –ene by Hanna-Peter Boehm, who described single-layer carbon foil in 1962.[2] Andre Geim and Konstantin Novoselov at the University of Manchester won the Nobel prize in physics in 2010 "For groundbreaking experiments regarding the two-dimensional material graphene".[3]

Graphene has many interesting properties of massless Dirac electronic structure, anomalous quantum Hall effects, high mobility, and extraordinary high thermal conductivity.[4] Graphene is a one atom thin graphite layer, transparent sheet and two-dimensional layers of sp^2 bonded carbon with surface area 2700 m^2/g shown in Figure 2.[4-6] That is about 50 meter times 50 meter and three times bigger than the size of a standard basketball court. Graphene is the largest surface area materials per mass that human being found out so far. Graphene also shows current densities six orders of magnitude higher than that of copper.[7] Graphene has a good mechanical properties which is 100 times stronger than steel.[8]

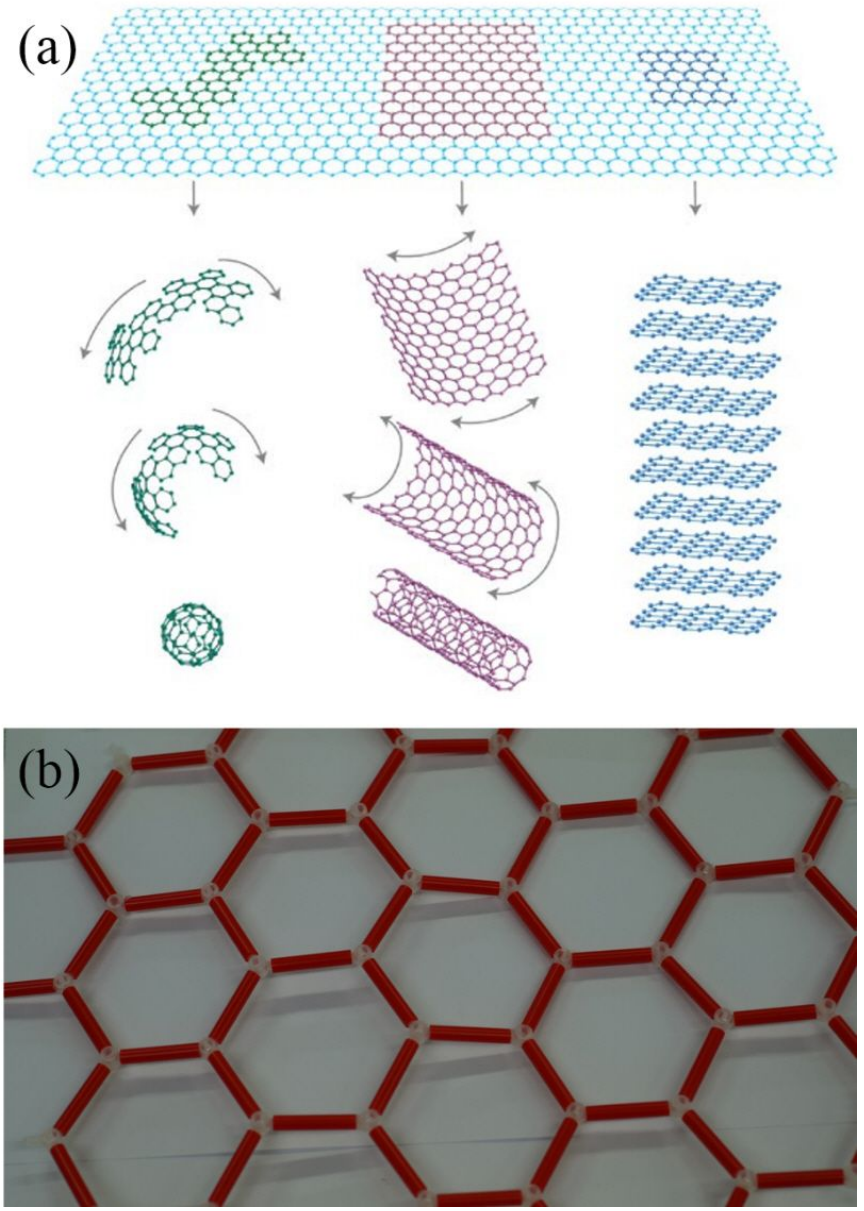

Figure 2. (a) Graphene as a 2D building material for fullerene, carbon nanotube, and bulk graphite [4] (b) Graphene structure

1.1.3 Application of graphene

Graphene has various potential application on chemical sensing, micro structuring, nano-electronics, hydrogen storage, corrosion-inhibiting coating, ultrasensitive photo detection, graphene transistor and membrane for gas separation (Figure 3).[9-18]

In bio-engineering field, it is already well known that carbon is compatible with cell, bacteria, and so on. Carbon nanotube which is well known allotrope of carbon had already many researches on DNA wrapping application. Graphene also has a bio application on label-free biosensor.[19]

Particularly, graphene has several advantages for energy production and storage applications because of a large surface per mass and volume, good mechanical properties of persistence and chemical stability. Graphene is already the key research topic such as lithium-ion batteries, a solar power, fuel cells, microbial bio-fuel cells and enzymatic bio-fuel cells.

Graphene is also accepted as a potential candidate for the electrodes in a supercapacitor because graphene-based materials have excellent electrical conductivity and extremely high specific surface area. To produce high quality graphene effectively, various kinds of processes and methods are tentatively employed in laboratories such as scotch tape method of mechanical graphite exfoliation, chemical vapor deposition growth of graphene, a thermal reduction or a photo-thermal reduction from graphene oxide, and other methods. In many kinds

of producing graphene methods among those, graphene obtained through a reduction process of graphite oxide (GO) is considered the most applicable.

An amount of energy stored in supercapacitor is very large compared to conventional capacitor because of the small charge separation in the order of nanometer brought by a separator. Most importantly, it is because of the enormous surface area per unit mass by using of porous material on the electrodes. This is the reason how graphene gains so much attention for active materials of supercapacitors and other high surface area applications.[20]

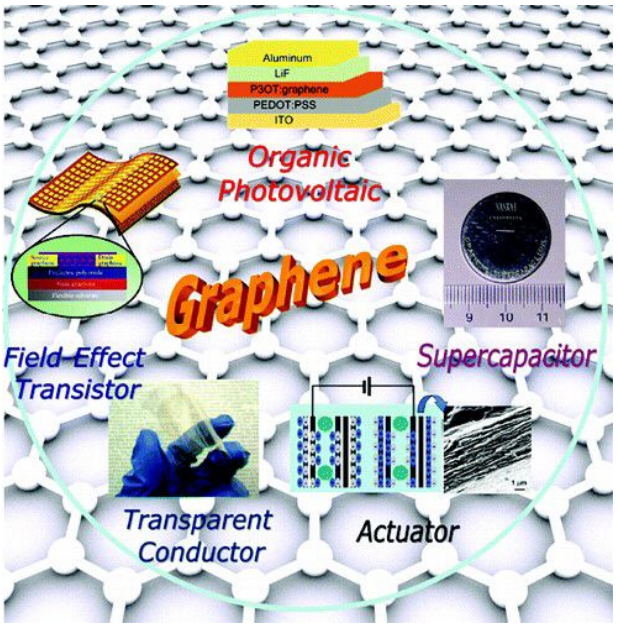

Figure 3. Emergent applications of graphene[21]

1.1.4 Introduction of graphite

Graphite is named by Abraham Gottlob Werner in 1789 from the Ancient Greek, normally used for writing pencils. Graphite is one of an allotrope of carbon which has an electrical conductor and the most stable form in standard conditions. There are principal types of natural graphite: crystalline flake graphite, amorphous graphite of fine particles, and lump graphite.

Graphite has a layered structure which is arranged in a honeycomb lattice with 0.142 nm and 0.335 nm plane distance.[22] The thermal properties of graphite is anisotropic which has a different properties in plane of sheet by structure direction because electrons travel very fast in carbon lattice plane and hard to pass through between the planes which makes low conductivity.

Graphite have been used in refractories, steel making, brake linings, lubricants, and so on. Especially, graphite has been widely used in writing pencils which is mixed with graphite and clay and still significant market for natural graphite. Natural and synthetic graphite are widely used at anode of lithium ion batteries in the last 30 years. Graphite fiber and carbon nanotubes are lately used in carbon fiber which is for reinforced plastics and heat resistant composites in many fields.

1.1.5 Comparison of graphene and graphite

Many graphene-based composite materials were produced for conducting electrode for energy storage devices such as supercapacitors and lithium ion batteries.[23-25] Among many kinds of modified graphene and graphite of carbon based materials, GO is the one of the best starting material for our process. In modern technology of graphene based, GO is only mass producible from inexpensive natural graphite.[26, 27]

Graphite is a stack of graphene reversely. Normally, graphite could be called in case of more than 10 layers of graphene. When graphite is oxidized or when graphite layer has oxygen functional groups instead of carbon bonding, graphite is changed into GO.[28, 29] One layer separated from GO is called as graphene oxide. When hydroxyl and oxygen (-OH, -O-, and -COOH) functionalities are removed from graphene oxide or GO, graphene oxide and graphite oxidized are called reduced graphene oxide or rGO.[30-35]

Graphene oxide can be reversibly reduced and oxidized by electricity.[36] Graphene oxide is hard to exist in normal condition and easily change into GO as iron get rusty, which is more stable state. Figure 4 shows a relationship between graphite, graphene, GO, graphene oxide, rGO, and reduced graphene oxide. For example, graphene could produce from graphite relatively easy method while it is hard to produce from rGO directly in modern technology.

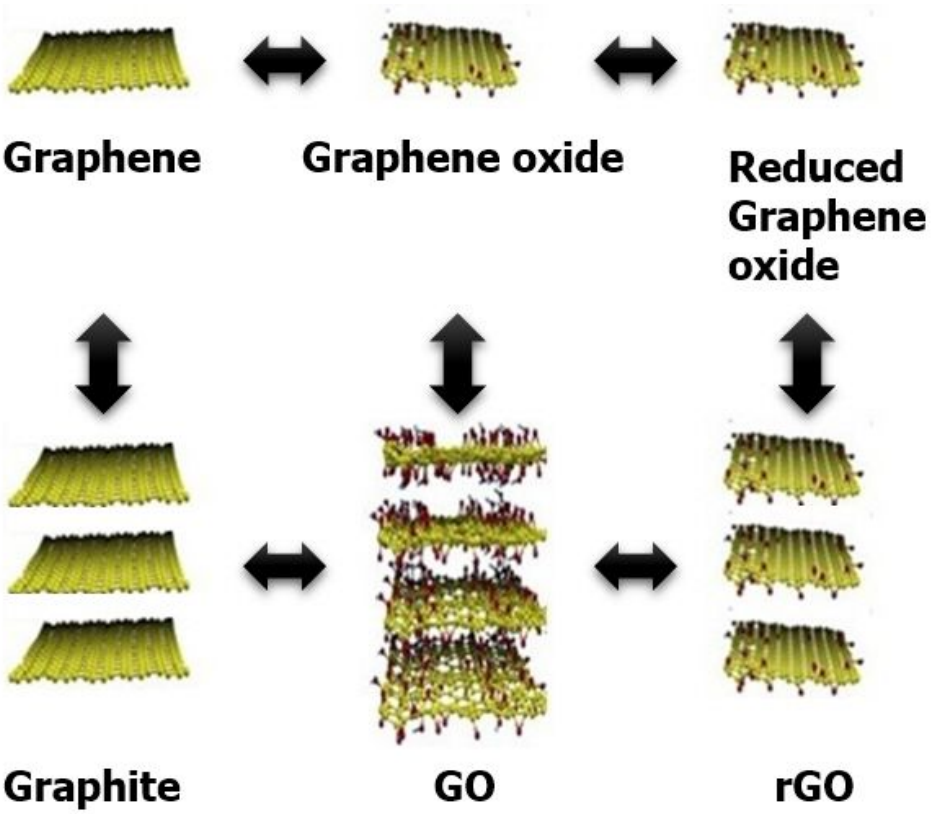

Figure 4. A schematic diagram of multiple graphene state

1.2 Graphite oxide (GO)

1.2.1 Introduction of graphite oxide (GO)

GO is also called graphitic oxide or graphitic acid because it is a mixture of carbon, oxygen, hydrogen and other components with various ratios and several kinds of bonding. Normally, GO is a form of graphite with oxidizers.

The structure of GO is determined by degree of oxidation and components ratio which proved by chemical analysis with Raman spectroscopy and X-ray photoelectron spectroscopy (XPS). While GO sustains the layer structure of graphite, the interlayer gap is 0.7 nm which is two times larger than that of graphite due to oxygen functional group. The edge of GO is combined with carboxyl and carbonyl group.[37]

Basically, GO is hydrophilic and hydrated to water with brown dark color and also easily incorporates other polar solvents. Conductivity of graphite is between 1 and 5 $\times 10^{-3}$ S/cm at a bias voltage of 10 V while it is insulator without biasing.[38]

GO and graphene oxide is partially reduced by treating with hydrazine hydrate, exposing to hydrogen plasma, exposing to light energy and so on. The versatile method of reduction of GO is a possible way to large scale production of graphene in practical industry.

1.2.2 Needs and reduction methods of graphite oxide (GO)

Graphene was produced via micro-mechanical exfoliation of highly ordered pyrolytic graphite, epitaxial growth, chemical vapor deposition with a relatively perfect structure and excellent properties.[39] Although a GO reduction method could not guarantee a quality of graphene, a GO reduction was wildly used in recent days due to straightforward manipulation.

A reduction of GO was needed to mass produce graphene-based materials. Graphene is still expensive to mass produce directly aimed at commercial manufacture. Reduced one from GO had a similar characteristic of graphene through a cost effective method with a high yield while rGO lost transparency and high conductivity of graphene.

One more merit of a GO reduction was a change of hydrophilic to hydrophobic characteristic when GO was changed to rGO. Therefore, GO was completely soluble in deionized water and could be used as an “ink” of a liquid dispenser in a solution injection without blocking or clogging nozzle of a liquid dispenser. After reduction, rGO was changed into patterned conducting material.

1.2.3 Photo-thermal reduction

Several reduction methods are technically feasible to produce rGO, such as a conventional thermal reduction at high temperature,[40] a chemical reduction using a reducing agent like hydrazine,[41] electrical reduction through electrophoretic deposition,[42] flame-induced reduction of a lighter and a microwave oven.[43, 44]

Among those mentioned reduction methods, we focused on a photo-thermal reduction method due to straightforward, environment-friendly, short time process and cost-effectiveness. A photo-thermal reduction could use various and strong light sources such as UV light, excimer laser, and camera flash. Xenon flash, which is an easily accessible camera add-on than can be used to deliver a photo-thermal effect for an in-depth reduction process that happened in a very short time (Figure 5). Being able to trigger deoxygenating reaction of GO by local heating, a photo-thermal reduction was desirable when a heating of a whole substrate, e.g., thin plastic film, needed to be avoided. Furthermore, optical reduction methods such as exposure to camera xenon flash, UV light, excimer laser and laser light source in a commercial DVD writer was a fast and clean process to produce rGO.[10, 45-47]. A reduction of GO was produced by pico-second pulsed laser irradiation.[48] The reduction process induced by optical energy was efficient from an aspect of processing time as energy transfers to GO instantaneously.

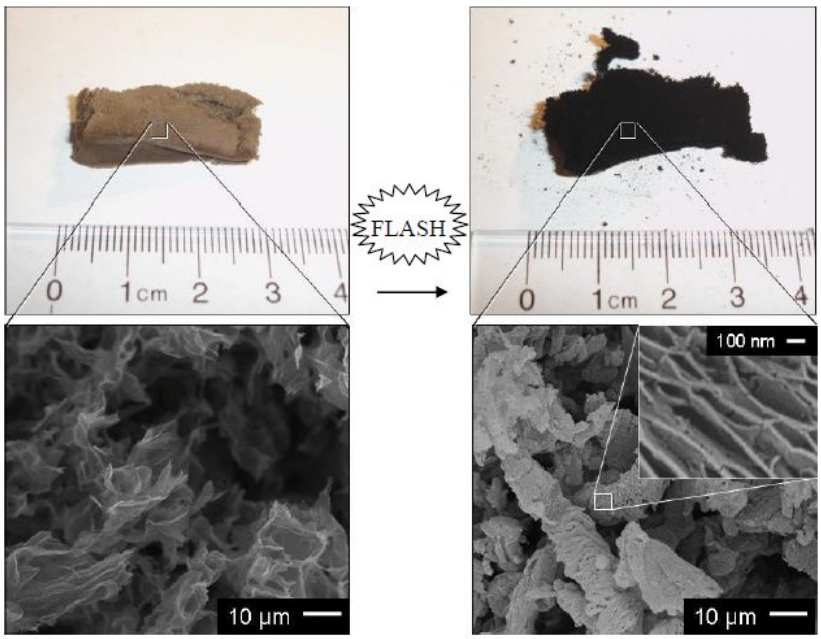

Figure 5. Before and after flash reduction[49]

1.2.4 Preparation of graphite oxide (GO)

A GO solution was synthesized by modified Hummers method.[50, 51] In our experiment, starting material was graphite power (4science, Korea). 1 mg graphite power was solved in 20 mL mixture of H_2SO_4: HNO_3 3.3 g potassium permanganate was added with checking temperature. A graphite solution was sonicated in an ultrasonic bath for 24 hours. The solution was passed through a 0.22 μm Teflon membrane in vacuum filtration shown in Figure 6. After 10 hours filtration, filted GO was stacked on the membrane. The membrane was rinsed copious amounts of deionized water to reach a neutral an aqueous solution which was continuously measured via pH meter, 7 pH. After a neutralized solution fully dried up, GO was obtained in a solid state. When GO was diluted in deionized water, a GO solution was adjusted to 5 g/L concentration.

A prepared GO solution was tested via Raman spectroscopy measurement. After reduced GO, Raman spectroscopy graph of GO showed the same result as other papers showed and mentioned in chapter 2. The GO solution was printed and reduced to rGO which comprised of reduced graphite and rGO. High surface area of rGO was one of the best candidates for good electrode materials of supercapacitors.

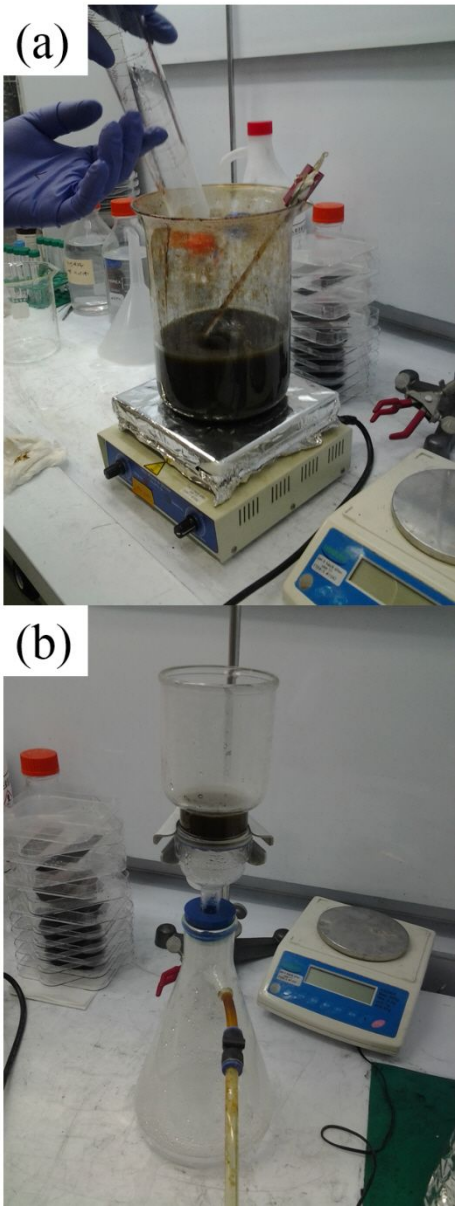

Figure 6. (a) Potassium permanganate was added (b) vacuum filtration with Teflon membrane

1.3 Supercapacitors

1.3.1 Introduction of supercapacitors

Supercapacitors are no longer uncommon these days as it has been receiving massive attention for its power density, thermal operating temperature, weight, and life cycle.[52] Performance of supercapacitors are mainly determined by active material of electrodes. Electrodes lying inside supercapacitor are undoubtedly the ultimate core element that directly influences and decides the performance of the device.

Graphene is widely accepted as a potential candidate for electrodes in a supercapacitor owing to excellent electrical conductivity and extremely high specific surface area.[53, 54] In an attempt of producing high quality graphene effectively, various sorts of a process and a method were employed in laboratories as well as industries. Among those, graphene obtained through a reduction process of GO was deemed the most applicable practically.

There were several reduction methods which were technically available at the moment to produce rGO, such as a conventional thermal reduction at high temperature, a chemical reduction using a reducing agent like hydrazine, and a photo-thermal reduction.[49, 55-58]

Photo-thermal reduction methods such as sunlight and UV light exposure as well as an excimer laser, microwave radiation were preferable approaches as they could be performed under a mild environment.[44, 59, 60] Furthermore, GO was reported

that it could be photo-thermally reduced under the exposure to a xenon flash lamp, which was a tube filled with xenon gas and widely used in a commercial camera. Being able to trigger deoxygenating reaction of GO by photo-thermal heating, a flash reduction method was mostly desirable as it was a chemical-free process and no high energy was required as in traditional thermal treatment.

By taking advantages of these reduction methods, GO was allowable to design and perform a patterning of rGO. A state-of-the-art patterning via an inkjet printing of GO offered a straightforward and fast way to produce a supercapacitor. The direct patterning became convenient as it was capable of making an efficient current collector free structure of electrodes in a supercapacitor. Meanwhile, a conventional supercapacitor had a current collector, separator, and binder in Figure 7.

In general, a supercapacitor has two configurations of sandwich and interdigitated type shown in Figure 8. Sandwich type supercapacitors are a symmetric structure which is sandwiched by two electrodes. Sandwich type supercapacitors were stable and used for the most of a commercial supercapacitor because active materials were concretely divided by a separator. Safety was proofed by electrolytic capacitor commonly used sandwich type. On the other hand, interdigitated type supercapacitors have both the electrodes on the same surface, with fingers of both electrodes arrayed next to each other.[61] Sandwich type supercapacitors have current collector, active material, electrolyte and a separator.

Meanwhile, interdigitated type supercapacitors did not need a separator to prevent both electrodes from coming into contact. Therefore, resistance due to a separator of

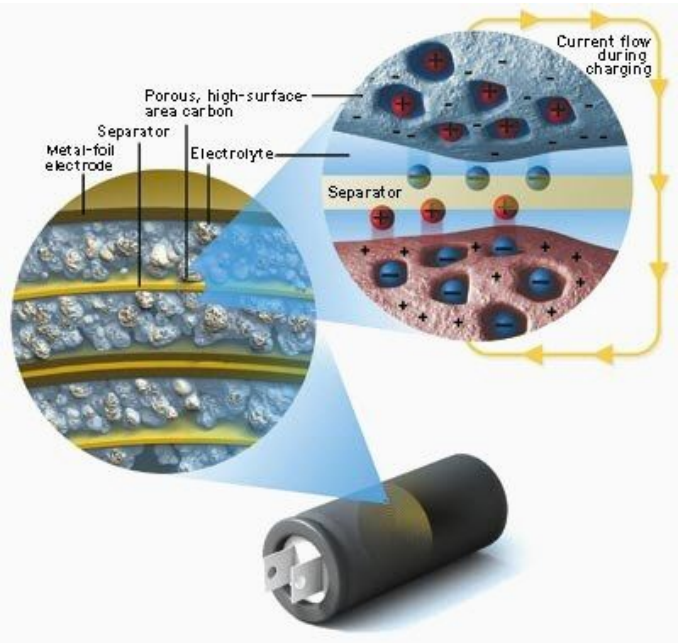

Figure 7. Structure of supercapacitor [62]

membrane can be avoided because the ions can migrate faster, resulting in high power density performance.

In two type of supercapacitors, we preferred interdigitated type supercapacitors because they were highly compatible with those on-chip circuitries. So, they became very convenient to be adopted in small smart devices. However, to produce a conventional interdigitated pattern, a photo-mask or clean room fabrication techniques were usually inevitable.[63-65]

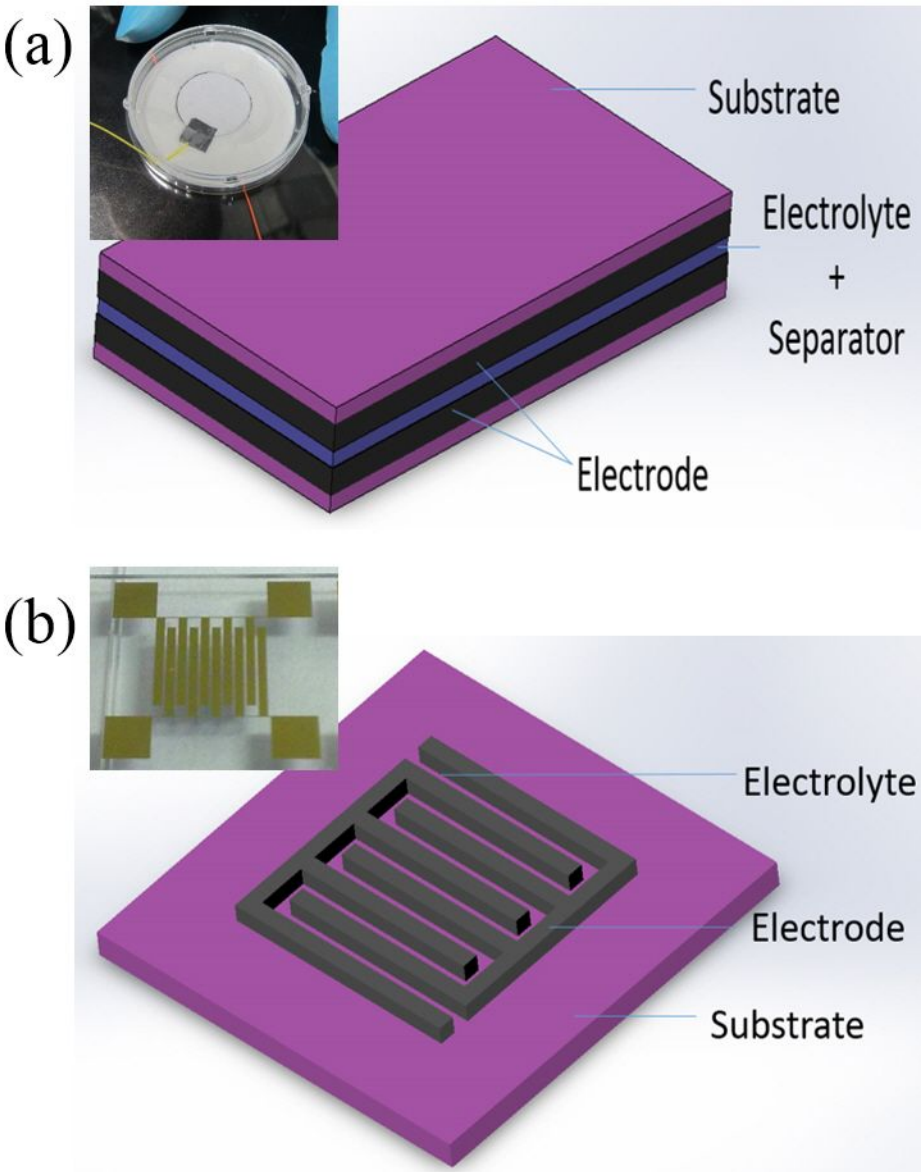

Figure 8. (a) A sandwich type supercapacitor (b) An interdigitated type supercapacitor

1.3.2 Commercial supercapacitors

A supercapacitor is also called EDLC (Electrical Double Layer Capacitor) which means ions are held between double layers using electric field. A distance of the static separation of charge is a few angstroms (0.3~ 0.8 nm).[66] A supercapacitor has double layers without a conventional solid dielectric.

A supercapacitor can be used with a combination of lithium-ion battery which can compensate for lack of energy density and power density each other. A lithium-ion battery and a fuel cell have high energy density while power density is low for fast charging-discharging. In between conventional capacitors and rechargeable batteries, supercapacitors could bridge the performance of energy and power density.

Supercapacitor normally has high specific capacitance, long life cycle, and fast charging-discharging rate. Using these characteristic, supercapacitor was specialized in low supply current device during long times for memory backup in PC, power electronics that require very short, high current and recovery of braking energy for vehicles or elevators.

There are many kind of commercial supercapacitors which used activated carbon as active materials shown in Figure 9. Commercial supercapacitors are being produced 1F, 10 F, 350 F, 500 F, 1000 F, and so on from APowerCap, BestCap, BoostCap and more than 20 companies. Capacitance of supercapacitor is 1000 times bigger than that of conventional capacitors. In high power electricity,

hundred and thousand farad supercapacitor has already replaced rechargeable battery.

Figure 9. (a) A commercial supercapacitor of 1 F and 350 F (b) A dissembled supercapacitor with activated carbon and separator

1.3.3 Supercapacitors vs lithium-ion batteries

Lithium-ion batteries are the most commonly used electrical energy storage device, which converts chemical energy to electrical energy and reverse is also possible for charging. Lithium-ion batteries are powered by redox reactions which simultaneously take place at cathode and anode electrodes. In contrast, charges are physically stored in a supercapacitor, without chemical reactions or phase changes involved, which makes a process very quick and highly reversible. Charging and discharging process can be repeated over and over again, more than 10 thousands of cycles before significant drop of performance is observed in Table 1.

A supercapacitor did not need additional management electric circuit while a lithium-ion battery needs a control circuit to protect over-charging or an explosion for over current. Meanwhile, a supercapacitor without any control circuit could be used safely. But a supercapacitor have to waste of remained energy in a certain level below voltage such as under one voltage. A supercapacitor also need control circuit to use energy below threshold voltage.

A lithium-ion battery showed slow a performance decrease in voltage with a flat discharge curve. When a lithium-ion battery dissipated energy, battery could deliver over 95% of its reserved energy. On the other hand, a supercapacitor showed linear charging and discharging characteristic in voltage. Therefore, a combination using of a supercapacitor and a lithium-ion battery needed a DC-to-DC converter circuit and a working voltage adjuster for better energy efficiency.

A commercial supercapacitor normally has 2.5 ~ 2.7 Voltage because organic electrolyte determines working voltage. Although 2.8 V or higher voltage could be used, they could decrease life cycles of a supercapacitor because a supercapacitor could occur electrolysis between electrodes and electrolyte.

Several supercapacitors were connected in series to supply higher voltage than 2.7 voltage. In this case, total capacitance was decreased by serial connection. However, voltage balancing was needed to protect over voltage from more than three supercapacitors serial connection.[67]

Table 1. Comparison between batteries and supercapacitor

Property	Batteries	Supercapacitor
Charge/discharge time	1 ~ 10 hrs	Seconds ~ Minutes
Operating temperature	-20 ~ 65 °C	-40 ~ 85 °C
Life cycles	1500 cycles	10,000 ++ cycles
Energy density	8 ~ 600 Wh/kg	1 ~ 5 Wh/kg
Power density	0.4 kW/kg	100 kW/kg
Cell voltage	3.6 ~ 3.7 V	2.3 ~ 2.7 V
Cost per Wh	$ 0.5 (Large system)	$ 20 (typical)

1.3.4 Micro device and micro sensor

A micro device such as Bluetooth® system operated in the range of 2400–2483.5 MHz. It needed standby energy to wake up the system and working energy which needed high power to generate all component. When a micro device, e.g., a Bluetooth module in sleep-mode, was a standby condition, a battery could supply low power to a device. But when a device was working, e.g., a Bluetooth module in work, a supercapacitor should supply big energy to a device rapidly.

When a system needed high energy like a vehicle to move, a supercapacitor should connect in series and parallel to increase working voltage and energy. However, when a supercapacitor connected in series, it diminished life cycles and needed a voltage adjuster. Therefore, it is the best condition that a micro device and a micro sensor were in small energy range covered by one cell of supercapacitor.

In medical diagnosis, a micro sensor system already used. Figure 10 shows graphene-based wireless bacteria detection on tooth enamel. In case of an implanted tooth, an energy storage system could be installed inside of a tooth for a short term and a long term medical health check. A capsule endoscopy was used to record images of digestive organ. After grabbing an image they target, a capsule endoscopy system could send data to a server and terminate energy of a system.

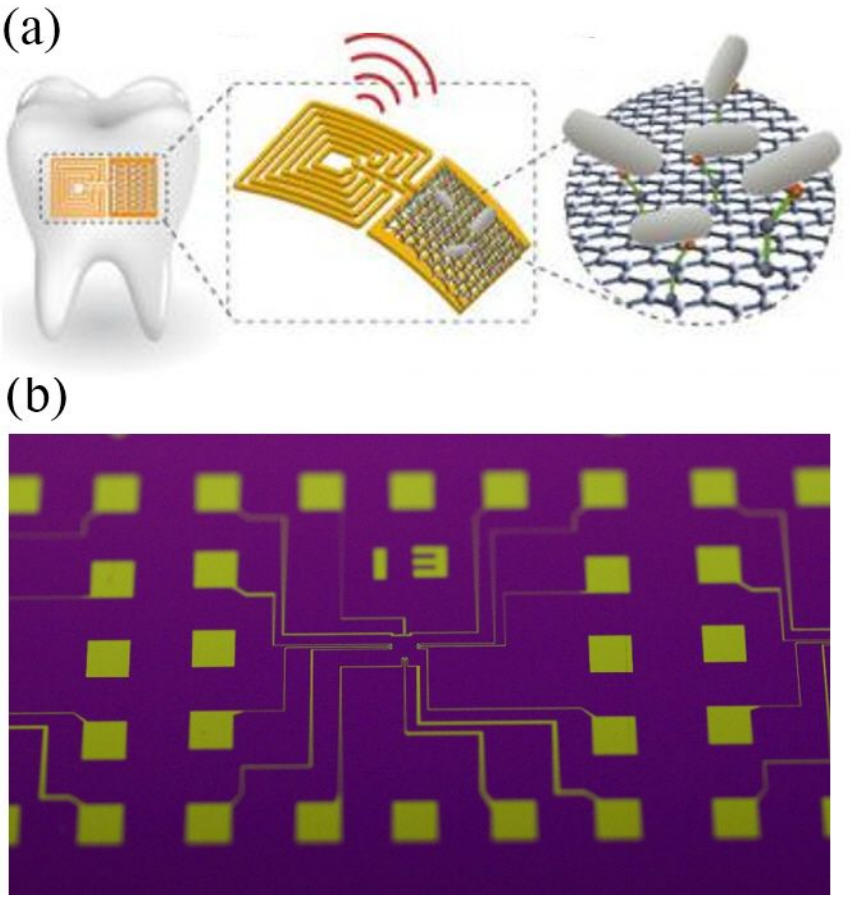

Figure 10. (a) A micro device with graphene-based wireless bacteria detection on a tooth enamel [68] (b) A micro FET sensor

1.4 Motivation and objective of study

1.4.1 Research goals

Graphene is a fascinating material which has a specific surface area and high electrical conductivity. It has a potential applications on sensing, structuring, nano-electronics, hydrogen storage, coating, photo detection, graphene transistor, and membrane. On the other hands, graphene has an inefficient problem in mass production because it still needs complex process with high cost.

In carbon based materials, carbon nanotube is hydrophilic and soluble in water. GO is also hydrophilic and completely soluble in water and rGO is conducting material and similar properties of graphene with economical mass production. Using characteristic of GO and rGO, we produced directing printing of supercapacitors with various condition in terms of contact angles and printing method and reduced via adjusted photo-thermal light energy. Patterned rGO produced supercapacitor with liquid electrolytes.

Supercapacitors with rGO are receiving strong attention and one of potential energy storage device for complementary to rechargeable battery. Current microelectronic device and sensor need high power energy storages for short sensing and scanning just as the same characteristic of supercapacitor.

1.4.2 Approach to achieve the goals

Nowadays, more and more electronics has been miniaturized when many smart equipment were invented shown in Figure 11. Many kinds of communications and sensing systems became so small that large and bulky energy storage devices altered a burden to the systems themselves. Accordingly, there has been growing interesting in small energy storage devices for generating systems.

Particularly, Samsung company unveiled galaxy S5 smartphone and new wearable gear device looked like conventional wristwatch several months ago. A gear device showed many functionality of camera, incoming call, emails, message and much more. A device still needed a high energy battery to communicate with a smartphone and to work properly, which meant more energy was recommended.

A micro device was our motivation to explore energy storage devices that were compatible and readily adopted through such small systems. Especially, in a mine detector system, devices were disposed after a micro detector was spread around high risk area for mine detection. A separately dispersed device just needed low energy enough to scan atmosphere and sent data to main server. In this micro sensor device, a micro-sized supercapacitor could be optimized at low energy but high power system also need to finish their mission of sending a gathered information.

Consequently, rGO of graphene based was produced in printed supercapacitors. It could be used an independent energy source and hybrid of conventional batteries for small portable devices.

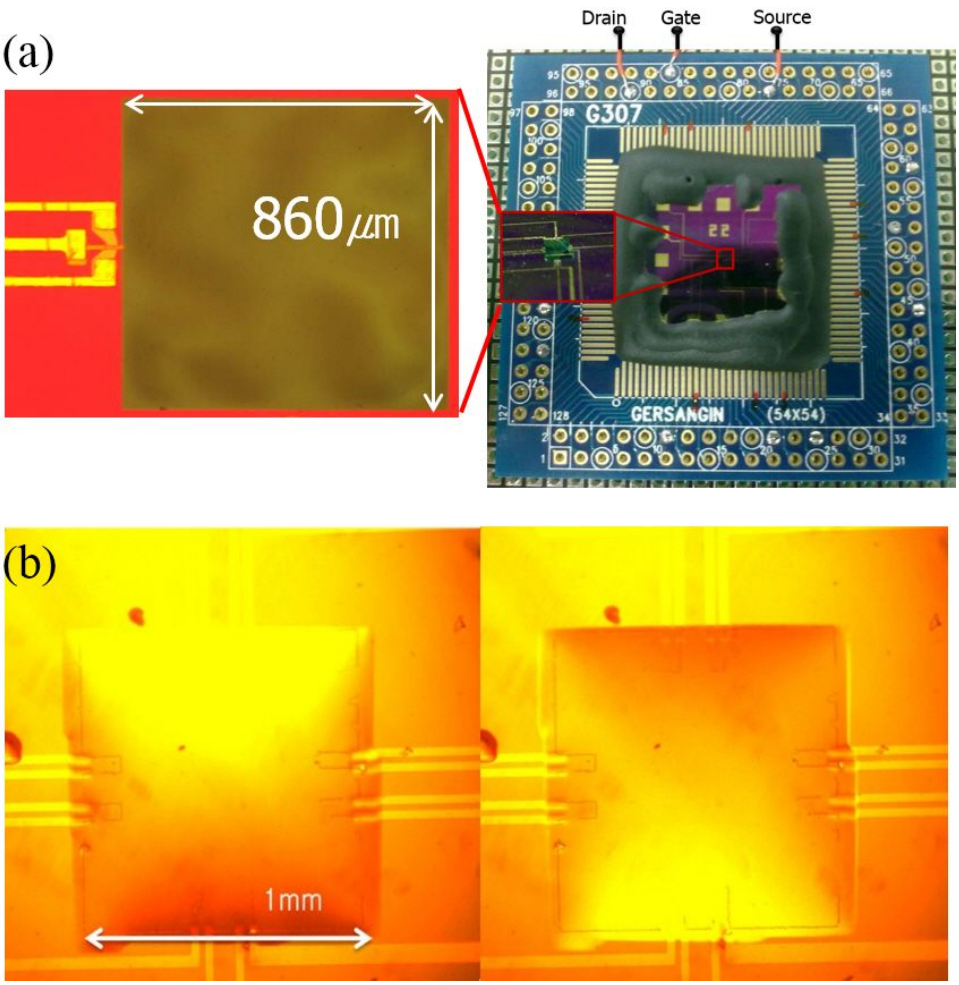

Figure 11. (a) Micro sensor for low pressure (b) micro membrane sensor [69]

1.5 Bibliography

[1]. *Allotropes of carbon*. Available from: http://en.wikipedia.org/wiki/Carbon.

[2]. Boehm, H.P., R. Setton, and E. Stumpp, "NOMENCLATURE AND TERMINOLOGY OF GRAPHITE-INTERCALATION COMPOUNDS (IUPAC RECOMMENDATIONS 1994)" *Pure and Applied Chemistry*, Vol. 66, No. 9, pp. 1893-1901, 1994.

[3]. *The offical web site of the Novel prize*. Available from: http://www.nobelprize.org/nobel_prizes/physics/laureates/2010/.

[4]. GEIM, A.K. and K.S. NOVOSELOV, "The rise of graphene" *Nature materials*, Vol. 6, No., pp. 183-191, 2007.

[5]. Butler, S.Z., S.M. Hollen, L.Y. Cao, Y. Cui, et al., "Progress, Challenges, and Opportunities in Two-Dimensional Materials Beyond Graphene" *Acs Nano*, Vol. 7, No. 4, pp. 2898-2926, 2013.

[6]. Stankovich, S., D.A. Dikin, G.H.B. Dommett, K.M. Kohlhaas, et al., "Graphene-based composite materials" *Nature*, Vol. 442, No. 7100, pp. 282-286, 2006.

[7]. Geim, A.K., "Graphene: Status and Prospects" *Science*, Vol. 324, No. 5934, pp. 1530-1534, 2009.

[8]. Andronico, M. and L.S. Writer. *5 Ways Graphene Will Change Gadgets Forever*. 2014; Available from: http://news.yahoo.com/5-ways-graphene-change-gadgets-155243022.html.

[9]. Jiang, D.E., V.R. Cooper, and S. Dai, "Porous Graphene as the Ultimate

Membrane for Gas Separation″ *Nano Letters*, Vol. 9, No. 12, pp. 4019-4024, 2009.

[10]. Moussa, S., A.R. Siamaki, B.F. Gupton, and M.S. El-Shall, "Pd-Partially Reduced Graphene Oxide Catalysts (Pd/PRGO): Laser Synthesis of Pd Nanoparticles Supported on PRGO Nanosheets for Carbon-Carbon Cross Coupling Reactions″ *Acs Catalysis*, Vol. 2, No. 1, pp. 145-154, 2012.

[11]. Lv, W., M. Guo, M.H. Liang, F.M. Jin, et al., "Graphene-DNA hybrids: self-assembly and electrochemical detection performance″ *Journal of Materials Chemistry*, Vol. 20, No. 32, pp. 6668-6673, 2010.

[12]. Li, W.W., X.M. Geng, Y.F. Guo, J.Z. Rong, et al., "Reduced Graphene Oxide Electrically Contacted Graphene Sensor for Highly Sensitive Nitric Oxide Detection″ *Acs Nano*, Vol. 5, No. 9, pp. 6955-6961, 2011.

[13]. Du, A.J., Z.H. Zhu, and S.C. Smith, "Multifunctional Porous Graphene for Nanoelectronics and Hydrogen Storage: New Properties Revealed by First Principle Calculations″ *Journal of the American Chemical Society*, Vol. 132, No. 9, pp. 2876, 2010.

[14]. Xi, Q., X. Chen, D.G. Evans, and W.S. Yang, "Gold Nanoparticle-Embedded Porous Graphene Thin Films Fabricated via Layer-by-Layer Self-Assembly and Subsequent Thermal Annealing for Electrochemical Sensing″ *Langmuir*, Vol. 28, No. 25, pp. 9885-9892, 2012.

[15]. Kim, B.J., S.K. Lee, M.S. Kang, J.H. Ahn, et al., "Coplanar-Gate Transparent Graphene Transistors and Inverters on Plastic″ *Acs Nano*, Vol. 6, No. 10, pp. 8646-8651, 2012.

[16]. Bergmair, I., W. Hackl, M. Losurdo, C. Helgert, et al., "Nano- and microstructuring of graphene using UV-NIL″ *Nanotechnology*, Vol. 23, No.

33, 2012.

[17]. An, X.H., F.Z. Liu, Y.J. Jung, and S. Kar, "Tunable Graphene-Silicon Heterojunctions for Ultrasensitive Photodetection" *Nano Letters*, Vol. 13, No. 3, pp. 909-916, 2013.

[18]. Prasai, D., J.C. Tuberquia, R.R. Harl, G.K. Jennings, et al., "Graphene: Corrosion-Inhibiting Coating" *Acs Nano*, Vol. 6, No. 2, pp. 1102-1108, 2012.

[19]. Ohno, Y., K. Maehashi, and K. Matsumoto, "Label-Free Biosensors Based on Aptamer-Modified Graphene Field-Effect Transistors" *Journal of the American Chemical Society*, Vol. 132, No. 51, pp. 18012-18013, 2010.

[20]. Yoo, J.J., K. Balakrishnan, J.S. Huang, V. Meunier, et al., "Ultrathin Planar Graphene Supercapacitors" *Nano Letters*, Vol. 11, No. 4, pp. 1423-1427, 2011.

[21]. *Google glass concept*. Available from: http://www.graphenebiz.com/.

[22]. Delhaes, P., *Graphite and Precursors*. 2001: CRC press.

[23]. Gomez, H., M.K. Ram, F. Alvi, P. Villalba, et al., "Graphene-conducting polymer nanocomposite as novel electrode for supercapacitors" *Journal of Power Sources*, Vol. 196, No. 8, pp. 4102-4108, 2011.

[24]. Huang, H.J., H.Q. Chen, D.P. Sun, and X. Wang, "Graphene nanoplate-Pt composite as a high performance electrocatalyst for direct methanol fuel cells" *Journal of Power Sources*, Vol. 204, No., pp. 46-52, 2012.

[25]. Zhu, X.J., Y.W. Zhu, S. Murali, M.D. Stoller, et al., "Reduced graphene oxide/tin oxide composite as an enhanced anode material for lithium ion batteries prepared by homogenous coprecipitation" *Journal of Power Sources*, Vol. 196, No. 15, pp. 6473-6477, 2011.

[26]. Wang, F. and K. Zhang, "Reduced graphene oxide-TiO2 nanocomposite with high photocatalystic activity for the degradation of rhodamine B″ *Journal of Molecular Catalysis a-Chemical*, Vol. 345, No. 1-2, pp. 101-107, 2011.

[27]. Robinson, J.T., M. Zalalutdinov, J.W. Baldwin, E.S. Snow, et al., "Wafer-scale Reduced Graphene Oxide Films for Nanomechanical Devices″ *Nano Letters*, Vol. 8, No. 10, pp. 3441-3445, 2008.

[28]. Huang, X., X.Y. Qi, F. Boey, and H. Zhang, "Graphene-based composites″ *Chemical Society Reviews*, Vol. 41, No. 2, pp. 666-686, 2012.

[29]. Kim, J.E., T.H. Han, S.H. Lee, J.Y. Kim, et al., "Graphene Oxide Liquid Crystals″ *Angewandte Chemie-International Edition*, Vol. 50, No. 13, pp. 3043-3047, 2011.

[30]. Sundaram, R.S., C. Gomez-Navarro, K. Balasubramanian, M. Burghard, et al., "Electrochemical modification of graphene″ *Advanced Materials*, Vol. 20, No. 16, pp. 3050-3053, 2008.

[31]. Si, Y. and E.T. Samulski, "Synthesis of water soluble graphene″ *Nano Letters*, Vol. 8, No. 6, pp. 1679-1682, 2008.

[32]. Gilje, S., S. Han, M. Wang, K.L. Wang, et al., "A chemical route to graphene for device applications″ *Nano Letters*, Vol. 7, No. 11, pp. 3394-3398, 2007.

[33]. Kim, S., S. Zhou, Y.K. Hu, M. Acik, et al., "Room-temperature metastability of multilayer graphene oxide films″ *Nature Materials*, Vol. 11, No. 6, pp. 544-549, 2012.

[34]. Dikin, D.A., S. Stankovich, E.J. Zimney, R.D. Piner, et al., "Preparation and characterization of graphene oxide paper″ *Nature*, Vol. 448, No. 7152,

pp. 457-460, 2007.

[35]. Kim, J., L.J. Cote, and J.X. Huang, "Two Dimensional Soft Material: New Faces of Graphene Oxide" *Accounts of Chemical Research*, Vol. 45, No. 8, pp. 1356-1364, 2012.

[36]. Ekiz, O.O., M. Urel, H. Guner, A.K. Mizrak, et al., "Reversible Electrical Reduction and Oxidation of Graphene Oxide" *Acs Nano*, Vol. 5, No. 4, pp. 2475-2482, 2011.

[37]. Schniepp, H.C., J.L. Li, M.J. McAllister, H. Sai, et al., "Functionalized single graphene sheets derived from splitting graphite oxide" *Journal of Physical Chemistry B*, Vol. 110, No. 17, pp. 8535-8539, 2006.

[38]. Gomez-Navarro, C., R.T. Weitz, A.M. Bittner, M. Scolari, et al., "Electronic Transport Properties of Individual Chemically Reduced Graphene Oxide Sheets. (vol 7, pg 3499, 2007)" *Nano Letters*, Vol. 9, No. 5, 2009.

[39]. Pei, S.F. and H.M. Cheng, "The reduction of graphene oxide" *Carbon*, Vol. 50, No. 9, pp. 3210-3228, 2012.

[40]. Schniepp, H.C., J.-L. Li, M.J. McAllister, H. Sai, et al., "Functionalized Single Graphene Sheets Derived from Splitting Graphite Oxide" *J. physical chemistry B*, Vol. 110, No., pp. 8535-8539, 2006.

[41]. Stankovich, S., D.A. Dikin, R.D. Piner, K.A. Kohlhaas, et al., "Synthesis of graphene-based nanosheets via chemical reduction of exfoliated graphite oxide" *Carbon*, Vol. 45, No. 7, pp. 1558-1565, 2007.

[42]. Ekiz, O.Ö., M. Ürel, H. Güner, A.K. Mizrak, et al., "Reversible electric reduction and oxidation of graphene oxide" *ACS Nano*, Vol. 5, No., pp. 2475-2487, 2011.

[43]. Sun, D., X. Yan, J. Lang, and Q. Xue, "High performance supercapacitor electrode based on graphene paper via flame-induced reduction of graphene oxide paper″ *Journal of Power Sources*, Vol. 222, No., pp. 52-58, 2013.

[44]. Zhu, Y., S. Murali, M.D. Stoller, A. Velamakanni, et al., "Microwave assisted exfoliation and reduction of graphite oxide for ultracapacitors″ *Carbon*, Vol. 48, No. 7, pp. 2118-2122, 2010.

[45]. El-Kady, M.F., V. Strong, S. Dubin, and R.B. Kaner, "Laser scribing of high-performance and flexible graphene-based electrochemical capacitors″ *Science*, Vol. 335, No. 6074, pp. 1326-1330, 2012.

[46]. Williams, G., B. Seger, and P.V. Kamat, "TiO2 graphene nanocomposites UV assisted photocatalytic reduction of graphene oxide″ *ACS NANO*, Vol. 2, No., pp. 1487-1491, 2008.

[47]. El-Kady, M.F. and R.B. Kaner, "Scalable fabrication of high-power graphene micro-supercapacitors for flexible and on-chip energy storage″ *Nature Communications*, Vol. 4, No., pp. 9, 2013.

[48]. Trusovas, R., K. Ratautas, G. Raciukaitis, J. Barkauskas, et al., "Reduction of graphite oxide to graphene with laser irradiation″ *Carbon*, Vol. 52, No., pp. 574-582, 2013.

[49]. Cote, L.J., R. Cruz-Silva, and J. Huang, "Flash reduction and patterning of graphite oxide and its polymer composite″ *J. AM. CHEM. SOC*, Vol. 131, No., pp. 7, 2009.

[50]. Byon, H.R., S.W. Lee, S. Chen, P.T. Hammond, et al., "Thin films of carbon nanotubes and chemically reduced graphenes for electrochemical micro-capacitors″ *Carbon*, Vol. 49, No. 2, pp. 457-467, 2011.

[51]. Stankovich, S., R.D. Piner, S.T. Nguyen, and R.S. Ruoff, "Synthesis and exfoliation of isocyanate-treated graphene oxide nanoplatelets″ *Carbon*, Vol. 44, No. 15, pp. 3342-3347, 2006.

[52]. Abbey, C. and G. Joos, "Supercapacitor energy storage for wind energy applications″ *Ieee Transactions on Industry Applications*, Vol. 43, No. 3, pp. 769-776, 2007.

[53]. Stoller, M.D., S. Park, Y. Zhu, J. An, et al., "Graphene-based ultracapacitors″ *Nano Lett*, Vol. 8, No. 10, pp. 3498-502, 2008.

[54]. Liu, C., Z. Yu, D. Neff, A. Zhamu, et al., "Graphene-Based Supercapacitor with an Ultrahigh Energy Density″ *Nano Lett*, Vol., No., 2010.

[55]. Park, S. and R.S. Ruoff, "Chemical methods for the production of graphenes″ *Nat Nanotechnol*, Vol. 4, No. 4, pp. 217-24, 2009.

[56]. Moon, I.K., J. Lee, R.S. Ruoff, and H. Lee, "Reduced graphene oxide by chemical graphitization″ *Nat Commun*, Vol. 1, No., pp. 73, 2010.

[57]. Park, S., Y.C. Hu, J.O. Hwang, E.S. Lee, et al., "Chemical structures of hydrazine-treated graphene oxide and generation of aromatic nitrogen doping″ *Nature Communications*, Vol. 3, No., 2012.

[58]. Lee, S., Y.J. Kim, D.H. Kim, B.C. Ku, et al., "Synthesis and properties of thermally reduced graphene oxide/polyacrylonitrile composites″ *Journal of Physics and Chemistry of Solids*, Vol. 73, No. 6, pp. 741-743, 2012.

[59]. Williams, G., B. Seger, and P.V. Kamat, "TiO2-graphene nanocomposites. UV-assisted photocatalytic reduction of graphene oxide″ *Acs Nano*, Vol. 2, No. 7, pp. 1487-1491, 2008.

[60]. Sokolov, D.A., C.M. Rouleau, D.B. Geohegan, and T.M. Orlando, "Excimer laser reduction and patterning of graphite oxide″ *Carbon*, Vol. 53,

No., pp. 81-89, 2013.

[61]. Chmiola, J., C. Largeot, P.L. Taberna, P. Simon, et al., "Monolithic Carbide-Derived Carbon Films for Micro-Supercapacitors" *Science*, Vol. 328, No. 5977, pp. 480-483, 2010.

[62]. *Ultracapacitors.org*. Available from: http://www.ultracapacitors.org/.

[63]. Makino, S., Y. Yamauchi, and W. Sugimoto, "Synthesis of electro-deposited ordered mesoporous RuOx using lyotropic liquid crystal and application toward micro-supercapacitors" *Journal of Power Sources*, Vol. 227, No., pp. 153-160, 2013.

[64]. Wang, S., P.K. Ang, Z.Q. Wang, A.L.L. Tang, et al., "High Mobility, Printable, and Solution-Processed Graphene Electronics" *Nano Letters*, Vol. 10, No. 1, pp. 92-98, 2010.

[65]. Xie, G.B., Z.W. Shi, R. Yang, D.H. Liu, et al., "Graphene Edge Lithography" *Nano Letters*, Vol. 12, No. 9, pp. 4642-4646, 2012.

[66]. Namisnyk, A.M., *A SURVEY OF ELECTROCHEMICAL SUPERCAPACITOR TECHNOLOGY*.2003

[67]. *Battery university*. Available from: http://batteryuniversity.com/learn/article/whats_the_role_of_the_supercapacitor.

[68]. Mannoor, M.S., H. Tao, J.D. Clayton, A. Sengupta, et al., "Graphene-based wireless bacteria detection on tooth enamel (vol 3, 763, 2012)" *Nature Communications*, Vol. 4, No., 2013.

[69]. Jung, H. and J. Lee, "A Polysilicon Field Effect Transistor Pressure Sensor of Thin Nitride Membrane Choking Effect of Right After Turn-on for Stress Sensitivity Improvement" *Journal of Sensor Science and Technology*,

Vol. 23, No. 2, pp. 114-121, 2014.

2 Photo-thermal reduction of GO

2.1 Introduction of light source

Visible light is electromagnetic radiation which have a wavelength in the range of 400 nm to 700 nm between the infrared, with longer wavelengths and the ultraviolet.[1] Primary properties of light are intensity, propagation direction, frequency or wavelength spectrum, and polarisation. Light is emitted and absorbed in photons which shows properties of wave and particles.

Generally, light sources used in optical reduction could be categorized into two groups, coherent and incoherent light source shown in Figure 12.[2] Coherence light source is an ideal condition of waves that enables temporal and spatial constant. Coherent light is a beam of photons that has same frequency and phase. Coherent light has high energy density and can focus on small spot. A laser is basically a type of coherent light source which does not spread and diffuse, but it can be focused to tiny spots in a digit micro meter. A high power coherent light source could engrave or make a cut on the surface of a metal material.

Incoherent light source is a beam of photons that have the same frequency and different phase or different frequency and phase between photons. So the transitions between energy levels in a photon are a random process and we cannot control. All conventional light sources except laser light source which is only

coherent light source are incoherent light source. LED (Light-emitting diode), fluorescent lamp, and xenon flash light are some of instances of incoherent light sources. In many type of incoherent light source, LED is same frequency and different phase of beam. A xenon flash tube is different frequency and different phase of beam.

Xenon flash unit needed high voltage to produce the light in short time, so it used a charged capacitor to deliver electrical current as soon as a xenon flash lamp was triggered. Among these incoherent light sources, xenon flash light was considered the most suitable means to reduce GO through a delivery of high energy to GO rapidly. A GO reduction through incoherent light source irradiation (ILSI) via a commercial xenon camera flash had been demonstrated in which high energy and high temperature environment were not required in conventional thermal treatment.

A GO reduction through ILSI by using a commercial xenon camera flash had been demonstrated in room temperature environment. The reduction process induced by optical energy was efficient from an aspect of processing time as energy transfers to GO instantaneously. Furthermore, a GO reduction by ILSI was environmental friendly because no harmful substances were produced throughout the process.

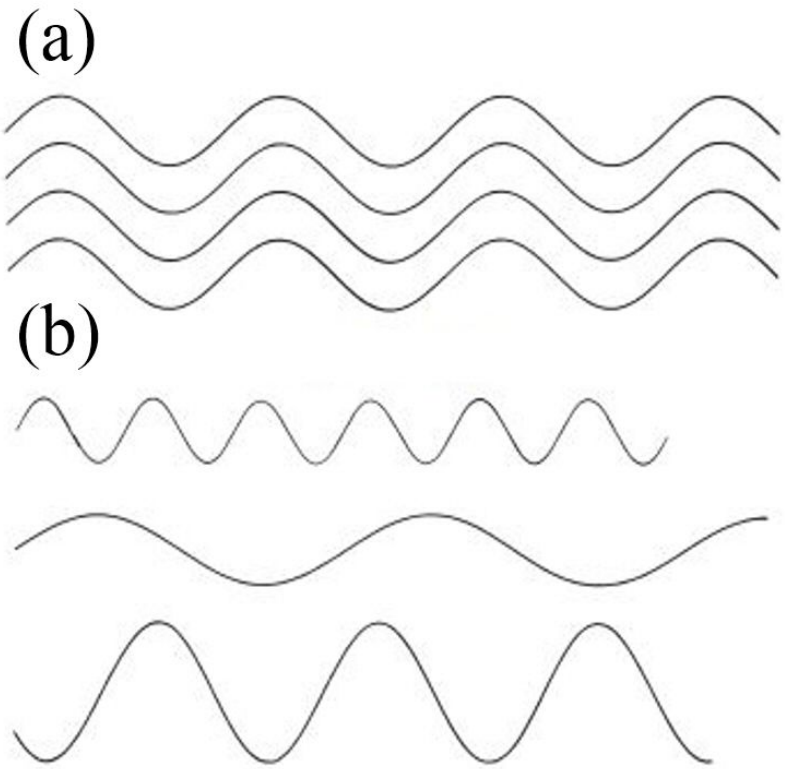

Figure 12. Light waves are coherent if they are all in phase with one another. The peaks and valleys of coherent light waves (a) are all lined up with each other. The peaks and valleys of incoherent light waves (b) do not line up. Stimulated emission is in phase with the light that stimulates it, so laser light is coherent. The sun, light bulbs, flames and other sources that generate spontaneous emission are incoherent.[3]

2.2 Coherent light source irradiation reduction

A laser is basically a type of coherent light source which does not spread and diffuse. A laser can be focused to tiny spots in a digit micro meter to transfer light energy. A high power coherent light source could engrave or make a cut on a surface of a metal material as well as rGO.

GO was reduced into rGO via coherent light source of pulsed laser.[4] Patterned rGO obtained through coherent light source irradiation (CLSI) via a laser DVD writer had been demonstrated as an excellent candidate for high performance supercapacitors. Coherent light source had enough energy to carve on rGO as well as reduce GO to rGO. Hundreds of GO sheets stacked together after a GO solution was dried up. CLSI craved lines on a surface of rGO sheet and reduced GO simultaneously. The width of crack line was less than 1 μm as focus point width of CLSI was approximately 0.9 μm. The rGO sheets only had crack lines in upper sheets while lower part of rGO sheets did not have a crack line.

An increase of total surface area of rGO was attributed to cracks in upper sheets while lower sheets which were reduced to electrically conductive rGO, functioned as a current collector when rGO sheets were used as an active material for electrodes in a supercapacitor.

CLSI in a DVD writer (SH-216, Samsung) that had a small dot of light beam was further focused at 900 nm spot size through annular mask lens. Writing velocity of a DVD writer was fixed at 250 mm per second while writing and reading power

were set at 50 mW (50% pulse duty ratio of 100 mW) and continuous 5 mW respectively. Zero focus offset was an indication of a laser focus location on a reflective layer of a DVD disk.

Tracks per inch (TPI) was a crucial parameter that defined width of every circular laser track made with one another. High TPI value implied more crack lines from a laser source was distributed on the same amount of surface area of a DVD disk. GO was reduced to rGO after receiving the optical energy from CLSI. Crack lines were produced and visible on a rGO layer surface under Scanning electron microscope (SEM) spectroscopy, which was essentially an outcome of laser focusing at the same spots repeatedly as shown in Figure 13. A distance between two crack lines could be precisely controlled through TPI manipulation.

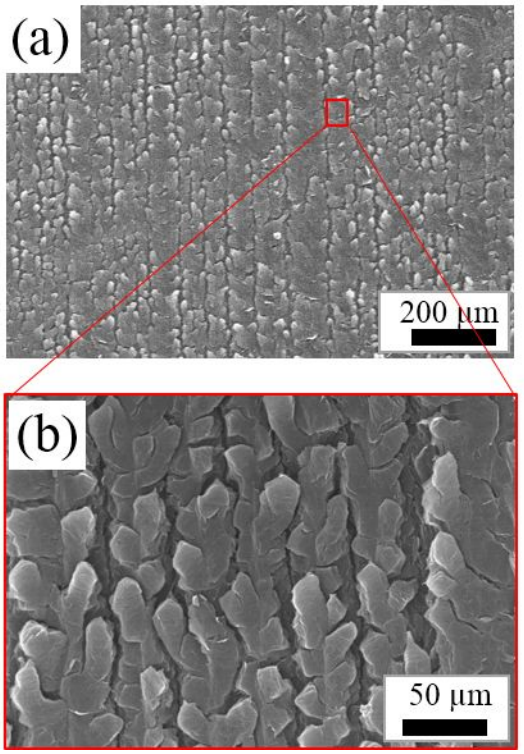

Figure 13. A laser reduction of GO. (a) CLSI rGO had aligned straight crack lines on the sheet surface (b) CLSI rGO showed small bump along with crack lines

2.3 Incoherent light source irradiation reduction

A xenon flash emitted extremely intense, full spectrum light which were a good characteristics to reduce GO.[5] In a literature, photo-thermally reduced graphene had high power anodes material for lithium-ion batteries.[6]

Xenon flash light source produced photo-thermal light energy in short time which occurred to reduce GO. Xenon flash light source needed high voltage to produce the light pulse, so it had to use a charged capacitor. Although there were several incoherent light sources of LED, light bulb, fluorescent light, and so on, xenon flash light could reduce GO in a short time of milliseconds . Therefore, xenon flash light was considered the most feasible and straightforward method to reduce GO through a delivery of high energy to GO in an extremely short duration.

In a ILSI process, light energy was provided by a xenon flash far exceeds 70 mJ/cm^2,[7] heat energy needed to raise a temperature of 1 μm thick of GO from a room temperature to 100°C at which deoxygenating reactions token place. The moment light energy was delivered to GO, an explosion sound effect of “pop” was audible, suggesting a rapid air expansion near a surface of GO due to degasing, which effectively exfoliated a stacked structure of GO layer. An increase of total surface of rGO was attributed to exfoliating mechanism where thickness of rGO expanded ten times after a ILSI reduction process shown in Figure 14.

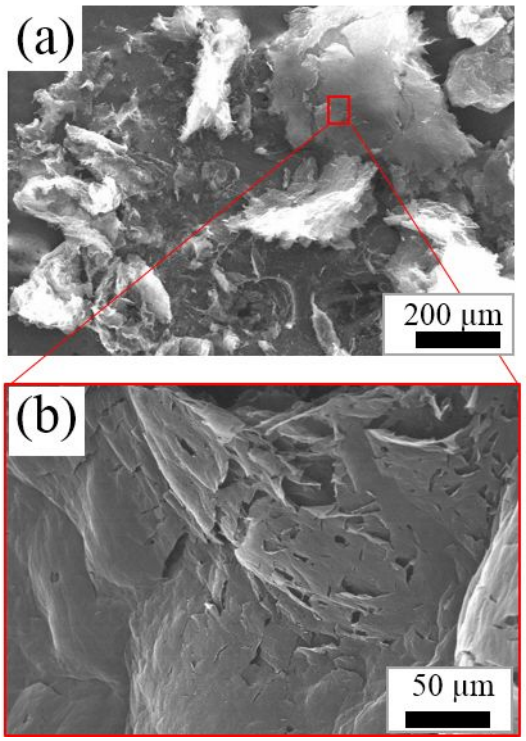

Figure 14. SEM image of a flash reduction. (a) Surface of ILSI rGO sheet (b) ILSI rGO had big surface area with small cracked flakes. It looked like arbitrary broken flakes.

2.4 Flash reduction

ILSI (Elinchrom, Style RX 1200, Switzerland) was employed to generate high intensity incoherent light to induce GO reduction (Figure 15). When photo-thermal light energy of ILSI of a xenon camera flash was too high, rGO surface tore out and split into small pieces. On the other hand, low photo-thermal light energy of ILSI did not trigger GO reduction as what shown in Figure 16. Prior to ILSI, GO film was positioned 4 cm away from the light source in a reduction process. ILSI of flash light had a flash power with precision, ranging from 2.5 f-stop (0.19 J/cm^2) to 7.5 f-stop (6.36 J/cm^2) with 0.1 f-stop intervals. F-stop value was a measurement of light energy emitted by a flash unit which maximum deliverable energy was 1200 J. During ILSI, a magnitude of 6.5 f-stop (3.18 J/cm^2) with equivalent 600 J of flash energy was delivered to rGO (Table 2).

Additional experiments had been executed to determine the optimum flash energy for ILSI. Flash energy of f-stop value lower than 4.5 f-stop could hardly activate an rGO reduction process while at 5.5 f-stop, only a partial of GO was reduced. At maximum 7.5 f-stop, GO was thoroughly reduced but produced rGO which could not retain a well-connected structure was fragmentized into tiny pieces.

In, photography, f-stop is also called focal ratio, f-number, f-ratio, or relative aperture. It is the ratio of the lens's focal length with dimensionless number. Stops mean a unit to quantify ratios of exposure in flash light source.

In a bulk GO reduction test, 6.5 f-stop value was the most appropriate flash power as a complete GO reduction is achievable while rGO can still maintain its structural network. Meanwhile, around 5.5 f-stop value was the most appropriate light energy because patterned electrode had narrow line. Therefore, reduction quality is one of important factors and sustaining a structure is also critical factor of flash light reduction.

$$N = \frac{f}{D} \tag{2.1}$$

Where f and D are focal length and diameter of the entrance pupil, respectively. For example, when focal length is long, high quantity of light energy is irradiated to compensate degradation from xenon flash light. Although camera has f-stop value of exposure, f-stop value of camera is opposite to that of flash light source.

Table 2. F-stop value to equivalent light energy

Energy to trigger reduction (F stop)	Energy (J)	Equivalent energy (J/cm^2)
7.5	1200	6.363
7.4	1120	5.937
7.3	1045	5.539
7.2	975	5.168
7.1	909	4.822
7	849	4.499
6.9	792	4.198
6.8	739	3.917
6.7	689	3.654
6.6	643	3.410
6.5	600	3.181
6.4	560	2.968
6.3	522	2.770
6.2	487	2.584
6.1	455	2.411
6	424	2.250
5.9	396	2.099
5.8	369	1.958
5.7	345	1.827
5.6	322	1.705
5.5	300	1.591
5.4	280	1.484
5.3	261	1.385
5.2	244	1.292
5.1	227	1.206
5	212	1.125
4.9	198	1.049
4.8	185	0.979
4.7	172	0.914
4.6	161	0.852
4.5	150	0.795
4.4	140	0.742
4.3	131	0.692
4.2	122	0.646
4.1	114	0.603
4	106	0.562
3.9	99	0.525
3.8	92	0.490
3.7	86	0.457
3.6	80	0.426
3.5	75	0.398
3.4	70	0.371
3.3	65	0.346
3.2	61	0.323
3.1	57	0.301
3	53	0.281
2.9	49	0.262
2.8	46	0.245
2.7	43	0.228
2.6	40	0.213
2.5	38	0.199

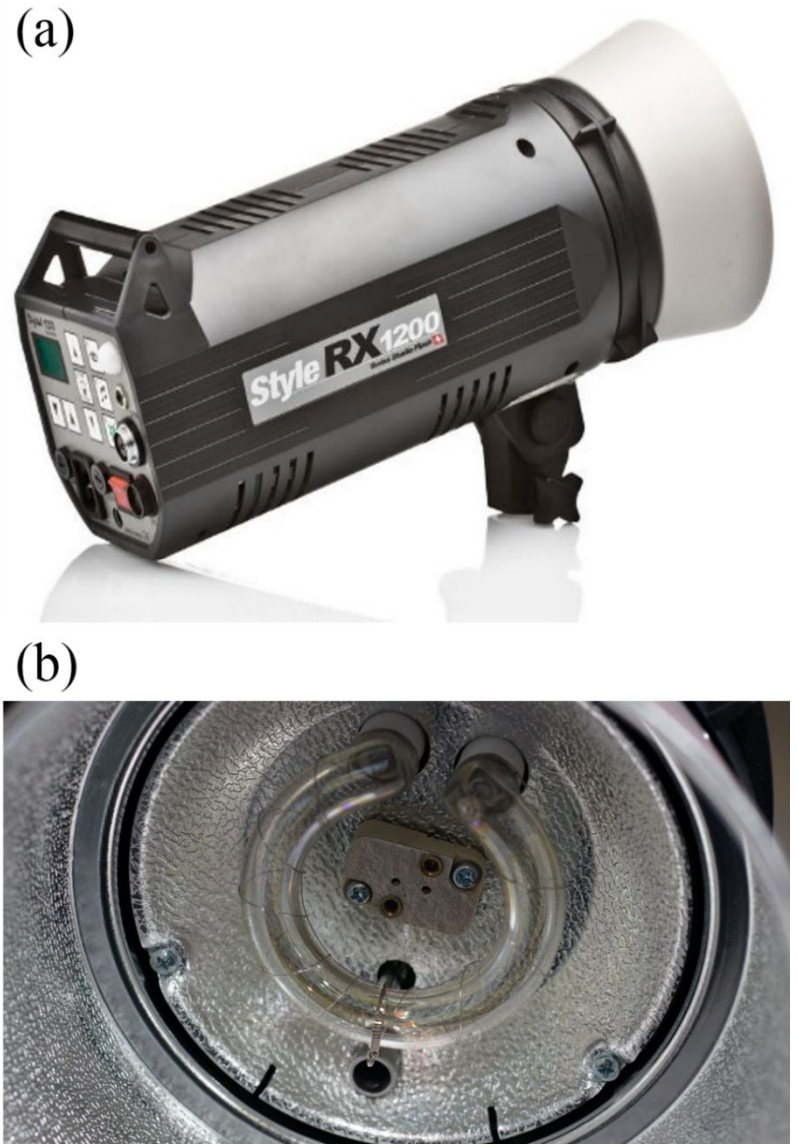

Figure 15. (a) Flash light source, style RX 1200 [8] (b) a xenon lamp inside

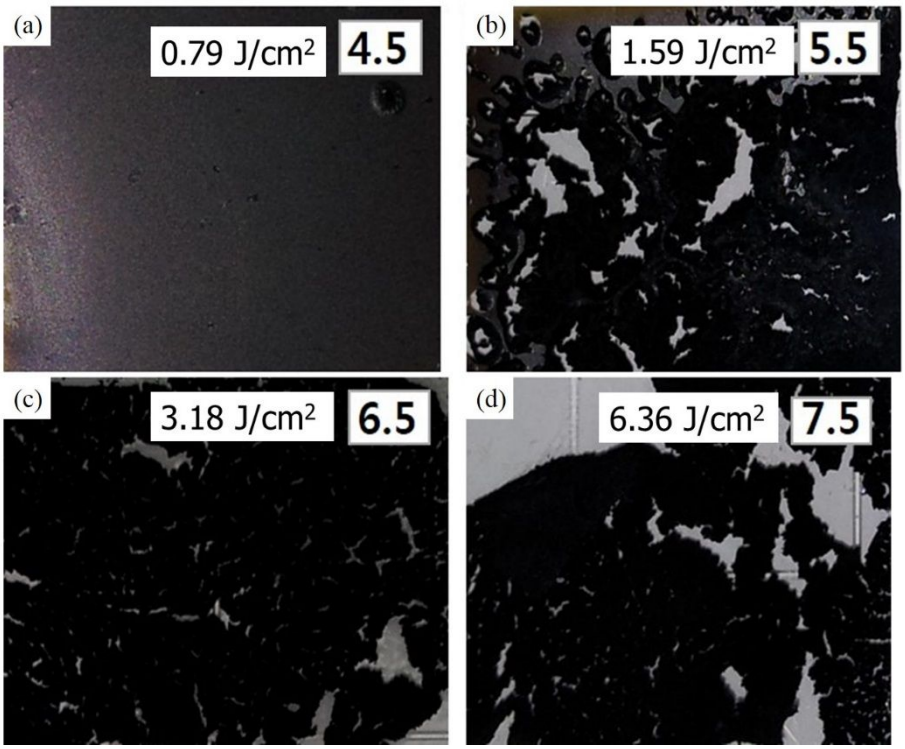

Figure 16. Different rGO surface results are shown in ILSI reduction condition of 4.5, 5.5, 6.5, and 7.5 f-stop value. (a) 4.5 f-stop. GO was not reduced (b) 5.5 f-stop. Some of GO was not reduced to rGO (c) 6.5 f-stop. GO was reduced evenly at whole surface area. In 6.5 f-stop, rGO surface showed the best results. (d) 7.5 f-stop. Although 7.5 f-stop reduced most of GO, rGO was tear out and break into pieces.[9]

GO thin layer shatters into tiny pieces when photo-thermal reduction was achieved by employing xenon flash light source in a short time. The thin structure suffered extensive damage during instantaneous degassing process of which a huge volume expansion takes place owing to the exfoliation of the stacked layers shown in Figure 17. When the moment of flash light was irradiated, debris of GO particle was dispersed arbitrary direction. Debris amount was increased by light energy level. Roughness of rGO surface was increased compared to that of GO.

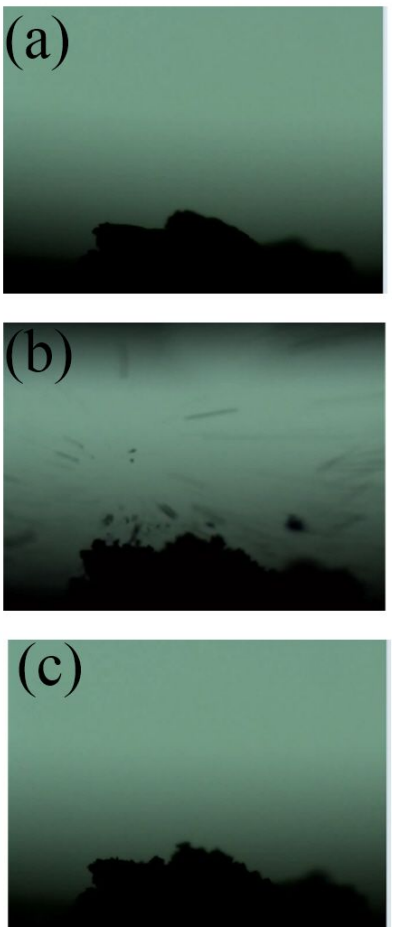

Figure 17. (a) GO surface had relatively smoother than after ILSI in Figure (c) (b) The moment of ILSI of xenon flash was lighted, and debris was dispersed every direction (c) After ILSI flash light, rGO surface changed to rough

2.5 Spectroscopy of GO and rGo

2.5.1 Raman spectroscopy

Raman spectroscopy is a spectroscopic technique used to observe vibrational, rotational, and other low-frequency modes in a system. Raman spectroscopy is commonly used to the chemical bonds and symmetry of molecules in chemistry.

Raman spectroscopy measurements of GO and rGO on different materials were performed in back scattering geometry with a LabRam HR which had 800 mm focal length monochromator with liquid-nitrogen cooled CCD (Charged-coupled device) multichannel detector.[10] A spectra of Raman shift were obtained using a 514.532 nm Ar-ion laser with power of 0.5 mW. Raman spectra of graphene and bulk graphite were a D peak (1350 cm^{-1}), a G peak (1580 cm^{-1}) and a 2D peak (2690 cm^{-1}) caused by in-plane optical vibration.[11-15] Raman shift of GO and other cases after GO reduction on the above substrates. In all cases expect for on glass, the Raman spectra shifted to the left. In particular such shift on PET film and paper resulted in the G peak at 1580 cm^{-1} which is a characteristic peak of graphene.

The D peak (1350 cm^{-1}) and G peak (1580 cm^{-1}) sharpness of Raman spectrum were increased and indicated crystallization of rGO was improved after photo-thermal flash reduction (1.50 J/cm^2). A remarkable increase of the 2D peak (2690 cm^{-1}) was observed, indicating better graphitization of rGO than GO shown in Figure 18. There was no 2D peak on GO. Oxygen functional groups of GO were removed and remained defected carbon structures that repair process was not occurred by a combination of carbon. Raman spectroscopy spectrum of GO at a

low (0.79 J/cm^2) photo-thermal flash reduction showed the same that of GO, which meant a reduction process was not occurred. Therefore, low light energy could not trigger the GO reduction process

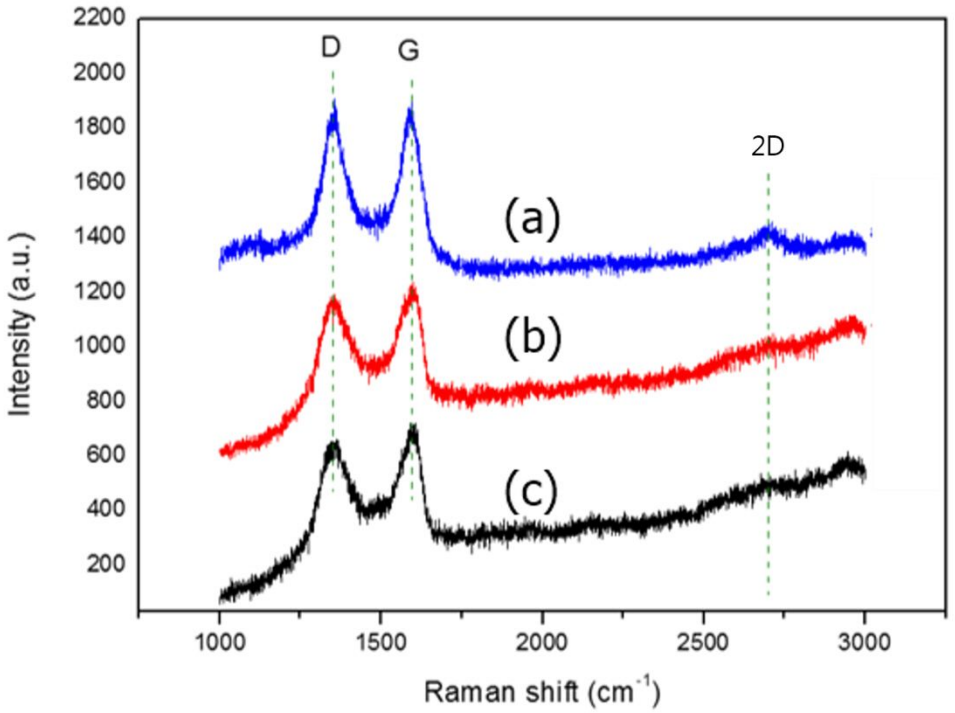

Figure 18. Raman shift of GO and rGO (a) GO (b) At a low photo-thermal light energy reduction of GO. (c) At a high photo-thermal light energy reduction of GO.[9]

2.5.2 X-ray photoelectron spectroscopy (XPS)

XPS (Kratos, AXIS-HSI) is a quantitative spectroscopic measurement to check elemental composition. XPS check with Raman spectroscopy measurement was powerful chemical component and bonding analysis techniques for nano scale surface depth. Focused beam of X-ray produced photo-emitted electrons measured kinetic energy of electron via electron energy analyzer. Minimum analytical area was 5 cm × 5 cm and base pressure was 5×10^{-10} Torr in basic condition. A software tool of kinetic energy analysis was used casaXPS commercial program.

XPS measurement was used to quantitatively analyze of GO and rGO while Raman spectroscopy could measure qualitatively carbon based materials. A total amount of oxygen was detected via XPS measurement (Figure 19). C-O (286.5 eV, hydroxyl and epoxy) and C=O (287.8 eV) bonding of GO were sustained from 19.8 at.% and 4.16 at.% to 21.2 at.% and 5.62 at.% at a low 0.79 J/cm^2 photo-thermal flash reduction while C-O and C=O bonding of GO were decreased to 6.09 at.% and 3.86 at.% at a 1.50 J/cm^2 photo-thermal flash reduction (Table 3).[9] Intensity of C-C/C=C is also increased. As a result, a decrease of oxygen showed oxygen functional groups in GO were partially removed at a 1.50 J/cm^2 photo-thermal flash reduction.[16]

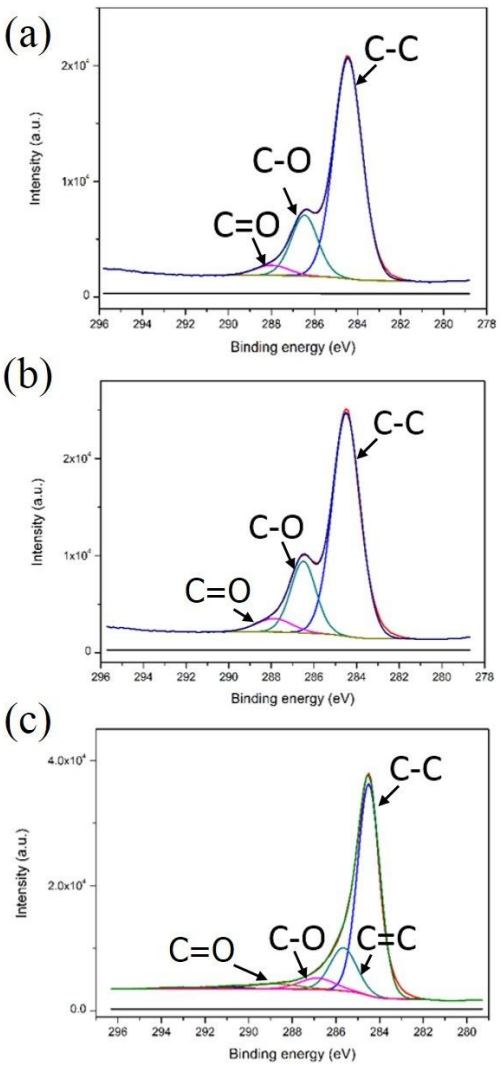

Figure 19. XPS of (a) GO, (b) low photo-thermal energy reduction of GO, and (c) high photo-thermal energy reduction of GO[9]

Table 3. Atomic composition of XPS result of GO[9]

Bonding (at.%) / Sample	C-O (286.5 eV)	C=O (287.8 eV)	C-C	C=C
GO	19.8	4.16	76.05	1>
0.79 J/cm^2 flash reduction	21.2	5.62	73.11	1>
1.50 J/cm^2 flash reduction	6.09	3.86	71.04	17.41

Conductivity affected a performance of a supercapacitor. Conductivity of rGO could be extracted from sheet resistance because patterned rGO electrodes were thin film. Sheet resistance was checked by a four point probe which measured a resistance of thin films.[17]

A patterned GO electrode could be tested by sheet resistance because rGO material was two digit of micro meter thick.[18] For example, 10 Ω/□ was conducting material while 10 MΩ/□ was almost non conducting material shown in Figure 20.

After a total GO amount was fixed at 3 nL, sheet resistance was measured to check a rGO reduction. Three printing methods were prepared such as a 3 nL GO single droplet, 0.6 nL GO of 5 droplets and 0.3 nL GO of 10 droplets. Only three methods could be executed because amount of droplets was determined by multiple number of 0.3 nL, a minimum dispensing amount. A reduction result showed that only 0.3 nL of 10 droplets was reduced when energy threshold value was 5.3 f-stop light energy.

To check a structure of rGO, microscope images was needed for detail investigation. A SEM is a type of electron microscope that produces image by scanning with an electron beam. A SEM (FE-SEM, S-4800, HITACHI, Japan) was operated after the samples were coated by platinum (Pt) conductive materials to prevent charging effect.[19]

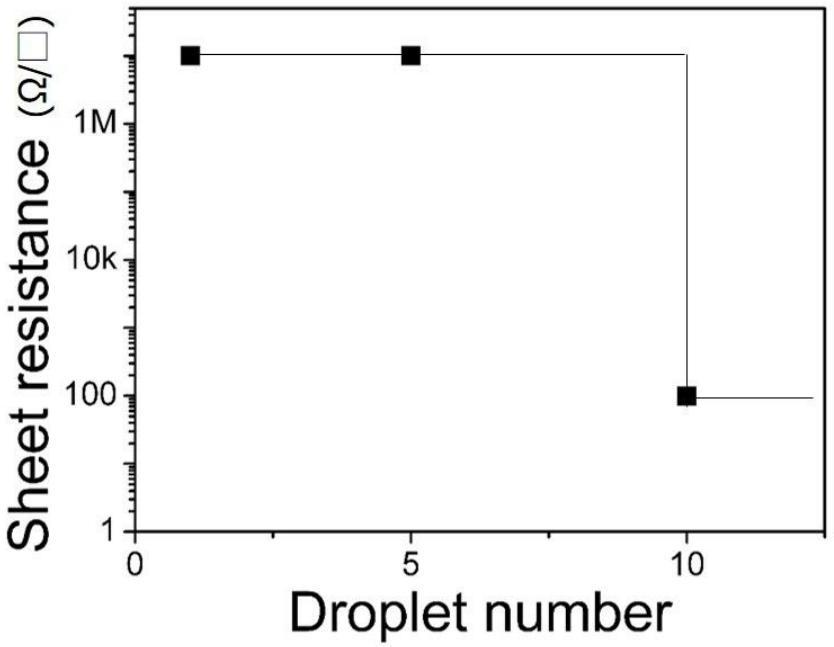

Figure 20. Sheet resistance by droplet number

Our samples were needed Pt conductive materials coating because GO and PET were non conducting materials. Although rGO was conducting material, A PET film substrate was non conducting material which distorted original images of rGO.

Figure 21 shows SEM image of cross-sectional view of an interdigitated supercapacitor. In SEM images, flash reduced rGO spread out arbitrary direction. After injection a liquid electrolyte, rGO parts shrank and height of rGO decreased. Structure of rGO is stable and stick tightly on PET film in figure.

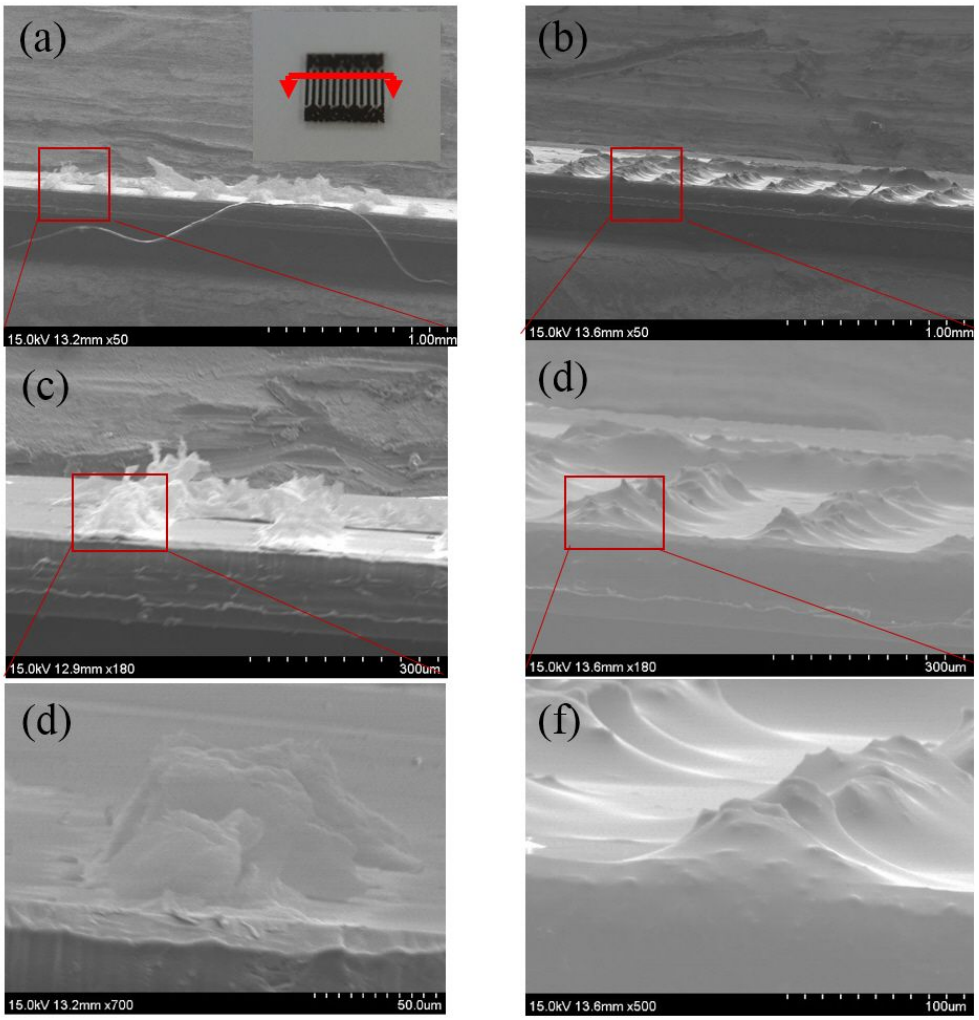

Figure 21. (a) Cross-section view of flash reduced rGO (b) After a reduction and electrolyte[9] (c) Magnified rGO (d) Magnified rGO (e) Height of GO (f) Shrink height

2.6 Bibliography

[1]. Pal, G.K. and P. Pal, *Textbook of Practical Physiology* 2001: Chennai: Orient Blackswan.

[2]. Schulz, T.J., "Optimal beams for propagation through random media" *Optics Lett.*, Vol. 30, No., pp. 1093-1095.

[3]. Hecht, J., *An entry-level guide Understanding Lasers*. Vol. 3. IEEE press.

[4]. Huang, L., Y. Liu, L.C. Ji, Y.Q. Xie, et al., "Pulsed laser assisted reduction of graphene oxide" *Carbon*, Vol. 49, No. 7, pp. 2431-2436, 2011.

[5]. Gilje, S., S. Dubin, A. Badakhshan, J. Farrar, et al., "Photothermal deoxygenation of graphene oxide for patterning and distributed ignition applications" *Adv Mater*, Vol. 22, No. 3, pp. 419-23, 2010.

[6]. Mukherjee, R., A.V. Thomas, A. Krishnamurthy, and N. Koratkar, "Photothermally Reduced Graphene as High-Power Anodes for Lithium-Ion Batteries" *Acs Nano*, Vol. 6, No. 9, pp. 7867-7878, 2012.

[7]. Cote, L.J., R. Cruz-Silva, and J. Huang, "Flash reduction and patterning of graphite oxide and its polymer composite" *J. AM. CHEM. SOC*, Vol. 131, No., pp. 7, 2009.

[8]. *Flash light source*. Available from: http://www.elinchrom.com/product/Style-RX-1200.html#content.

[9]. Jung, H., C.V. Cheah, N. Jeong, and J. Lee, "Direct printing and reduction of graphite oxide for flexible supercapacitors" *Applied Physics Letters*, Vol. 105, No., 2014. [http://dx.doi.org/10.1063/1.4890840].

[10]. *Raman research center, Korea*. Available from: http://www.raman.re.kr/.

[11]. Trusovas, R., G. Račiukaitis, J. Barkauskas, and R. Mažeikienė, "Laser

Induced Graphite Oxide/Graphene Transformation″ *Journal of Laser Micro/Nanoengineering*, Vol. 7, No., 2012.

[12]. Zhu, Y.W., S. Murali, W.W. Cai, X.S. Li, et al., "Graphene and Graphene Oxide: Synthesis, Properties, and Applications″ *Advanced Materials*, Vol. 22, No. 35, pp. 3906-3924, 2010.

[13]. Niyogi, S., E. Bekyarova, M.E. Itkis, H. Zhang, et al., "Spectroscopy of Covalently Functionalized Graphene″ *Nano Letters*, Vol. 10, No. 10, pp. 4061-4066, 2010.

[14]. Bergmair, I., W. Hackl, M. Losurdo, C. Helgert, et al., "Nano- and microstructuring of graphene using UV-NIL″ *Nanotechnology*, Vol. 23, No. 33, 2012.

[15]. Allen, M.J., V.C. Tung, and R.B. Kaner, "Honeycomb Carbon: A Review of Graphene″ *Chemical Reviews*, Vol. 110, No. 1, pp. 132-145, 2010.

[16]. Wang, M., J. Oh, T. Ghosh, S. Hong, et al., "An interleaved porous laminate composed of reduced graphene oxide sheets and carbon black spacers by in situ electrophoretic deposition″ *Rsc Advances*, Vol. 4, No. 7, pp. 3284-3292, 2014.

[17]. Jaeger, R.C., *Introduction to Microelectronic Fabrication (2nd ed.)*. 2003, New Jersey: Prentice Hall. 81–88.

[18]. Zhu, Y.W., W.W. Cai, R.D. Piner, A. Velamakanni, et al., "Transparent self-assembled films of reduced graphene oxide platelets″ *Applied Physics Letters*, Vol. 95, No. 10, 2009.

[19]. *Inter-university semiconductor research center, Seoul National University*. Available from: http://www.isrc.snu.ac.kr/.

3 Droplet printing technology

3.1 Introduction of printing technology

There were several printing technologies of conducting materials on a flexible substrate.[1-3] In carbon based materials, thin film supercapacitors were printed using single walled carbon nanotubes.[4] Pattern with photo mask method was printed.[5] Laser scribing of commercial DVD writer was patterned with thin film GO solution coating,[6] However, there technology are hard to pattern on slanted and curved surface.

There are already commercialized mass producing printing methods. Slot die printing process is to produce stripes coatings which is on flexible substrates in fast speed. On the other hand, control of thickness and non-continuous pattern has limitation. Another poplar and long history printing method is screen printing method. Screen printing method uses a woven mesh to block ink to receive a designed image. However, patterning resolution is limited in micro size in screen printing.

A printing method of a liquid dispenser affected a line resolution and porosity, when a GO solution was dispensed. We tested several printing conditions to reach high electrode resolution. As a result, a multiple dispensing printing method had the best performance.

We shows a direct patterning method of a GO solution using particular inkjet printing method. Hydrophilic GO can be dissolved in deionized water to be used as an “ink” for a patterning on a slanted plastic substrate.

To verify a multiple dispensing printing method, we compared to a single dispensing printing method. A liquid dispenser should drop a 3 nL GO solution on every spot to produce electrodes. Both a multiple dispensing printing method and a single dispensing printing method were tested for producing high resolution electrodes pattern.

First, in a multiple dispensing printing method, a 3 nL GO solution was divided into 10 portions of 0.3 nL GO and ejected 10 times separately. A small droplet dried up in a second, before a following droplet was ejected exactly on the top of the previous one, to create a stacking structure. Meanwhile, in a single dispensing method, only one droplet containing a 3 nL solution was dispensed at one spot to print out a 3 nL solution. Therefore, total amount of GO solution was the same of 3 nL.

3.2 Printing on a non-flat surface

3.2.1 Significance of direct printing technology

Direct printing technology has many advantage of curved surface printing, minimum quantity of GO solution, and environment-friendly process. Although direct printing has several merits, control problem make it hard to use widely.

To pattern carbon based materials, several methods was used. Onion-like carbon was patterned electrophoretic deposition technique which used semiconductor fabrication of high temperature and chemical reaction.[7] Later, several straightforward method was proposed. Flash reduction of photo mask, laser scribbling method, and commercial inkjet printer only conducted on flat substrate and was not good for a curved surface. Direct printing can pattern not only on flat substrate but also a curved surface.

Nowadays, there are already commercialized wearable devices such as google glass or Samsung galaxy gear (Figure 22). Wearable devices basically has a curved surface to fit our body. Furthermore, it sometimes needs a flexible properties to feel comfortable.

For example, google glass still had display device on flat surface. For a convenience, glasses surface will need a display on itself. While it look normally

glasses, glasses need on conducting lines on a curved glasses surface. Direct printing will be a useful tool to pattern on a curved surface in mass production.

Figure 22 (a) Wearable device of Google glass[8] (b) Watch concept [9] (c) iWatch concept [10]

3.2.2 Limitations of previous approaches

Flash reduction of GO patterned interdigitated electrodes of nitrogen sensor.[5] It used photo mask on top of a GO film to block an area which a light could not pass through. When substrate had a caved or curved surface, light could penetrate gap between the substrate and photo mask. Therefore, patterning was difficult on curved surface with photo mask method.

Laser scribing DVD writer patterned on disk which was coated thin GO film.[6] In a commercial DVD writer, disk with thin film substrate was only allowed to install in disk chamber. When disk had on rough surface, disk writer could occur an operation error and broken down due to losing focus point. Furthermore, substrate which has curved surface is hard to install on the DVD writer for patterning. Although attached film on a disk could be patterned in the DVD writer, attached film decrease transparency of final products.

A commercial inkjet printer had been put into test in GO patterning, but the droplets of quantity was too small so that conducting line could not produce. An inkjet printer had loading of curved substrate. Although inkjet printer could load a substrate, a droplet could not be controlled a curved surface.

Although previous technologies process was complicate, it was difficult to print a curved surface. Therefore, liquid dispensing is only method of direct printing on curved surface.

3.2.3 Dispensed printing on different depths

We estimated droplet dispensing on different depth surfaces in Figure 23. Printing was tested to draw a line on a slanted surface with 5 g/L concentration GO solution. Furthermore, 5 field was printed to produce a straight line with multiple dispensing printing method. Center to center was 0.08 mm distance. Maximum depth was 3 mm from reference height which is main surface of device. When reference height was included, maximum depth was 3.5 mm from the dispensing nozzle.

We printed straight lines on reference surface, 1 mm, 2 mm, and 3 mm depth surface. Maximum depth was determined by working distance of nozzle module. A specification of liquid dispenser was limited in 3 mm depth. Dispensing nozzle was positioned 0.5 mm from reference surface. Straight lines of GO solution on 1 mm, 2 mm, and 3 mm depth surface were produced like the one on reference surface. Each line gap was 80 μm resolution. Printing quality was sustained in 3 mm depth surface to produce GO electrode line. On the other hand, GO lines width start to widen which showed misalignment started.

In different depth surfaces printing test, GO droplets was spread evenly to produce a straight line. Therefore, we showed that direct printing of GO solution could produce a curved surface such as eye glasses.

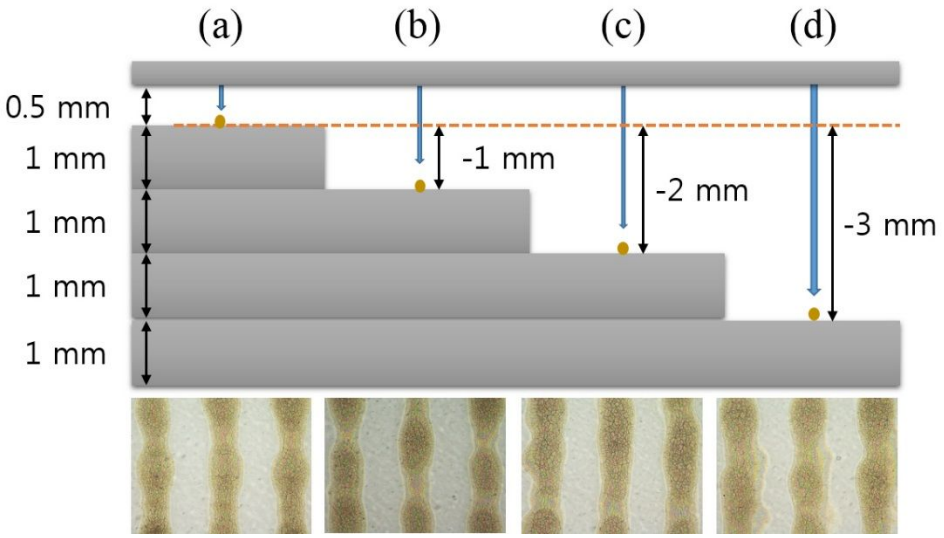

Figure 23 (a) Reference printing (b) 1 mm depth printing (c) 2 mm depth printing (d) 3 mm depth printing

3.2.4 Dispensed printing on a slanted surface

In laser scribing of DVD writer patterning, GO solution was needed to coat on the disk evenly.[6] When GO film was on a curved surface, laser disk could not work and even install. In addition, GO part was remained as non-conducting material except patterned rGO whereas laser scribing only patterned on designated area.

Ejected 300 pL droplet could attach on a slanted substrate without chemical, physical, and any other treatment because droplet is too small, so that surface tension is bigger than weight of droplet to slide down. Droplets which dispensed 5 fields with 10 times multiple dispensing printing method were printed to produce conducting line of rGO on slanted surfaces on flat, 10, 8, 6, and 4 mm PET film length in Figure 24. GO solution was 5 g/L concentration and center to center of droplets was 0.08 mm. 10 mm film length was defined as a slanted span which measured from the top of 1 mm substrate to bottom substrate the same as in 8, 6, and 4 mm slanted film.

Quality of printed GO solution at 10 mm slanted film produced the same of flat substrate. After reduction, it also sustained straight line of conducting material. However, in 8 mm slanted film, droplets started to coalesce into next droplets. Furthermore, in 6 mm and 4 mm slanted film, droplets were completely coalesced.

To check a gradient degree, samples were calculated by known length. 10, 8, 6 and 4 mm slanted film estimated approximately 5.7°, 7.1°, 9.6° and 14.4°, respectively. In the above test, printing of GO solution was feasible on 7.1° tilted angle substrate. In 5 g/L concentration GO, disconnection percentage get higher when slanted surface degree increased due to coalescence rate. Another low concentration GO solution was tested for disconnection rate. The test condition was the same as 5 g/L concentration GO solution except concentration. In 2.5 g/L concentration GO, line patterning failed because absolute GO amount was lack after GO solution was dried.

Figure 25 shows only 5.7° and 7.1° slanted surface has the same quality of flat surface printing with 5 g/L concentration GO solution. Every slanted angle had 8 sample lines with 30 dots of GO solution. Every sample was measured by resistance via Keithley 2400 meter. In 5.7° and 7.1° slanted surface, resistance of rGO printed line had under 1 M ohm, which showed conducting line was patterned. In the other hands, resistance was rapidly increased over 9.6° slanted surface. One of mis-aligned GO printing conclude a disconnection of electrode line. Resistance of disconnection was overflow range in measurement meter. In 2.5 g/L concentration, all slanted surface fail to produce an electrode line because absolute amount of GO was lack to connect each other.

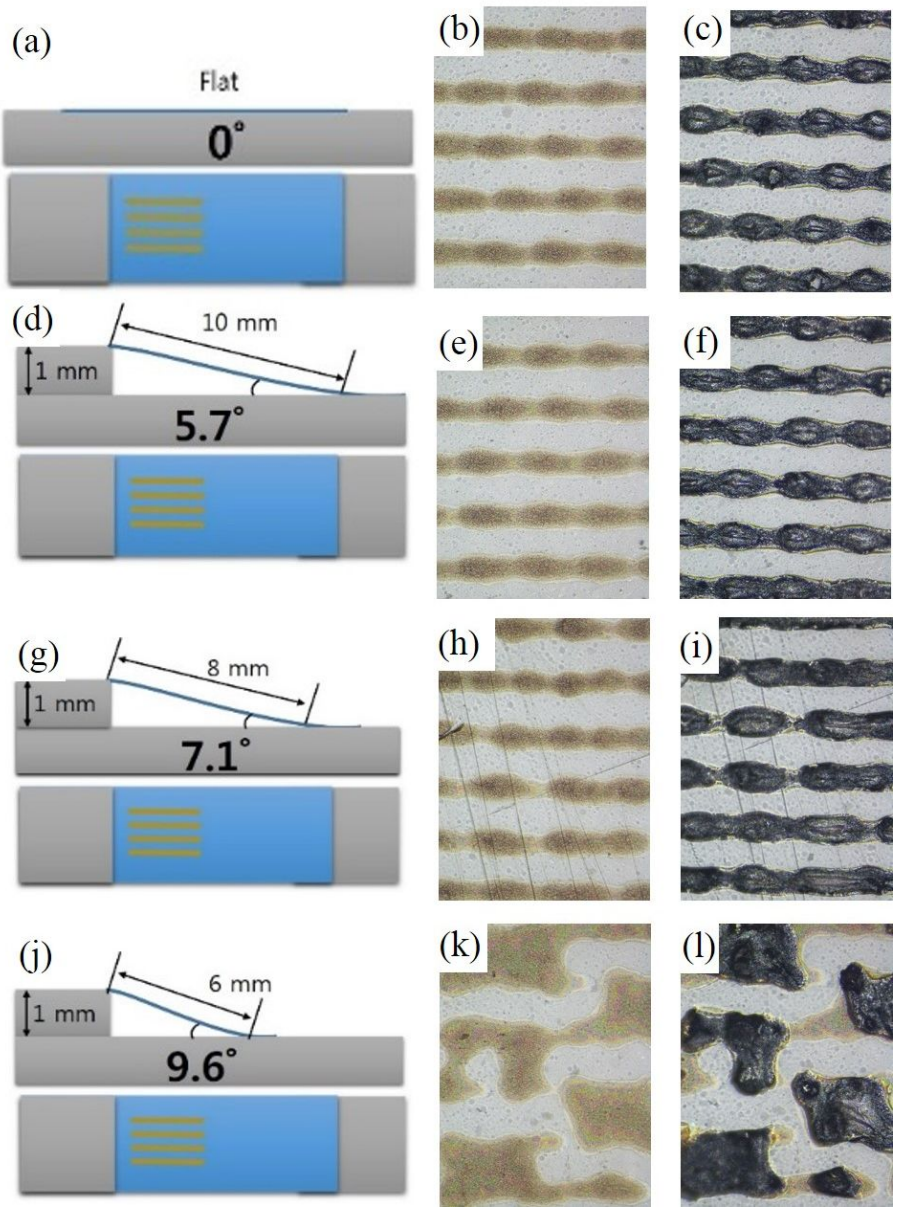

Figure 24 Conducting line on slanted surface. Flat substrate of (a) cross-sectional view, (b) GO, and (c) rGO. 10 mm slanted substrate of (d) cross-sectional view, (e) GO, and (f) rGO. 8 mm slanted substrate of (g) cross-sectional view, (h) GO, and (i) rGO. 6 mm slanted surface

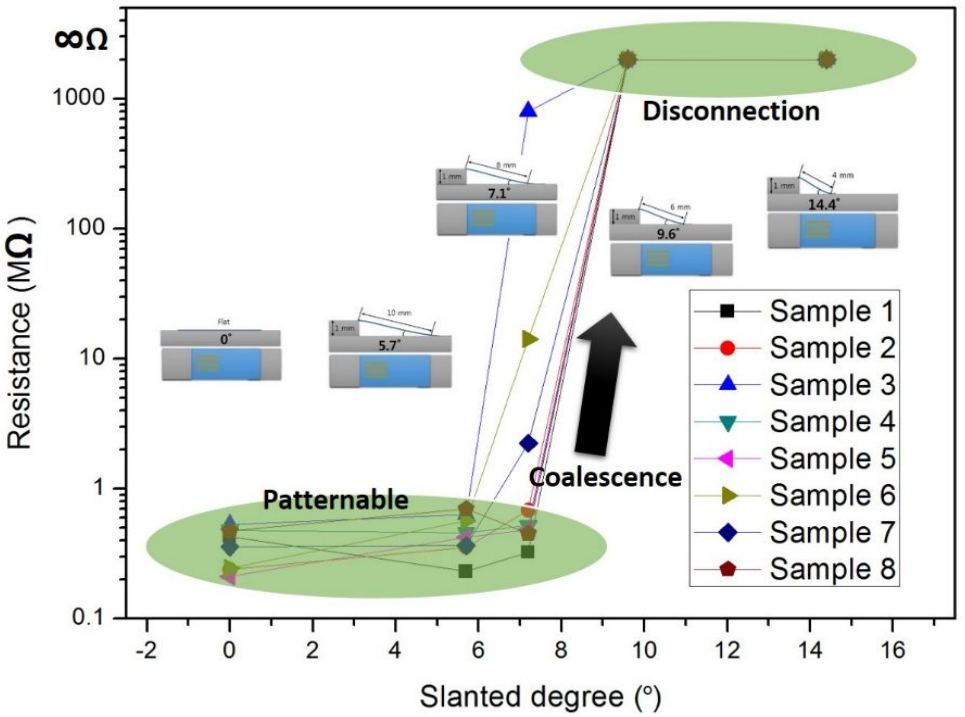

Figure 25. Resistance of 5 g/L concentration GO on slanted surface

3.3 Liquid dispenser device

A liquid dispenser (sciFLEXARRAYER DW, Scienion, Germany) originally designed for bio applications was a dedicated tool for highly precise deposition of picoliter or nanoliter amount via a piezo dispensing nozzle in Figure 26. A user could program to continuously eject 300 pL a GO suspension (5 g/L, HC-Graphene oxide aqueous solution, Graphene supermarket, USA) at every designated spot on a flexible substrate to produce a high resolution interdigitated pattern.

Due primarily to a hydrophilic property of GO particles, GO was completely dispersed in deionized water and used as an ink.[11, 12] Electrodes of a supercapacitor were printed via a liquid dispenser as we designed an interdigitated pattern. After a printed GO solution was dried up, only remained GO particles via a photo-thermal flash could reduce into printed-reduced graphite oxide (PRGO).[13, 14] Conducting PRGO lines which had hundreds-of-micrometer width and tens-of-micrometer thickness could be formed under 10 times 300 pL droplet condition. Droplets were easily merged to an adjacent droplet when next droplet was printed without a GO solution drying on PET film.

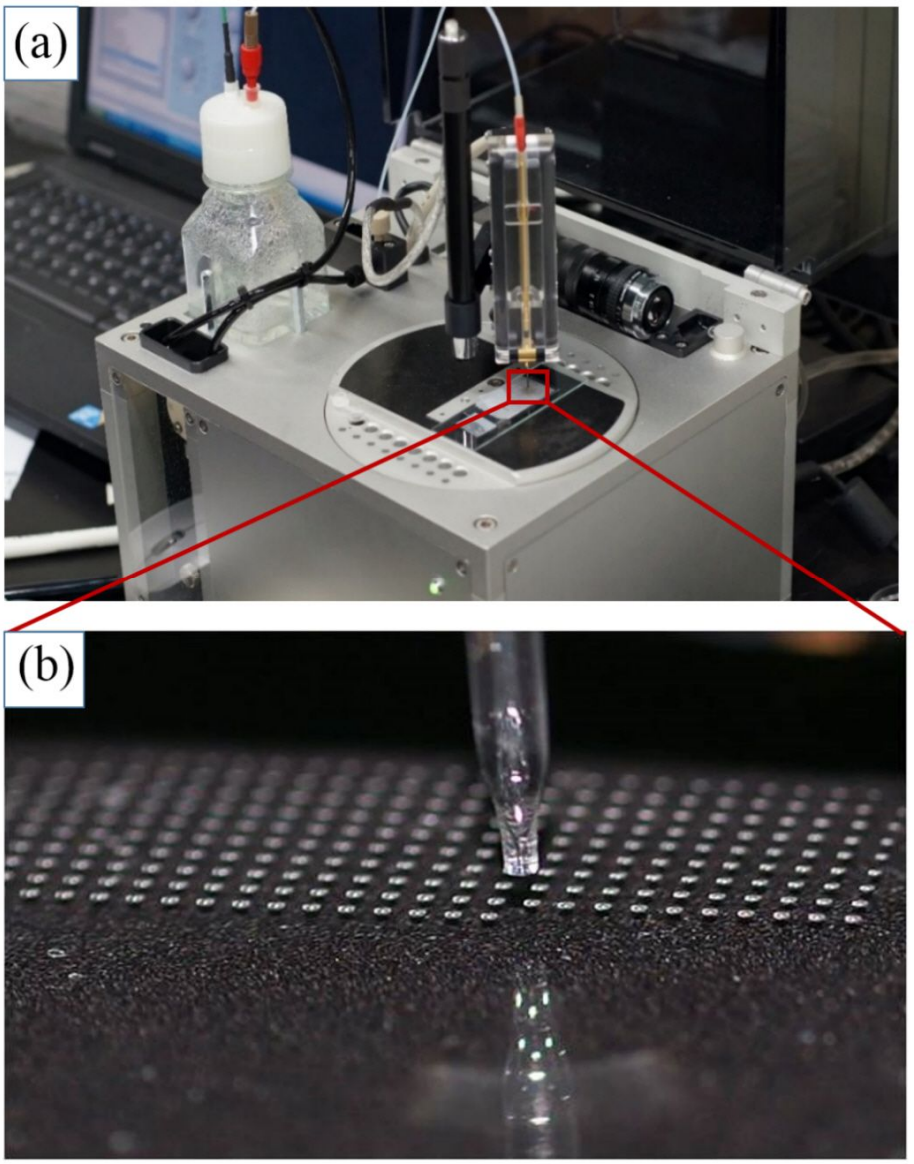

Figure 26. (a) A liquid dispenser with programmable software (b) Micro liter droplets by a piezo nozzle [http://microaqua.eu/sites/default/files/styles/ partners_img/public/partners_img]

3.4 Substrate material selection

Substrate material selection was a vital process leading to effective a GO reduction and good adhesion of rGO electrode for flexible supercapacitors. Several potential substrate materials were chosen such as transparent glass, transparent polyethylene terephthalate (PET) film, white copy paper, polydimethylsiloxane (PDMS), and CYTOP (CTL-809A, Asahi Glass, Japan) shown in Table 2.[15, 16] Potential substrate materials were selected by criteria of flexibility, transparency, and possibility of bio compatible.

Transparent materials were placed on a piece of white paper prior to being flashed to rule out flash light reflection effect. A GO droplet formed a wide range of a contact angle (30° ~ 110°) on a surface of different materials due to a distinctive degree of hydrophobicity of material.

A contact angle was measured with using a contact angle goniometer. A contact angle was finally determined by an optical subsystem to capture a profile of a droplet on substrate material. A measurement system had a high resolution camera and software to capture and analyze a contact angle of a GO droplet on different substrates in Table 2. Accuracy of a contact angle was determined by a quality of image from camera.

The contact angle of GO on the material surface was an essential feature that had an effect on a GO reduction and an adhesion of rGO on a substrate material after a photo-thermal flash reduction. A photo-thermal reduction took an effect on rapid

volume expansion of GO material, especially vertical direction. Volume change affected that a GO material deposited on a substrate with a larger contact angle showed higher an oxygen-functional group removing reduction compared to those with a smaller contact angle such as a glass substrate verified by a color change, Raman spectroscopy measurement, and XPS measurement in chapter 2.3.2.

Adhesive behavior of rGO was also associated with a contact area between rGO and a substrate surface, which was vital to prevent delamination of rGO. A contact angle of a GO droplet on a substrate surface had an inversely proportional relationship with a GO-surface contact area. A GO droplet that formed a large surface contact angle, for instance, 110° on a CYTOP substrate was prone to delamination after a photo-thermal flash irradiation. Some parts of an rGO spot were partially detached and removed from PDMS and CYTOP surfaces because poor adhesion between rGO and a substrate.

As a consequence, considering a delamination problem, a substrate material should be under a 90° to prevent rGO materials from removing. A substrate material that supported a GO material with a moderate surface contact angle, approximately 80° as shown by PET film was considered the most suitable for a high resolution printing.

Table 4. A contact angle on different materials[17]

Materials	Droplet	Contact angle
Glass	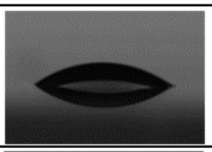	30°
PET Film	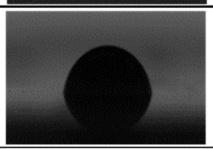	80°
Paper	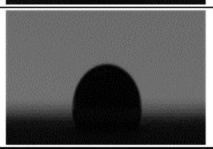	90°
PDMS	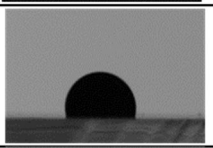	100°
CYTOP	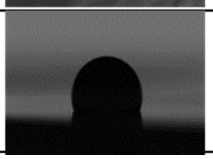	110°

3.4.1 Reduction characteristic on different substrates

There were several rGO characteristics of a photo-thermal light energy reduction of a xenon camera flash on different substrates. 10 nL GO droplets with 5 g/L concentration were dispensed on different materials such as glass slide, PET film, copy paper, PDMS, and CYTOP.

The rGO reduced from GO showed a color change from brown to black except glass substrate in Figure 27, also verified by Raman spectroscopy and XPS measurement. Some spots remained unchanged color when local light energy delivered. No color change was because photo-thermal energy was below threshold light energy to cause a reduction which oxygen-functional groups was not changed and verified by Raman spectroscopy and XPS measurement. On all substrates except for the transparent glass, all GO spots were completely photo-thermally reduced.

Owing to different hydrophobicity of the substrate material, GO droplets formed specific contact angles on the surface, ranging from 30° to 110°. GO droplets spread widely on the glass slide with a small contact angle. On the other hand, GO droplets maintained high contact angles with hydrophobic substrates such as PDMS and CYTOP. Photo-thermal flash reduction of GO did not take place on the glass slide while an effective reduction occurred on the other materials.

However, some rGO spots were detached and removed from PDMS and CYTOP surfaces which had high contact angle of 100° and 110°, respectively because of

poor adhesion after a reduction. A GO material regardless of underlying substrate material can be photo-thermally reduced, except GO material deposited on a glass slide. Particularly, GO reduction hardly took place on glass slide where GO droplet flattens to the largest extent due to hydrophilic attraction.

Materials	Before reduction	After reduction
Glass	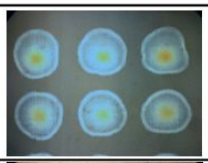	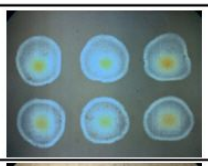
PET Film	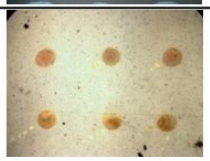	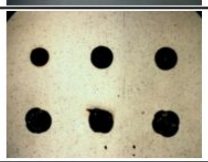
Paper	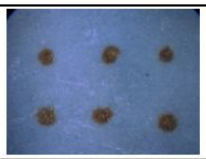	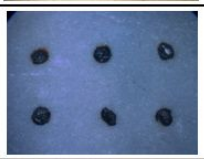
PDMS	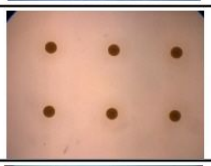	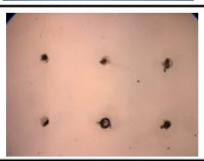
CYTOP	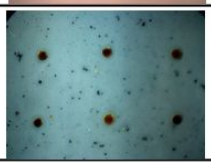	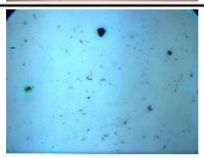

Figure 27. Before and after a reduction on different materials[17]

3.4.2 Resolution by contact surface area

We could estimate a printed line resolution from a contact angle of a GO solution. Figure 28 shows diagram for a geometrical configuration of a GO droplet on a substrate. When droplet volume was known on a specific substrate, printed line width could be calculated by an equation (3.1). Surface area of a GO droplet was gained from an equation (3.2).

$$V = \frac{\pi R^3}{3}(1-\cos\theta)^2(2+\cos\theta) \tag{3.1}$$

$$S_{LS} = \pi R^2 \sin^2\theta \tag{3.2}$$

And

$$R = \sqrt[3]{\frac{3V}{\pi(2+\cos\theta)(1-\cos\theta)^2}} \tag{3.3}$$

where S_{LS} is the contacting area between the liquid and the surface, R is the radius of the GO sphere that the liquid surface form, and θ is the contact angle. R is the function of a contact angle and volume of a liquid drop. The general formula for R and r of contact circle radius is as following,

$$\cos(90° - \theta) = \frac{r}{R} \tag{3.4}$$

$$r = R \sin \theta \tag{3.5}$$

And

$$r = \sqrt[3]{\frac{3V}{\pi(2+\cos\theta)(1-\cos\theta)^2}} \sin\theta \tag{3.6}$$

where r is projected radius of half width of GO electrode line. An equation (3.5) is induced in Figure 28 and put an equation (3.3) to an equation (3.5). r is expressed by a contact angle in an equation (3.6). Using an equation (3.6), we can finally express relation between r and θ.

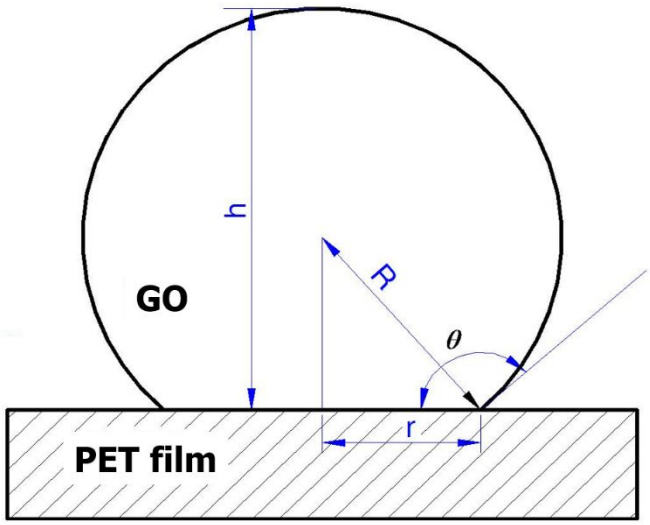

Figure 28. A contact angle between a droplet and PET film and projected radius of a GO droplet

Figure 29 shows a relationship between a contact angle and width of patterning line. A blue line was drawn by a calculation of a contact angle and projected radius. For example, we could expect 280 μm radius of a droplet, total 560 μm width line in the glass substrate and 190 μm radius of a droplet, total 280 μm width line in a CYTOP substrate when total droplets volume was 10 nL amount of GO solution.

However, dried GO radius of glass, PET, paper, PDMS and CYTOP substrates was practically measured 271 μm, 154 μm, 121 μm, 98 μm and 67 μm, respectively in Figure 30 when we measured dried GO droplets radius directly through micro scope pictures. While the gap of calculation and measurement was 11 μm difference on glass substrate, 123 μm gap was observed on a CYTOP substrate. The difference of calculation and measurement was increased with growth of a contact angle, e.g. CYTOP substrate difference of calculation and measurement was the biggest of other substrates. The difference was because GO solution of a high contact angle was shrank during evaporation of deionized water.

Therefore, we could estimate a printed electrode resolution by a total amount of a GO solution and a substrate material. But, we could not obtain exact resolution value because a GO droplet was shrank during evaporation. An additional condition was needed to exact calculation like temperature and humidity.

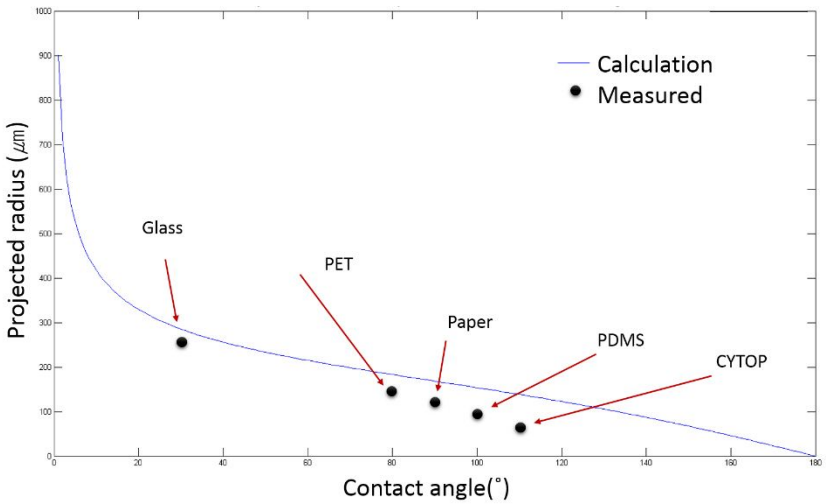

Figure 29. Calculation and measurement of a contact angle and projected radius of a GO droplet

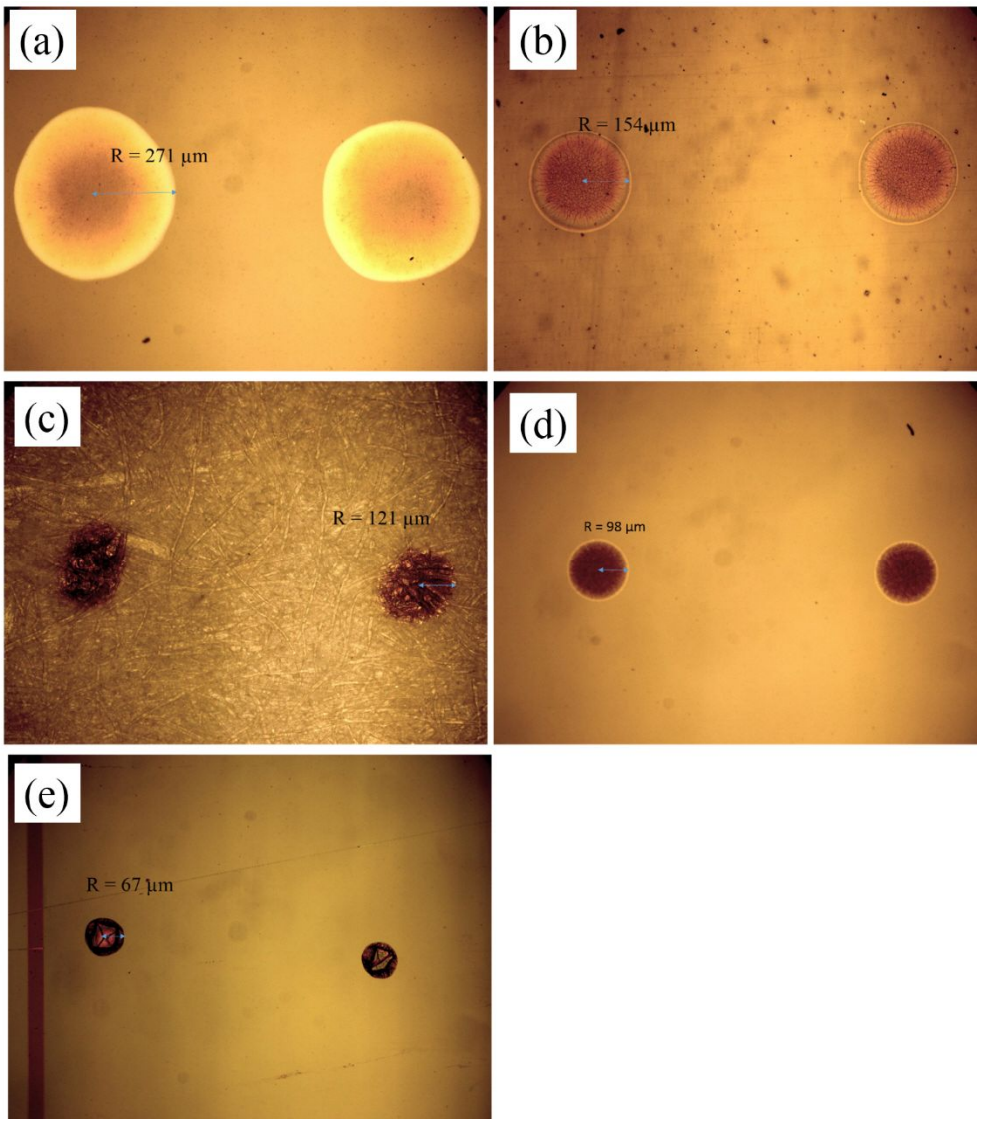

Figure 30. Droplets diameter on glass, PET, paper, PDMS, and CYTOP

3.5 Adjustment of GO quantity

There needed to adjust GO amount to produce rGO electrodes. In previous chapter, substrate material selection was one of the main factors to produce rGO electrodes line. In a reduction test, a certain amount of GO was needed to start flash reduction. On the other hand, when a GO amount was increased too much, it met reduction depth and electrode resolution problem.

A moderate amount of GO solution was changed via printing methods of a liquid dispenser. Although an increase of a GO amount developed a performance of a supercapacitor, a high flash reduction needed to reduce increased a GO amount could destroy an electrode structure of a supercapacitor. That was because an increased GO amount was needed more light energy. However, a multiple dispensing printing method could decrease photo-thermal light energy without increasing a GO amount.

3.5.1 Multiple dispensing printing method

When a liquid dispenser ejected GO droplets, a particular printing method was used as a multiple dispensing produced by ten times of a multiple 0.3 nL droplet with drying between each droplet dispensing shown in Figure 31. There needed to be a multiple dispensing printing method to produce rGO electrodes with high resolution and enough porosity, in addition to preventing coalescence of GO droplet. A multiple dispensing printing method was a process which had a drying process before a next droplet was dispensed. A drying process of GO prevent droplets from spreading undesirable direction.

When we produced a patterning field, which was one layer of every droplet, every field was printed after previous field was fully dried up. One field was composed of 300 pL droplet in each location. In a view of one designated spot, every 300 pL was printed via a multiple dispensing printing method.

A multiple dispensing printing method made 300 pL droplet fields which was dried up in a second before next field was printed. Furthermore, an overlapping of droplets at their outer radius with one another was the main key to ensure lines of a pattern were well-defined and continuous.

However, a distance between the centers of two droplets should have been maintained at minimum distance to prevent coalescence of small droplets into a large droplet. Minimum gap was 240 μm (80% of 300 μm) limited by a liquid dispenser specification in order to produce a desired pattern.

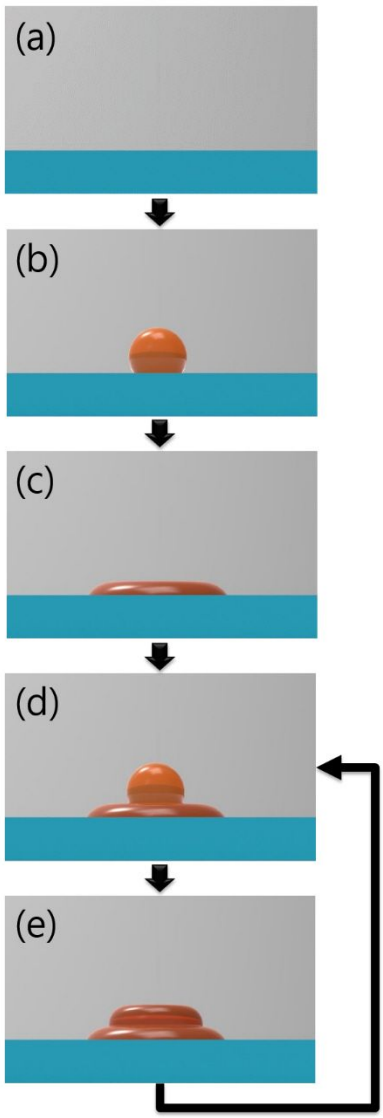

Figure 31. A multiple dispensing sequence. (a) Substrate material preparation (b) A first droplet (c) Evaporation of deionized water and remained GO (d) Second droplet on dried GO (e) A dried GO solution stacked on GO.

3.5.2 Comparison of a multiple and single dispensing

A total amount of printed GO was determined by a number of droplet dispensing. For example, one time dispensing droplet amount was 300 pL in a liquid dispenser. Two times dispensing was 600 pL. A total amount of GO solution was a multiple number of 300 pL because minimum droplet volume was determined by a liquid dispenser specification. Actually, a piezo nozzle in a liquid dispenser limited a minimum solution amount. Therefore, ten times dispensing was 3000 pL, i.e., a 3 nL GO solution.

In this chapter, we compared a droplet characteristic by different dispensing methods of a multiple and a single dispensing in the same total amount of a GO solution. A single dispensing printing method was one time dispensing of whole amount of a GO solution in Figure 32.

A multiple dispensing printing method was referred to a procedure which one 0.3 nL GO droplet was deposited on the formerly ejected one that had already dried to create a multilayer structure at every spot. A pair of well-defined interdigitated patterns, consisted of straight lines were produced by overlapping of 0.3 nL droplets at their outer radius with one another. One GO droplet stacked on another to minimize contact area with a material surface to prevent spreading of a droplet on a substrate surface. Contact area minimization and stacking configuration led to a high resolution pattern equipped with sufficient porosity.

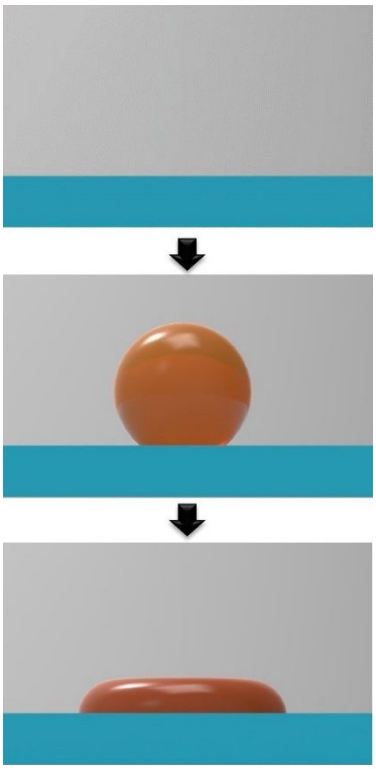

Figure 32. A single dispensing sequence

A distance between the centers of two droplets should be maintained at 100 μm to prevent coalescence of small droplets in order to produce a desired pattern. In our experiment, a GO pattern was made by depositing ten droplets of a 0.3 nL GO solution in the same manner. Although adjacent droplets overlapped with one another, droplets could still sustain their shape because they were so small that they would not collapse.

However, in a single dispensing printing process, 3 nL droplets were easily merged to adjacent droplets when a droplet was printed at the next spot. Even though both single dispensing and multiple dispensing printing methods used the same amount of a GO solution and substrate materials, a single dispensing printing method could not produce a line due to coalescence of GO droplets.

In a multiple dispensing, the diameter of dried GO was 92 μm. Meanwhile, in a single dispensing, the diameter of dried GO was 230 μm with 3 nL total GO amount shown in Figure 33. A difference was over two times more. A gap of diameter difference was because a dispensed GO was stacked by every droplet in a multiple dispensing printing method. A minimum dispensing was the smallest amount of a GO droplet to occur a photo-thermal reduction in specific light energy of a camera flash. For example, in high photo-thermal energy of a 1.50 J/cm^2 xenon flash, GO droplets of ten multiple dispensing started restoration of sp^2 hybridized C-C bonds, while GO droplets of two multiple dispensing did not start recombination of carbon bonding. More light was needed to reduce two multiple dispensed droplets.

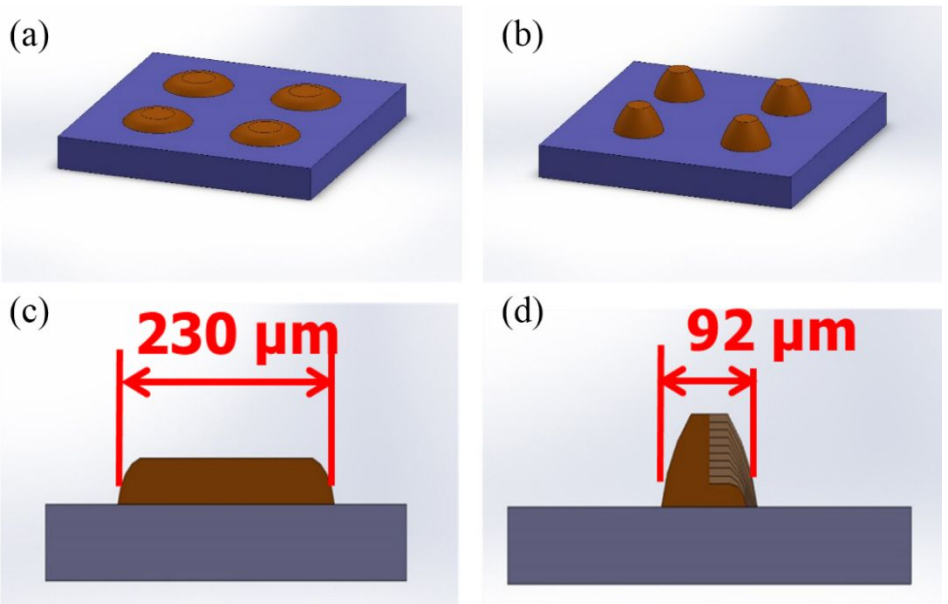

Figure 33. (a) A single dispensing (b) A multiple dispensing (c) Side view of single dispensing (e) Side view of multiple dispensing

After photo-thermal light energy was decreased to 0.79 J/cm^2, Go amount did not affect the minimum light energy to start removing oxygen functional groups of GO. At 6.36 J/cm^2 light energy, 15 times multiple dispensing was also reduced. In this condition, ten multiple dispensing was the minimum dispensing and the best choice for performance of a supercapacitor.

Figure 34(a) ~ (b) compares the two cases, i.e., a multiple dispensing of 10 times and a single dispensing with the same target volume. While the line pattern with a multiple dispensing showed that spacing of 80 μm can be readily achieved, the line pattern failed with the single dispensing of the whole volume. A merger of big droplets resulted in disconnection and loss of spacing between lines.

Figure 34(c) ~ (e) compare a multiple dispensing of 300 pL ten times on different materials of glass, PET, and PDMS. Glass and PDMS substrate had coalescence of droplets. Adjacent two GO droplets were combined and moved to another position. Subsequently, coalescence caused disconnection of GO electrode line. Although GO droplets sustained their designed position on paper substrate, paper absorbed the water of GO droplets and disconnection sometimes happened. Therefore, though a multiple dispensing printing method was adapted in glass, paper and PDMS substrate, printing of GO droplets on PET substrate made the best result for pattern of electrodes.

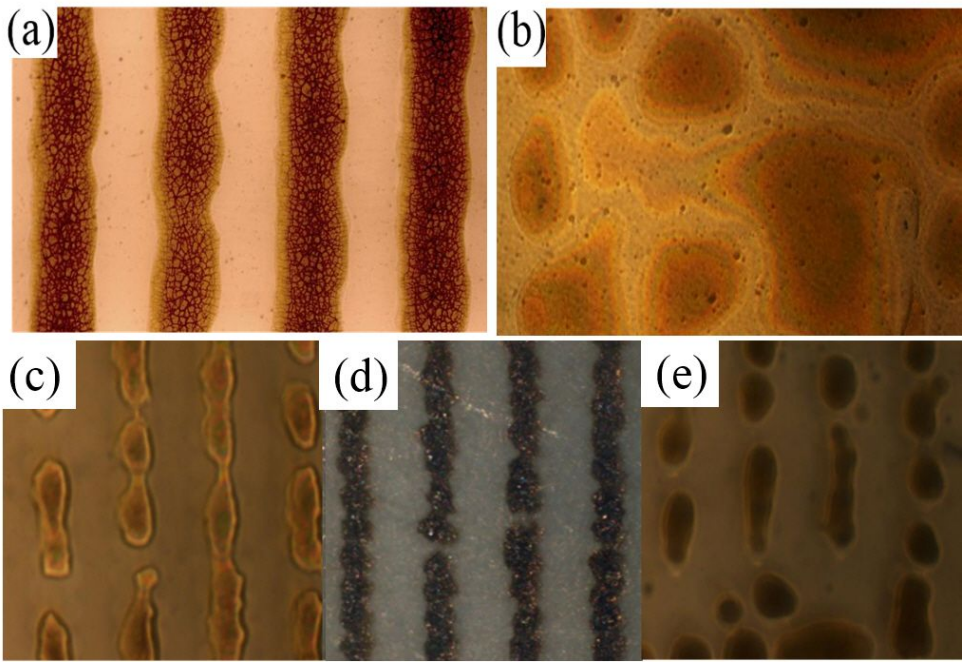

Figure 34. A multiple dispensing of 10 times and a single dispensing with the same target volume (a) A multiple dispensing on PET film[17] (b) A single dispensing on PET film[17] (c) A multiple dispensing on glass slide substrate (d) A multiple dispensing on paper substrate (e) A multiple dispensing on PDMS substrate

3.5.3 Reduction of a dispensed patterns

High photo-thermal light energy irradiation could destroy the rGO structure due to rapid degassing during a reduction process. Therefore, a low photo-thermal light energy irradiation was needed in a photo-thermal reduction process for sustaining a patterned structure.

Patterns produced by both a single dispensing printing method and a multiple dispensing printing method were exposed to the same magnitude of a flash irradiation simultaneously in Figure 35. There was 25 dots of 5 g/L concentration GO solution. GO droplet of multiple dispensing showed the dark color which stacked GO compared to that of single dispensing printing method. A GO pattern obtained by 10 times multiple dispensing printing method was reduced whereas that patterned by a single dispensing printing method was not reduced into rGO in photo-thermal energy of a 1.50 J/cm^2 xenon flash light source.

Compared to a single dispensing printing method, a multiple dispensing printing method could produce GO pattern with high thickness in previous chapter. Furthermore, in a multiple dispensing printing method, one GO droplet stacked on another to minimize contact area with a material surface so as to prevent spreading of a droplet on a substrate surface. Therefore, it resulted in thinner lines and better resolution patterns.

After printing of GO patterns, a xenon flash emitting device was used as a convenient tool to convert a dried insulating GO pattern to electrically conducting

PRGO electrodes. Flash light energy intensity and irradiation distance were adjusted at 1.50 J/cm^2 and 4 cm to meet an optimal condition so as to ensure fine integrity of an rGO structure as PRGO could be disintegrated due to excessive volume expansion by receiving high photo-thermal energy.

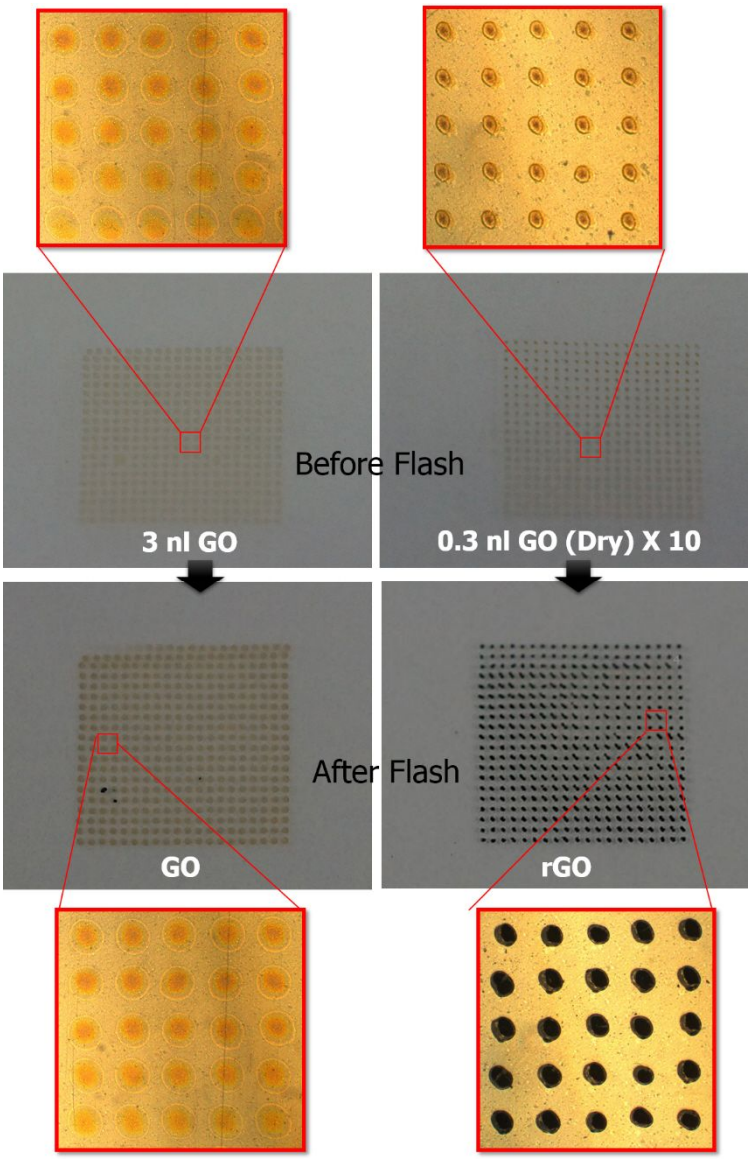

Figure 35. Before and after a flash reduction of a single dispensitng and a multiple dispensitng

3.6 Results and discussions

To produce high resolution patterning, there needed to be a specific combination of a substrate material, a particular printing method, and a particular amount of GO solution for a useful charge storage.

A substrate material was selected by analysis of a contact angle and rGO condition. A PET film substrate had moderate a contact angle and flash reduction effect compared to glass, paper, PDMS, and CYTOP. A particular printing method was tested for high resolution and flash reduction of GO electrodes. A multiple dispensing printing method produced fine straight electrode without coalescence. A minimum dispensing was determined by total GO amount with threshold value of photo-thermal light energy.

A high performance supercapacitor was produced from combining substrate material selection, a multiple dispensing printing method and adjusted minimum dispensing all together.

3.7 Bibliography

[1]. Kong, D., L.T. Le, Y. Li, J.L. Zunino, et al., "Temperature-Dependent Electrical Properties of Graphene Inkjet-Printed on Flexible Materials" *Langmuir*, Vol. 28, No. 37, pp. 13467-13472, 2012.

[2]. Luechinger, N.A., E.K. Athanassiou, and W.J. Stark, "Graphene-stabilized copper nanoparticles as an air-stable substitute for silver and gold in low-cost ink-jet printable electronics" *Nanotechnology*, Vol. 19, No. 44, 2008.

[3]. Leigh, S.J., R.J. Bradley, C.P. Purssell, D.R. Billson, et al., "A Simple, Low-Cost Conductive Composite Material for 3D Printing of Electronic Sensors" *Plos One*, Vol. 7, No. 11, 2012.

[4]. Kaempgen, M., C.K. Chan, J. Ma, Y. Cui, et al., "Printable Thin Film Supercapacitors Using Single-Walled Carbon Nanotubes" *Nano Letters*, Vol. 9, No. 5, pp. 1872-1876, 2009.

[5]. Cote, L.J., R. Cruz-Silva, and J. Huang, "Flash reduction and patterning of graphite oxide and its polymer composite" *J. AM. CHEM. SOC*, Vol. 131, No., pp. 7, 2009.

[6]. El-Kady, M.F., V. Strong, S. Dubin, and R.B. Kaner, "Laser scribing of high-performance and flexible graphene-based electrochemical capacitors" *Science*, Vol. 335, No. 6074, pp. 1326-1330, 2012.

[7]. Pech, D., M. Brunet, H. Durou, P. Huang, et al., "Ultrahigh-power micrometre-sized supercapacitors based on onion-like carbon" *Nat Nanotechnol*, Vol. 5, No. 9, pp. 651-4, 2010.

[8]. ; Available from: http://quique123.wordpress.com/2014/02/18/google-glass-pros-cons/.

[9]. *iWatch*. Available from: http://readwrite.com/2014/04/14/google-glass-buy#awesm=~oELLooumgOsleh.

[10]. *Google glass concept*. Available from: http://www.graphenebiz.com/.

[11]. Li, D., M.B. Muller, S. Gilje, R.B. Kaner, et al., "Processable aqueous dispersions of graphene nanosheets" *Nature Nanotechnology*, Vol. 3, No. 2, pp. 101-105, 2008.

[12]. Park, S., J.H. An, I.W. Jung, R.D. Piner, et al., "Colloidal Suspensions of Highly Reduced Graphene Oxide in a Wide Variety of Organic Solvents" *Nano Letters*, Vol. 9, No. 4, pp. 1593-1597, 2009.

[13]. Abdelsayed, V., S. Moussa, H.M. Hassan, H.S. Aluri, et al., "Photothermal Deoxygenation of Graphite Oxide with Laser Excitation in Solution and Graphene-Aided Increase in Water Temperature" *Journal of Physical Chemistry Letters*, Vol. 1, No. 19, pp. 2804-2809, 2010.

[14]. Watcharotone, S., D.A. Dikin, S. Stankovich, R. Piner, et al., "Graphene-silica composite thin films as transparent conductors" *Nano Letters*, Vol. 7, No. 7, pp. 1888-1892, 2007.

[15]. Hu, L.B., J.W. Choi, Y. Yang, S. Jeong, et al., "Highly conductive paper for energy-storage devices" *Proceedings of the National Academy of Sciences of the United States of America*, Vol. 106, No. 51, pp. 21490-21494, 2009.

[16]. Yan, C., K.S. Kim, S.K. Lee, S.H. Bae, et al., "Mechanical and Environmental Stability of Polymer Thin-Film-Coated Graphene" *Acs Nano*, Vol. 6, No. 3, pp. 2096-2103, 2012.

[17]. Jung, H., C.V. Cheah, N. Jeong, and J. Lee, "Direct printing and reduction of graphite oxide for flexible supercapacitors" *Applied Physics Letters*, Vol. 105, No., 2014. [http://dx.doi.org/10.1063/1.4890840].

4 Supercapacitor fabrication

4.1 Fabrication process

A patterning process of rGO interdigitated electrodes on a flexible substrate through a direct printing was illustrated in Figure 36. A liquid dispenser was programmed to continuously eject 300 pL GO suspension at every designated spot on a flexible substrate to produce a high resolution interdigitated pattern.

Thickness of GO pattern could be precisely controlled by means of a direct printing because a structure of GO pattern was stacked up like a thin layer. A pair of 4-interdigitated patterns was precisely produced by a direct printing of GO in this manner on a thin PET film with dimensions of 1.750 mm × 1.890 mm which included spacing between interdigitated fingers.

Due to hydrophilic nature of GO, it was soluble in water, allowed us to use it as ink.[1] Then, we used an equipment to perform a patterning of GO on a PET film substrate. The beauty of our approach was that we could literally print a GO material on any substrate we want. After the patterning, we carried out the reduction process to recover electrical conductivity of the material. Lastly, we proceeded to a packaging of a device with Kapton® tape.[2]

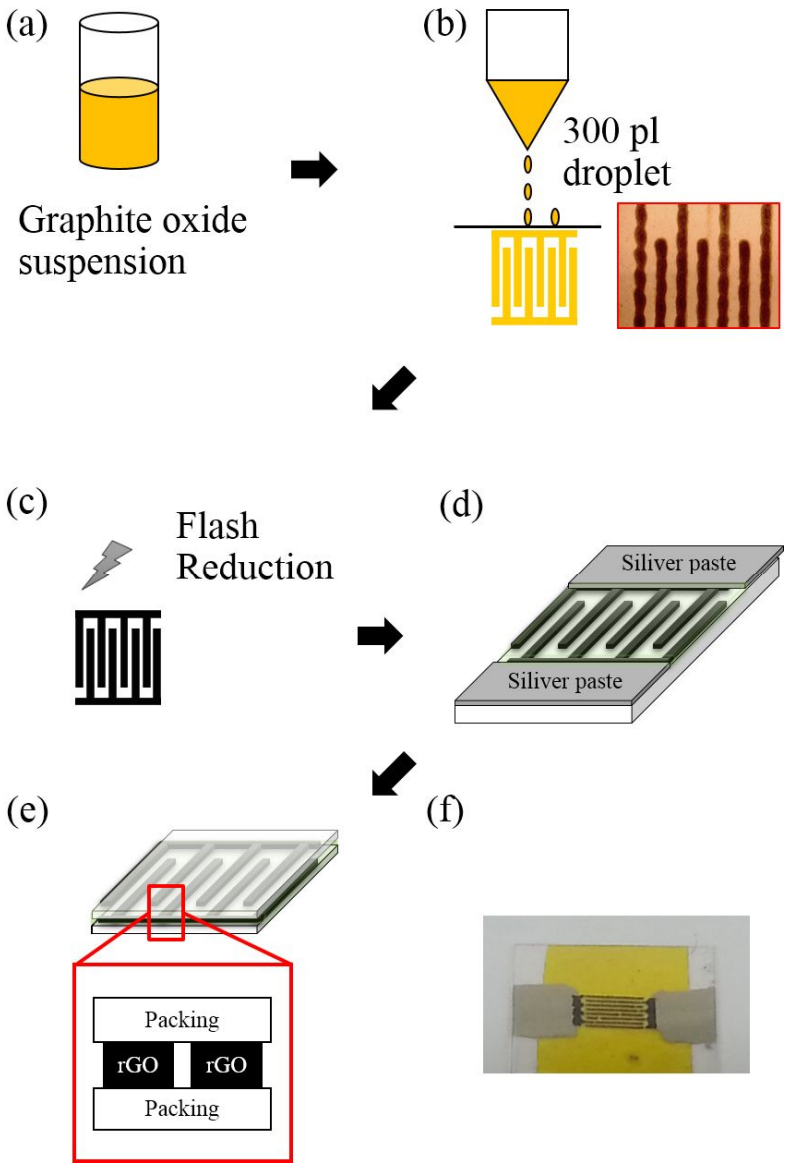

Figure 36. A fabrication process of a supercapacitor[3] (a) GO solution preparation (b) direct printing of GO with 300 pl injection (c) a xenon flash reduction (d) paste for connection to output (e) Package with PET film (f) Covered with Kapton tape

4.2 Layout of dispensing

A liquid dispenser produced 22 by 40 dots pattern in Figure 37. A electrode was used by 22 x 22 dots as active area. Both sides of 9 dots was used for connection of carbon paste. Several dots which is adjacent active area were covered by covering tape, so a liquid electrolyte could not contact rGO pattern used for connection.

First, gap of 22 dots pattern had 100 μm spacing. To increase density of a supercapacitor electrode, a pattern was diminished by horizontal 80% and vertical 90%. Total horizontal length was 22 dots x 100 μm x 80% = 1760 μm. Total vertical length was 22 dots x 100 μm x 90% = 1980 μm. However, dimensions of 1750 μm × 1890 μm was measured practically due to liquid dispenser error.[4]

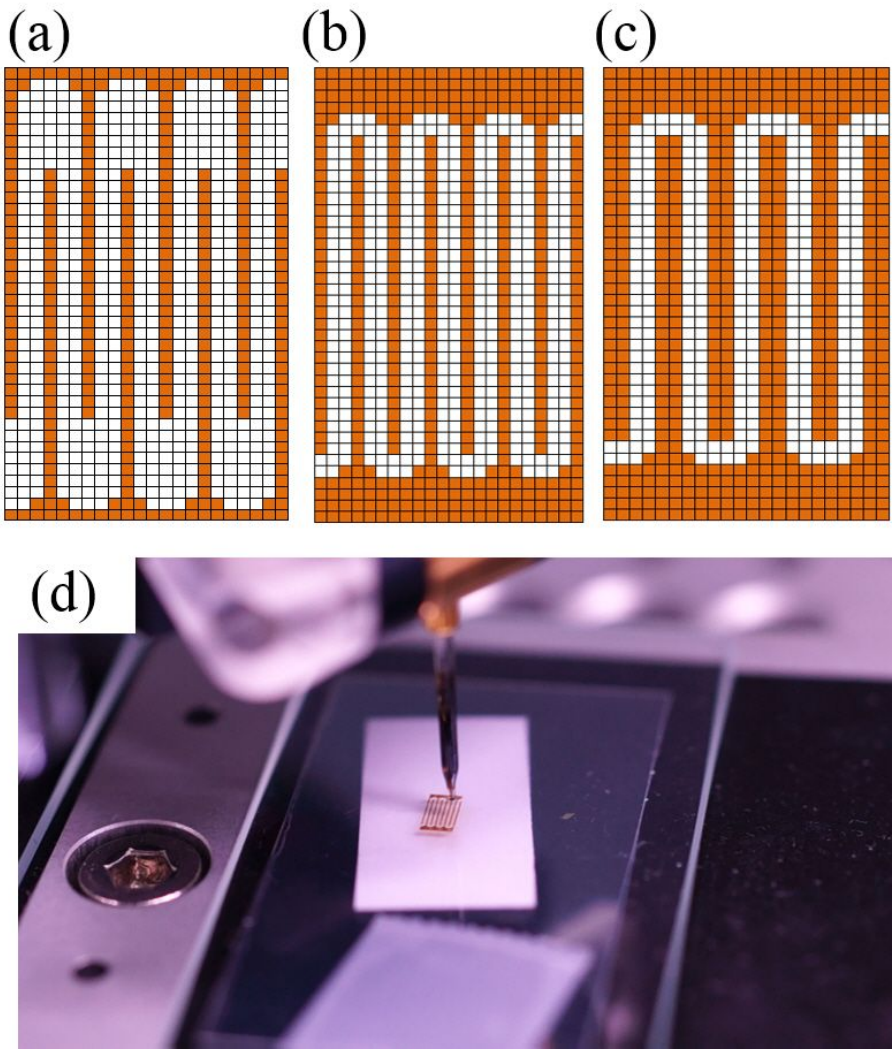

Figure 37. (a) Modified 8 interdigitated electrode (b) 8 interdigitated electrode and (c) 6 interdigitated electrode (d) Printed 8 interdigitated electrode on PET

film

We demonstrated fabrication process in previous chapter. During producing a process of a supercapacitor, defect of electrodes happened all the times. A patterned GO solution could had disconnection in an electrode and connection between electrodes. Even though patterned GO was succeed in printing, rGO could have disconnection and connection by a flash reduction. Sometime, some part of GO electrode was not reduced fully so that performance of a supercapacitor ran short of other one.

In Figure 38, it shows before and after a reduction of GO electrode. Especially, Figures were taken in the same brightness for accurate description. Before a reduction of GO, magnified GO had crack arbitrary lines and almost transparent.

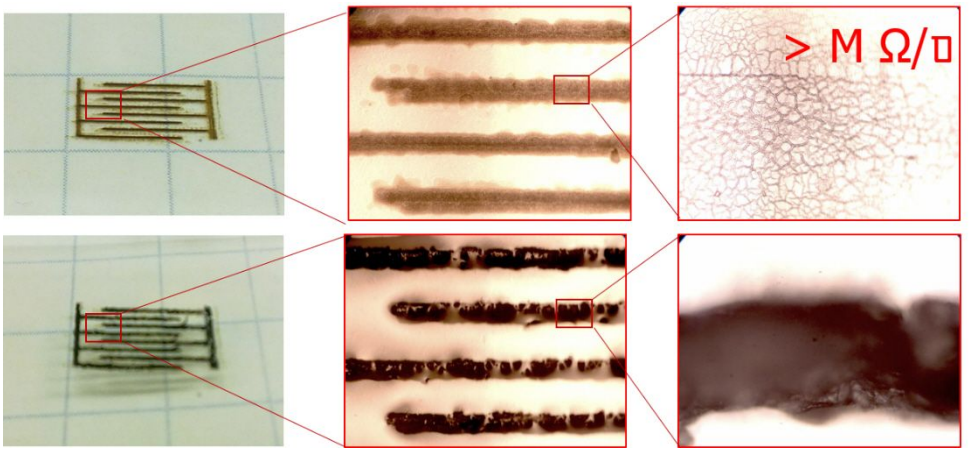

Figure 38. A flash reduction on the same brightness

We demonstrated fabrication process. A GO electrode was connected by carbon paste (CANS, ELCOAT, Resistivity 10^{-4} Ω·cm). Carbon paste was thinly coated to prevent electrolyte leakage. carbon paste should also decrease a contact resistance between GO electrodes and connector to a system (Figure 39).[5]

Normally, a resistance was dominant at a contact resistance between a current collector and an electrode.[6] After patterning an electrode and putting a liquid electrolyte, the same PET film was symmetrically covered upside. Kapton® tape was used for sealing for electrolyte leakage and supported a structure (Figure 40). 3M transparent thin adhesive tape could be used for alternatives of Kapton® tape.[7] Kapton® tape was a polyimide film developed by DuPont that remains stable across a wide range of temperatures.

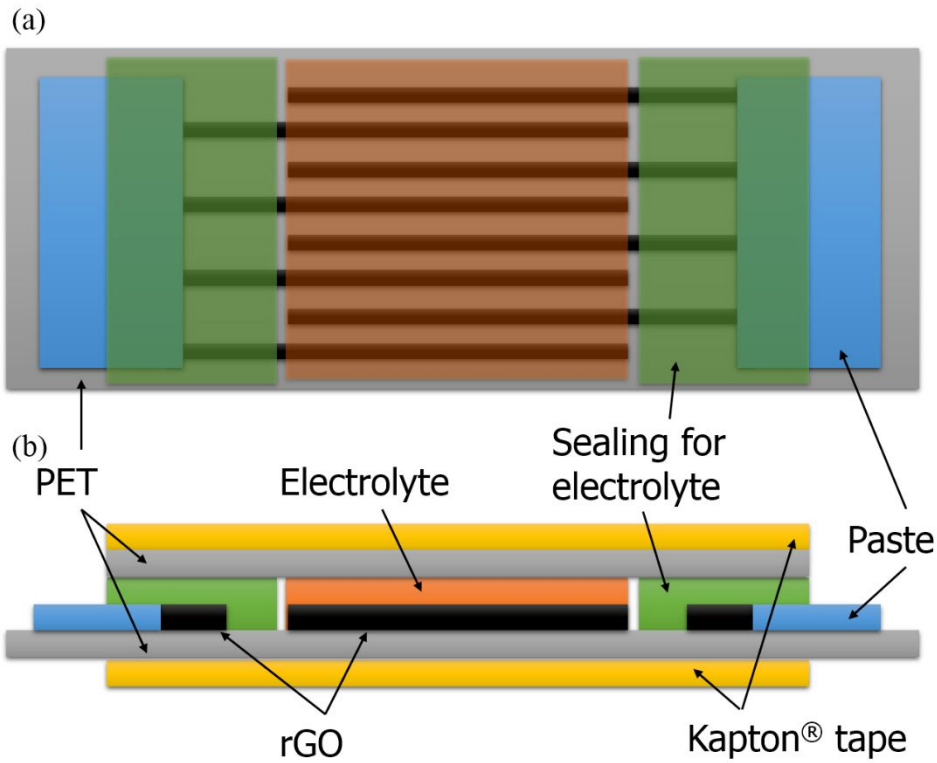

Figure 39. (a) Top view of package of a supercapacitor (b) Cross-sectional view of a supercapacitor

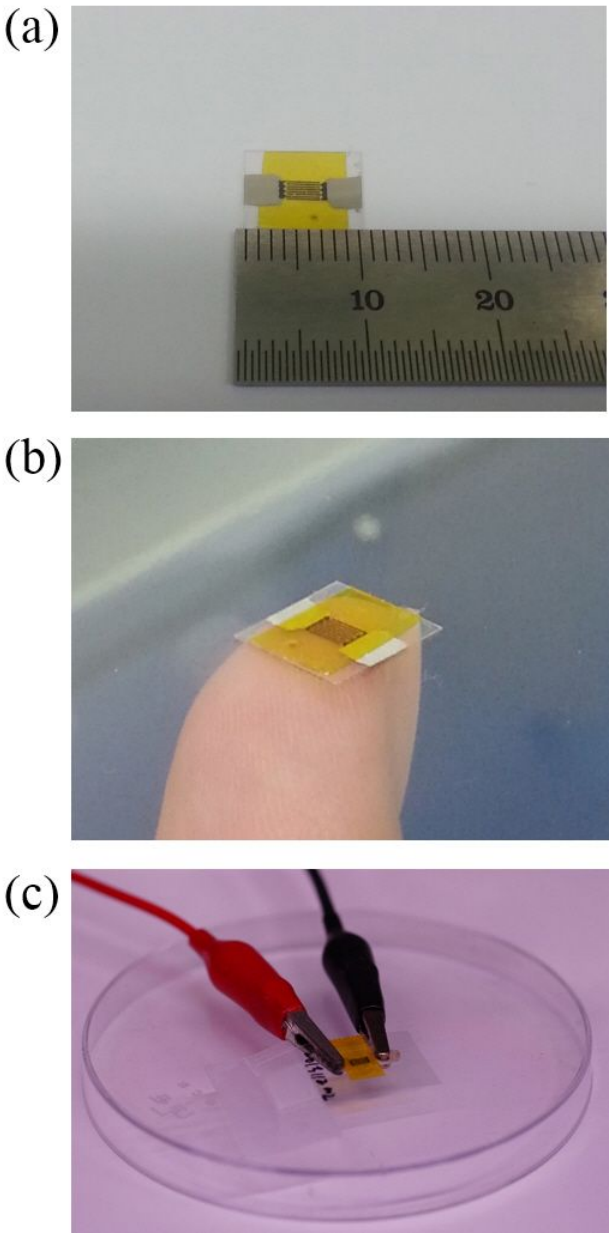

Figure 40. (a) Packed supercapacitor with PET film and Kapton tape (b) Side view of packed supercapacitor (c) connection with an alligator clip

4.3 Electrolytes

An electrolyte was a composite that ionizes when liquefied in appropriate ionizing solvents. A liquid electrolyte was commonly used and several solid electrode of polymer were invented nowadays. Some gases, such as hydrogen chloride could also work as electrolytes. Electrolyte solutions could also result from dissolution of some biological and synthetic polymers.

There is two kind of solid and liquid electrolyte basically shown in Figure 41. Solid electrolyte is good mechanical strength and safe for flexible solid-state electronics.[8, 9] A performance of a supercapacitor was similar with aqueous electrolyte. However electric conductivity of solid electrolyte is generally lower than that of organic liquid electrolyte.

When electrodes is deposited in an electrolyte, electrodes should sustain its structure and have no electrolysis. When a voltage was applied within potential window, electrodes should conduct electricity and remained as there were. Furthermore, effect of water contamination also decreased performance of capacitance.[10]

After a supercapacitor worked as capacitor, a chemical reaction took place at the cathode consuming electrons and at the anode producing electron transferred to the cathode. For example, in a solution of ordinary salt in water, the cathode reaction was

$$2H_2O + 2e^- \rightarrow 2OH^- + H_2$$

And anode reaction was

$$2NaCl \rightarrow 2Na^+ + Cl_2 + 2e^-$$

In this thesis, four kinds of ionic liquid, organic with acetonitrile (AN, Dae Jung, Korea) or propylene carbonate solvent (PC, Dae Jung, Korea), and aqueous electrolytes were used: 1-ethyl-3-methylimidazolium tetrafluoroborate ($EMIMBF_4$, Sigma Aldrich), a 1.0 M solution of tetraethylammonium tetrafluoroborate ($TEABF_4$, Alfa Aesar) and a 1.0 M solution of sulfuric acid (H_2SO_4, Dae Jung).

An aqueous liquid was used as electrolyte for a supercapacitor such as $(NH_4)_2SO_4$, KCl, KOH, and Na_2SO_4.[11, 12] Generally, an aqueous liquid electrolyte has advantages of cheap, environment friendly, and easy producible than organic electrolyte.

Our group chose sulfuric acid as an aqueous liquid electrolyte.[13] An aqueous electrolyte was solved in deionized water which worked as a solvent.[14] Our group prepared 1.0 M H_2SO_4 as an aqueous electrolyte. An aqueous electrolyte had an advantage of a low internal resistance and electrolyte leakage. High conductivity of electrolyte and current collectors was needed to achieve a low equivalent series resistance.[15]

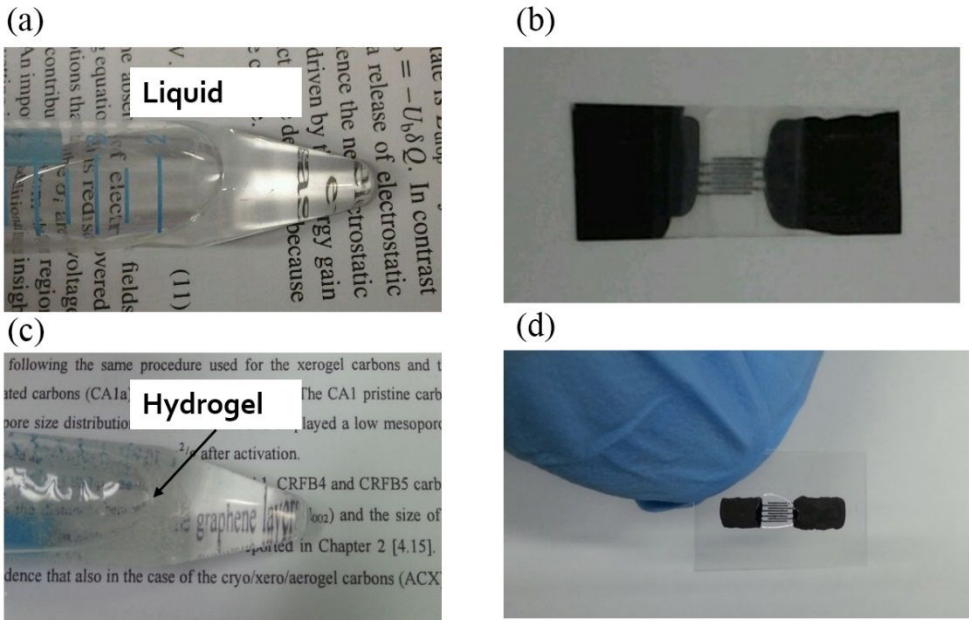

Figure 41. (a) A liquid electrolyte (b) Packaged and sealed with liquid electrolyte supercapacitor (c) A solid electrolyte (d) Pasted gel electrolyte supercapacitor without package

First, we considered molecular weight of H_2SO_4 = 98 g/mol, so we had to add 98 g concentrated sulfuric acid and made up to 1 liter water.

density = mass / volume

which was said on a bottle to be about 1.84 g/mL, so then we had: volume = 98 g / 1.84 (g/mL) = 53.2 mL. We had to consider acid purity, usually 98% then we had to do this. If acid were 100% pure convert in mL given with purity of 98%, so 100% x 53.2 mL / 98% = 54.3 mL of (98%) concentrated acid. Finally, add 54.3 mL sulfuric acid to about 0.9 L deionized water while continuously stirring with evolving heat. After it filled up to 1.00 L with also deionized water. Finally, 1 M sulfuric acid was produced as an aqueous electrolyte (Figure 42).

$$1\,M = 1\,mol/l$$

An organic electrolyte was prepared by dissolving a solid quaternary ammonium salt, tetraethylammonium tetrafluoroborate ($TEABF_4$) in high dielectric constant solvent PC (Figure 42). While performance of AN solvent was better than that of PC, PC solvent was safe and convenient to handle.[16] An organic electrolyte had theoretically had 3 voltage potential window. However, a supercapacitor with an organic electrolyte could reach 2.7 V potential window practically.[17]

A 1.0 M solution of $TEABF_4$ was dissolved in PC. Tetraethylammonium (TEA) is a quaternary ammonium cation. Tetrafluoroborate is anion BF_4^-.[18] To prepare 1

M of an organic electrolyte, 10.85 g $TEABF_4$ salt of 217.06 g/mol molar mass, is dissolved into 50 mL PC.

$$1\,M = 1\,mol/l$$

To make 50 mL organic solution of 1 M concentration, 0.05 mol of $TEABF_4$ /PC was need.

$$0.05\,mol\ \times 217.06\frac{g}{mol}\ = 10.85\,g$$

A 1.0 M solution of $TEABF_4$ with PC produced as an organic electrolyte. In the same manner, a 1.0 M solution of $TEABF_4$ was dissolved in AN. To prepare 1 M of an organic electrolyte, 10.85 g $TEABF_4$ salt of 217.06 g/mol molar mass, was dissolved into 50 mL AN.

$$1\,M = 1\,mol/l$$

To make 50 mL organic solution of 1 M concentration, 0.05 mol of $TEABF_4$ /AN was need.

$$0.05\,mol\ \times 217.06\frac{g}{mol}\ = 10.85\,g$$

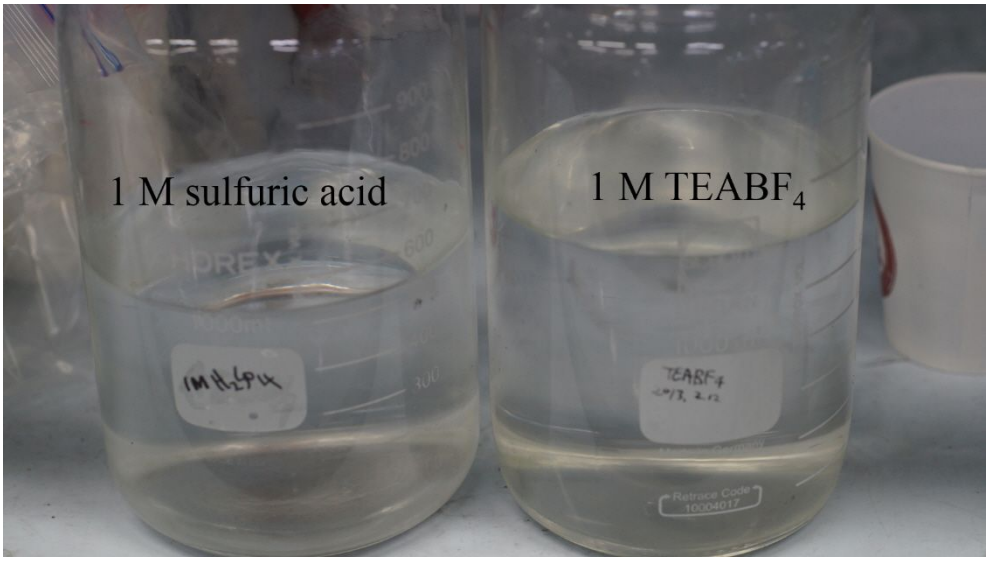

Figure 42. A 1 M sulfuric acid electrolyte and a 1 M $TEABF_4$ electrolyte

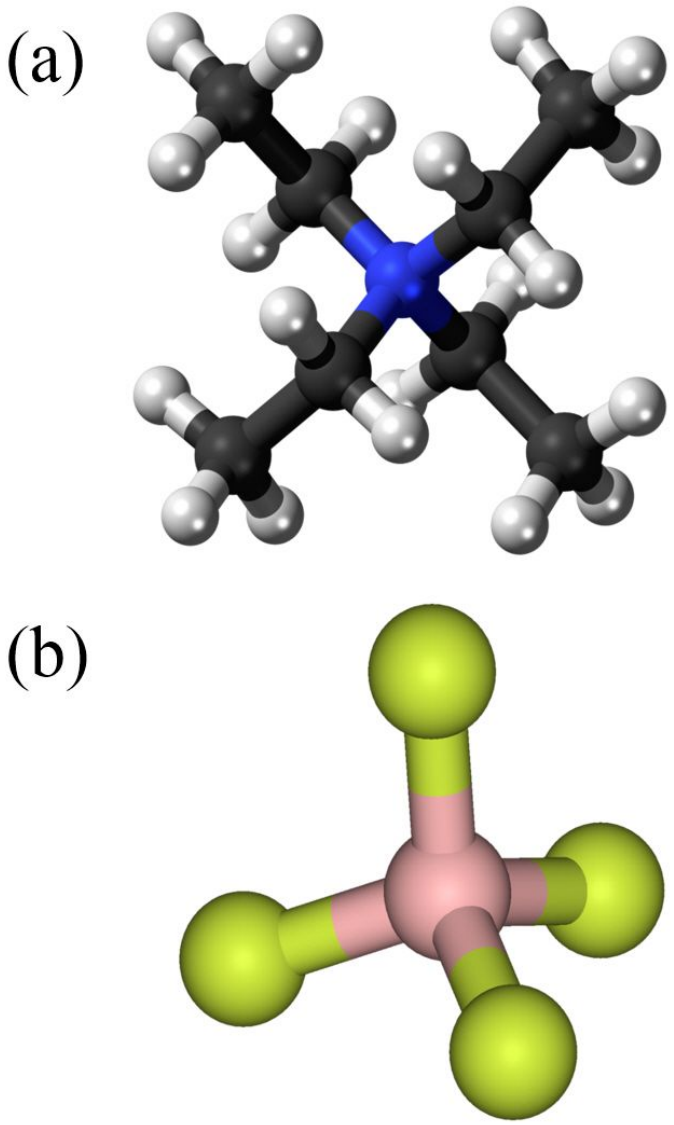

Figure 43. (a) Tetraethylammonium (b) Tetrafluoroborate-ion

A 1.0 M solution of $TEABF_4$ with AN produced as an organic electrolyte.

An ionic liquid electrolyte was used for high performance because of wide potential window.[19, 20] Ionic liquid electrolytes had merits such as wide potential window of 4 voltage, non-volatility, low toxicity, and high decomposition temperatures. In a supercapacitor, an ionic liquid electrolyte was environmentally friendly material.[21] However, ionic liquid electrolytes had low ion conductivity and price of ionic liquid electrolyte were expensive than that of both an aqueous electrolyte and an organic electrolyte.[22] Therefore, an ionic electrolyte was needed to research to increase the ion conductivity and decrease production cost for commercially wide spread.

$EMIMBF_4$ is an ionic liquid electrolyte and could be used without any other treatments. The cation consists of a five-membered ring with two nitrogen and three carbon atoms.

Energy density of an ionic liquid electrolyte PRGO supercapacitor showed approximately one order higher than that of an aqueous electrolyte PRGO supercapacitor, because ionic liquids had high potential window was 3.5 V, relatively high compared to 1 V of an aqueous electrolyte in our test.[23] On the other hand, it had similar energy density of an organic electrolyte PRGO supercapacitor. However, power density of an ionic electrolyte PRGO supercapacitor had the best performance in four type electrolytes

4.4 Results and discussions

Four electrolytes, aqueous, organic /AN, organic /PC and ionic liquid, were used respectively to test performance of a PRGO supercapacitor. An aqueous, organic and ionic liquid electrolyte have 1 V, 2.7 V, 2.75 V, and 3.5 V working potential voltage. Performance of a PRGO supercapacitor which used an ionic liquid electrolyte was the best in terms of energy and power density among the three electrolytes.

There were many electrolyte researches to improve performance. For example, there were a mixed-solvent strategy to increase performance of energy storage device. Especially, a solid electrolyte is safe in outer physical stress of device such as mechanical strength and safe for flexible solid-state electronics. Meanwhile, solid electrolyte is still lower performance than liquid electrolytes.

4.5 Bibliography

[1]. Chen, P., H. Chen, J. Qiu, and C. Zhou, "Inkjet Printing of Single-Walled Carbon Nanotube/RuO2 Nanowire Supercapacitors on Cloth Fabrics and Flexible Substrates" *Nano Research*, Vol. 3, No. 8, pp. 594-603, 2010.

[2]. *Kapton tape*. Available from: http://en.wikipedia.org/wiki/Kapton.

[3]. Jung, H., C.V. Cheah, N. Jeong, and J. Lee, "Direct printing and reduction of graphite oxide for flexible supercapacitors" *Applied Physics Letters*, Vol. 105, No., 2014. [http://dx.doi.org/10.1063/1.4890840].

[4]. *Scienion enabling life science*. Available from: http://www.scienion.com/products/sciflexarrayer/s1-compact-entry-model/.

[5]. Moon, J.S., M. Antcliffe, H.C. Seo, D. Curtis, et al., "Ultra-low resistance ohmic contacts in graphene field effect transistors" *Applied Physics Letters*, Vol. 100, No. 20, 2012.

[6]. Zheng, J.P., "Resistance distribution in electrochemical capacitors with a bipolar structure" *Journal of Power Sources*, Vol. 137, No. 1, pp. 158-162, 2004.

[7]. *Adhesive tape*. Available from: http://en.wikipedia.org/wiki/Adhesive_tape.

[8]. Angell, C.A., C. Liu, and E. Sanchez, "RUBBERY SOLID ELECTROLYTES WITH DOMINANT CATIONIC TRANSPORT AND HIGH AMBIENT CONDUCTIVITY" *Nature*, Vol. 362, No. 6416, pp. 137-139, 1993.

[9]. Xu, Y.X., Z.Y. Lin, X.Q. Huang, Y. Liu, et al., "Flexible Solid-State Supercapacitors Based on Three-Dimensional Graphene Hydrogel Films"

Acs Nano, Vol. 7, No. 5, pp. 4042-4049, 2013.

[10]. Cericola, D., P.W. Ruch, A. Foelske-Schmitz, D. Weingarth, et al., "Effect of Water on the Aging of Activated Carbon Based Electrochemical Double Layer Capacitors During Constant Voltage Load Tests" *International Journal of Electrochemical Science*, Vol. 6, No. 4, pp. 988-996, 2011.

[11]. Demarconnay, L., E. Raymundo-Pinero, and F. Beguin, "A symmetric carbon/carbon supercapacitor operating at 1.6 V by using a neutral aqueous solution" *Electrochemistry Communications*, Vol. 12, No. 10, pp. 1275-1278, 2010.

[12]. Deng, L.J., G. Zhu, J.F. Wang, L.P. Kang, et al., "Graphene-MnO2 and graphene asymmetrical electrochemical capacitor with a high energy density in aqueous electrolyte" *Journal of Power Sources*, Vol. 196, No. 24, pp. 10782-10787, 2011.

[13]. Engstrom, A.M. and F.M. Doyle, "Exploring the cycle behavior of electrodeposited vanadium oxide electrochemical capacitor electrodes in various aqueous environments" *Journal of Power Sources*, Vol. 228, No., pp. 120-131, 2013.

[14]. Wang, Q., Q. Cao, X.Y. Wang, B. Jing, et al., "A high-capacity carbon prepared from renewable chicken feather biopolymer for supercapacitors" *Journal of Power Sources*, Vol. 225, No., pp. 101-107, 2013.

[15]. Zhang, X.Y., X.Y. Wang, L.L. Jiang, H. Wu, et al., "Effect of aqueous electrolytes on the electrochemical behaviors of supercapacitors based on hierarchically porous carbons" *Journal of Power Sources*, Vol. 216, No., pp. 290-296, 2012.

[16]. Wang, Y., Z.Q. Shi, Y. Huang, Y.F. Ma, et al., "Supercapacitor Devices

Based on Graphene Materials″ *Journal of Physical Chemistry C*, Vol. 113, No. 30, pp. 13103-13107, 2009.

[17]. Khomenko, V., E. Raymundo-Pinero, and F. Beguin, "High-energy density graphite/AC capacitor in organic electrolyte″ *Journal of Power Sources*, Vol. 177, No. 2, pp. 643-651, 2008.

[18]. Thevenin, J.G. and R.H. Muller, "IMPEDANCE OF LITHIUM ELECTRODES IN A PROPYLENE CARBONATE ELECTROLYTE″ *Journal of the Electrochemical Society*, Vol. 134, No. 2, pp. 273-280, 1987.

[19]. Zhu, Y.W., S. Murali, M.D. Stoller, K.J. Ganesh, et al., "Carbon-Based Supercapacitors Produced by Activation of Graphene″ *Science*, Vol. 332, No. 6037, pp. 1537-1541, 2011.

[20]. Fu, C.P., Y.F. Kuang, Z.Y. Huang, X. Wang, et al., "Supercapacitor based on graphene and ionic liquid electrolyte″ *Journal of Solid State Electrochemistry*, Vol. 15, No. 11-12, pp. 2581-2585, 2011.

[21]. Kim, T.Y., H.W. Lee, M. Stoller, D.R. Dreyer, et al., "High-Performance Supercapacitors Based on Poly(ionic liquid)-Modified Graphene Electrodes″ *Acs Nano*, Vol. 5, No. 1, pp. 436-442, 2011.

[22]. Lu, W., L.T. Qu, K. Henry, and L.M. Dai, "High performance electrochemical capacitors from aligned carbon nanotube electrodes and ionic liquid electrolytes″ *Journal of Power Sources*, Vol. 189, No. 2, pp. 1270-1277, 2009.

[23]. Kim, T.Y., H.W. Lee, M. Stoller, D.R. Dreyer, et al., "High performance supercapacitors based on poly(ionic liquid)-Modified graphene electrodes″ *ACS NANO*, Vol. 5, No., pp. 436-442, 2010.

5 Performance evaluation

5.1 Cyclic voltammetry and charging/discharging test

Performance of a high power density supercapacitor was measured with potentiostatic and galvanostatic methods.[1-4] A graphene-based supercapacitor was also measured with conventional potentiostatic and galvanostatic methods.[5-9] We used cyclic voltammetry (CV) test and galvanostatic charging/discharging (CC) test for a performance test.[10] CV was a type of potentio dynamic electrochemical measurement.[10, 11]

In a CV test, a working electrode was ramped linearly by time while a counter electrode stayed a reference voltage. CV was generally used to test electrochemical properties of an analyte in a solution. In a CC test, when given current flowed both electrodes of supercapacitor voltage showed how fast it absorb electrons by time. Both a CV and a CC test can give calculation of energy density, power density, and capacitance density. In this chapter, a CV and CC test was calculated to estimate the performance of a supercapacitor. An IVIUMSTAT electrochemical workstation (Ivium technologies BV Co., The Netherlands) was used for a CV and a CC test shown in Figure 44.

A result of a CV curve showed in potential window of 0 ~ 1 V and 0.2, 1, 20, 100 V/s scan rate under room temperature shown in Figure 45.

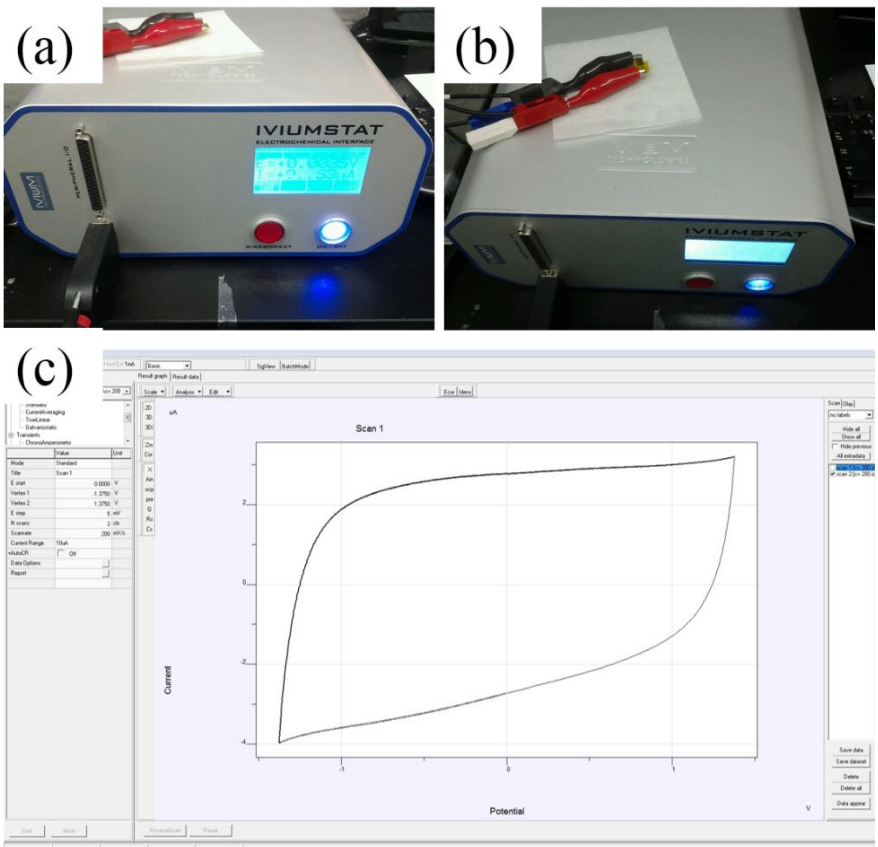

Figure 44. (a) An IVIUMSTAT electrochemical workstation (b) A working electrode and a counter electrode on electrochemical workstation (c) Measurement software for an electrochemical workstation

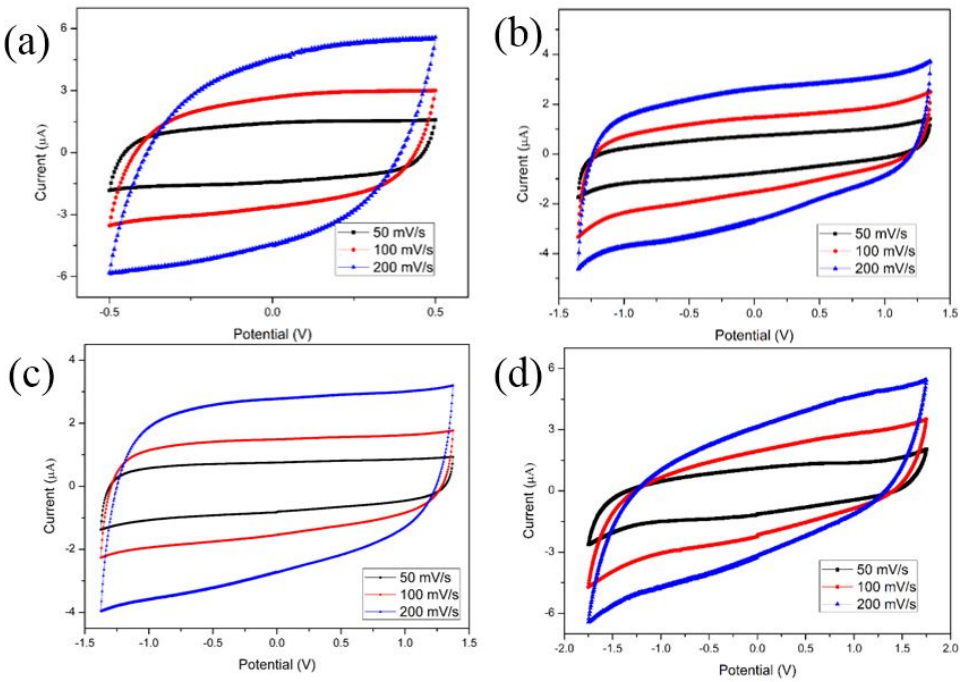

Figure 45. 50 mV/s, 100 mV/s, and 200 mV/s of CV measurement with (a) 1M aqueous electrolyte (b) 1M organic electrolyte in PC (2.7 V) (c) 1M organic electrolyte in AN (2.75 V)[12] (d) ionic electrolyte (3.5 V)

A potentiostat worked with three electrodes of working, reference and counter. Counter and reference electrodes were shorten and connected to one electrode when working electrode was connected to the other electrode because electrodes were a symmetrical structure in a PRGO supercapacitor. Three electrodes system was used for scientific analysis by a reference electrode.[13]

However, anode and cathode electrodes were used in our experiment like practical usage. Current was measured at each potential applied through symmetric electrodes of a PRGO supercapacitor. A CV test was used to measure capacitance, energy and power density of a PRGO supercapacitor.

In a CC test, voltage with given current was measured by time flow shown in Figure 46. Voltage connected between electrodes of a supercapacitor showed how fast it storage or consume energy.

When galvanostatic meter measured, constant current was given at 8 μA at first for charging of a supercapacitor. Voltage was measured every 0.01 second. In an aqueous electrolyte supercapacitor, voltage increased to one voltage which was maximum voltage limited an aqueous electrolyte in hundred milliseconds.

After voltage reached one voltage of a supercapacitor, current was given opposite direction for discharging, minus 8 μA. Given current sustained until voltage approached zero voltage which meant that a supercapacitor finished discharging completely. Two cycles of charging/discharging repeated for ensuring a measurement. After 8 μA current measurement was finished, 7 μA constant current

was applied in the same electrode of a supercapacitor. Discharging time took 1.9 second with 0.85 voltage drop. Voltage drop was caused by equivalent series resistance. When constant current decreased to 1 μA, it took 23 seconds for discharging. Relatively high constant current showed lineal voltage change while low constant current had a slanted voltage graph.

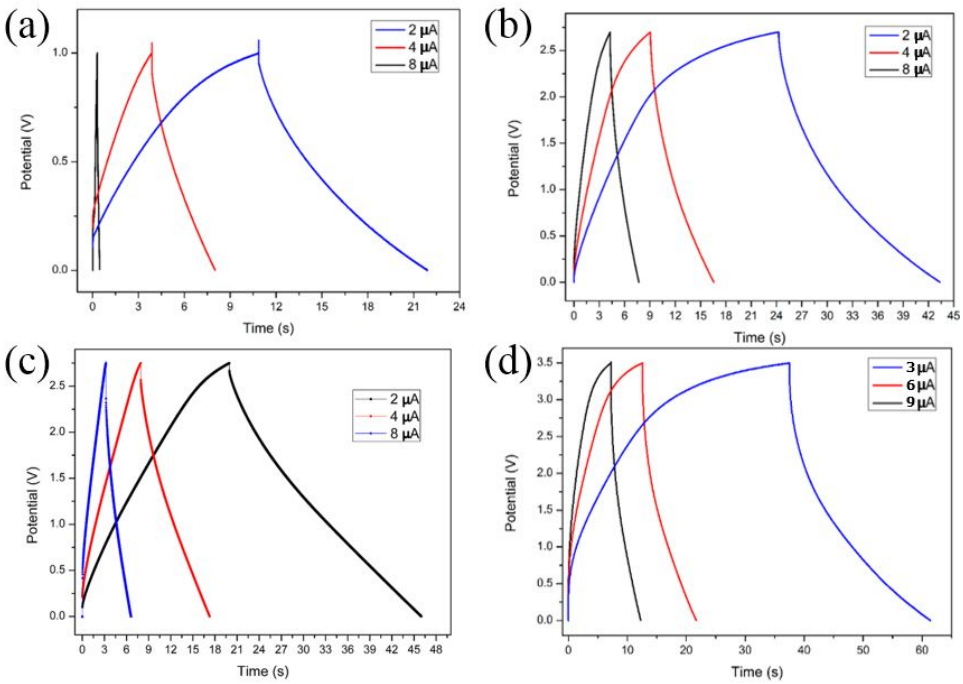

Figure 46. CC graph by time and voltage (a) 1M aqueous electrolyte (b) 1M organic electrolyte in PC (2.7 V) (c) 1M organic electrolyte in AN (2.75 V)[12] (d) ionic electrolyte (3.5 V)

5.2 Energy density and power density

Energy density and power density is commonly used to check and compare a performance for capacitors, fuel-cells, supercapacitors, and lithium-ion batteries. Energy density is an amount of energy in a system and the most important parameter for evaluating a performance. Power density is also another important parameter to check the speed of energy translation of a supercapacitor.

Specific capacitance, C_{sp} is defined as capacitance per mass or volume between plates associated with accommodation of charge. C_{sp} was calculated by integrating the area of a closed curve in a CV graph over a potential window, ΔE from 0 V to 1 V at particular scan rate and the projected area of electrodes. Charge is essentially the area integration over scan rate, representing the sum of anodic and cathodic voltammetry charges, where I, E and v are electric current, potential and scan rate, respectively.

$$C_{SP} = \frac{1}{\Delta E V v} \int_{E_1}^{E_2} I(E) dE \tag{5.1}$$

Likewise, energy density was referred to energy density of a supercapacitor per unit volume, given as

$$E_d = \frac{1}{2 \times 3600} C_{sp} \Delta E^2 \tag{5.2}$$

On the other hand, power density is simply obtained from the integral area of a CV curve over the corresponding total volume of a capacitor, shown by

$$P_{\mathrm{d}} = \frac{E_{\mathrm{d}}}{\Delta t} \tag{5.3}$$

Table 5. Energy and power density from CV test

Sample	Cv Area (mAV)	Scan rate (V/s)	Active area (cm2)	Thickness (μm)	Potential Window (v)	Csp (F/cm3)	ED (Wh/cm3)	PD (Wh/cm3)
Aqueous electrolyte	0.00177	0.05	0.033075	10	1	1.070	0.000149	0.027
	0.00335	0.1	0.033075	10	1	1.013	0.000141	0.051
	0.006	0.2	0.033075	10	1	0.907	0.000126	0.091
Organic ($TEABF_4$/ PC)	0.00401	0.05	0.033075	10	2.7	0.898	0.000909	0.061
	0.00738	0.1	0.033075	10	2.7	0.826	0.000837	0.112
	0.01287	0.2	0.033075	10	2.7	0.721	0.000730	0.195
Organic ($TEABF_4$/ AN)	0.004322	0.05	0.033075	10	2.75	0.950	0.000998	0.065
	0.007587	0.1	0.033075	10	2.75	0.834	0.000876	0.115
	0.0134	0.2	0.033075	10	2.75	0.737	0.000774	0.203
Ionic electrolyte	0.006564	0.05	0.033075	10	3.5	1.134	0.001929	0.099
	0.01223	0.1	0.033075	10	3.5	1.056	0.001797	0.185
	0.0185	0.2	0.033075	10	3.5	0.799	0.001359	0.280

However, in a CC graph, specific capacitance was obtained. Total charge was from a given current multiply discharging time. Then charge was divided by potential window and volume. Specific capacitance in specific area was calculated by dividing the total volume with the size of a potential window: $\Delta E=1\ V$.

$$C_{sp} = \frac{It}{\Delta EV} \tag{5.4}$$

where I, t, E, and V are the electric current, discharging time, potential, and volume, respectively.

Energy density and power density were also calculated from equation (5.2) and (5.3). Energy density and power density were 0.9×10^{-4} Wh/cm^3 and 0.015 W/cm^3, respectively at 0.1 μA in a 1.0 M solution of H_2SO_4 aqueous electrolyte. Thickness and area of a supercapacitor were 10 μm and 0.033 cm^2, respectively.

A PRGO supercapacitor showed high energy density and power density even though current collectors, separator and chemical binders were eliminated from the structure of a supercapacitor. The active area of a PRGO supercapacitor was only comprised of active electrodes and an electrolyte.

Table 6. Energy and power density from CC test[12]

Sample	I(A)	delta t	delta V	Active area (cm2)	Thickness (μm)	Cs(F/cm3)	ED (Wh/cm3)	PD (W/cm3)
Aqueous electrolyte	0.000001	23	1	0.033075	10	0.70	0.0000966	0.015117158
	0.000002	10	0.98	0.033075	10	0.62	0.0000823	0.02962963
	0.000003	6.4	0.92	0.033075	10	0.63	0.0000742	0.041723356
	0.000004	4.1	0.9	0.033075	10	0.55	0.0000620	0.054421769
	0.000005	3.1	0.89	0.033075	10	0.53	0.0000579	0.067271353
	0.000006	2.2	0.88	0.033075	10	0.45	0.0000488	0.079818594
	0.000007	1.9	0.85	0.033075	10	0.47	0.0000475	0.08994709
Organic electrolyte ($TEABF_4$/ PC)	0.000002	19	2.7	0.033075	10	0.43	0.0004308	0.081632653
	0.000003	12	2.7	0.033075	10	0.40	0.0004082	0.12244898
	0.000004	8	2.65	0.033075	10	0.37	0.0003561	0.160241875
	0.000005	6	2.64	0.033075	10	0.34	0.0003326	0.199546485
	0.000006	4.5	2.63	0.033075	10	0.31	0.0002982	0.238548753
	0.000007	4	2.5	0.033075	10	0.34	0.0002939	0.264550265
	0.000008	3.3	2.5	0.033075	10	0.32	0.0002771	0.302343159
Organic electrolyte ($TEABF_4$/ AN)	0.000001	75	2.75	0.033075	10	0.82	0.0008661	0.041572184
	0.000002	27	2.72	0.033075	10	0.60	0.0006168	0.082237339
	0.000003	14.3	2.7	0.033075	10	0.48	0.0004864	0.12244898
	0.000004	9	2.69	0.033075	10	0.40	0.0004067	0.16266062
	0.000005	7	2.64	0.033075	10	0.40	0.0003880	0.199546485
	0.000006	5	2.55	0.033075	10	0.36	0.0003212	0.231292517
	0.000007	4.2	2.45	0.033075	10	0.36	0.0003025	0.259259259
Ionic electrolyte	0.000003	23.5	3.4	0.033075	10	0.63	0.0010066	0.154195011
	0.000004	17	3.3	0.033075	10	0.62	0.0009423	0.199546485
	0.000005	11	3.2	0.033075	10	0.52	0.0007391	0.241874528
	0.000006	9.3	3.1	0.033075	10	0.54	0.0007264	0.281179138
	0.000007	8	3	0.033075	10	0.56	0.0007055	0.317460317
	0.000008	6.5	3	0.033075	10	0.52	0.0006551	0.362811791
	0.000009	4.8	3	0.033075	10	0.44	0.0005442	0.408163265

Capacitance density, C_{sp} is defined by voltage difference between the plates associated with accommodation of charge. C_{sp} was calculated by integrating the area of a closed curve in a CV graph, where *I, E, m* and *v* are electric current, potential, mass and scan rate, respectively.

$$C_{SP} = \frac{1}{\Delta E m v} \int_{E_1}^{E_2} I(E) dE \tag{5.5}$$

Likewise, energy density is referred to energy density of a supercapacitor per unit mass, unit is Wh/kg, given as

$$E_d = \frac{1}{2 \times 3600} C_{sp} \Delta E^2 \text{ (Wh/kg)} \tag{5.6}$$

On the other hand, power density is simply obtained from dividing energy density by discharging time, unit is W/kg, shown by

$$P_d = \frac{E_d}{\Delta t} \text{ (W/kg)} \tag{5.7}$$

Table 7. Specific energy and specific power density from CV test

Sample	Cv Area (mAV)	Scan rate (V/s)	Potential Window (v)	Mass (g)	Cm (F/g)	S.Energy (Wh/kg)	S.Power (W/kg)
Aqueous electrolyte	0.001770	0.05	1	0.000000528	67.045	9.31	3352
	0.003350	0.1	1	0.000000528	63.447	8.81	6345
	0.006000	0.2	1	0.000000528	56.818	7.89	11364
Organic ($TEABF_4$/ PC)	0.004010	0.05	2.7	0.000000528	56.257	56.96	7595
	0.007380	0.1	2.7	0.000000528	51.768	52.41	13977
	0.012870	0.2	2.7	0.000000528	45.139	45.70	24375
Organic ($TEABF_4$/ AN)	0.004322	0.05	2.75	0.000000528	59.532	62.53	8186
	0.007587	0.1	2.75	0.000000528	52.252	54.88	14369
	0.013400	0.2	2.75	0.000000528	46.142	48.47	25378
Ionic electrolyte	0.006564	0.05	3.5	0.000000528	71.039	120.86	12432
	0.012230	0.1	3.5	0.000000528	66.180	112.60	23163
	0.018500	0.2	3.5	0.000000528	50.054	85.16	35038

In a CC test, specific capacitance, $C_{sp,}$ could also be calculated from mass by dividing potential window as specific capacitance was calculated from volume in previous chapter. ΔE from 0 V to 2.7 V and mass of electrodes, m which took into account the whole active material of electrodes at a particular scan rate, given by

$$C_{sp} = \frac{It}{\Delta Em} \tag{5.8}$$

where *I, t, E,* and *m* are the electric current, discharging time, potential, and mass, respectively.

Energy density and power density were also calculated from equation (5.6) and (5.7). The specific energy and specific power of a PRGO-based supercapacitor is 63.0 Wh/kg and 9659 W/kg, respectively in an ionic electrolyte.

Table 8. Specific energy and specific power density from CC test[12]

Sample	I(A)	delta t	delta V	Mass (g)	Cm (F/g)	Specific energy (Wh/kg)	Specific power (W/kg)
Aqueous electrolyte	0.000001	23	1	0.000000528	43.561	6.050	946.970
	0.000002	10	0.98	0.000000528	38.652	5.156	1856.061
	0.000003	6.4	0.92	0.000000528	39.526	4.646	2613.636
	0.000004	4.1	0.9	0.000000528	34.512	3.883	3409.091
	0.000005	3.1	0.89	0.000000528	32.984	3.629	4214.015
	0.000006	2.2	0.88	0.000000528	28.409	3.056	5000.000
	0.000007	1.9	0.85	0.000000528	29.635	2.974	5634.470
Organic electrolyte ($TEABF_4$/PC)	0.000002	19	2.7	0.000000528	26.655	26.989	5113.636
	0.000003	12	2.7	0.000000528	25.253	25.568	7670.455
	0.000004	8	2.65	0.000000528	22.870	22.306	10037.879
	0.000005	6	2.64	0.000000528	21.522	20.833	12500.000
	0.000006	4.5	2.63	0.000000528	19.443	18.679	14943.182
	0.000007	4	2.5	0.000000528	21.212	18.413	16571.970
	0.000008	3.3	2.5	0.000000528	20.000	17.361	18939.394
Organic electrolyte ($TEABF_4$/AN)	0.000001	75	2.75	0.000000528	51.653	54.253	2604.167
	0.000002	27	2.72	0.000000528	37.600	38.636	5151.515
	0.000003	14.3	2.7	0.000000528	30.093	30.469	7670.455
	0.000004	9	2.69	0.000000528	25.346	25.473	10189.394
	0.000005	7	2.64	0.000000528	25.109	24.306	12500.000
	0.000006	5	2.55	0.000000528	22.282	20.123	14488.636
	0.000007	4.2	2.45	0.000000528	22.727	18.947	16240.530
Ionic electrolyte	0.000003	23.5	3.4	0.000000528	39.271	63.052	9659.091
	0.000004	17	3.3	0.000000528	39.027	59.028	12500.000
	0.000005	11	3.2	0.000000528	32.552	46.296	15151.515
	0.000006	9.3	3.1	0.000000528	34.091	45.502	17613.636
	0.000007	8	3	0.000000528	35.354	44.192	19886.364
	0.000008	6.5	3	0.000000528	32.828	41.035	22727.273
	0.000009	4.8	3	0.000000528	27.273	34.091	25568.182

A Ragone plot, also called Ragone chart, is a plot used for performance comparison of energy storage devices by the value of energy density and power density with volume and mass.[14]

The Ragone plot shows energy density and power density expressed by two type of volume and mass of material. Normally, energy density means energy per volume while specific energy density or specific energy mean energy per mass. In case of power density and specific power is the same meaning.

The Ragone plot with volume density from CV test shows energy density and power density of a PRGO supercapacitor aqueous electrolyte, a PRGO supercapacitor organic electrolyte ($TEABF_4$/PC), a PRGO supercapacitor organic electrolyte ($TEABF_4$/AN), a PRGO supercapacitor ionic electrolyte, respectively shown in Figure 47. The Ragone plot with volume density from CC test also shows energy density and power density of a PRGO supercapacitor shown in Figure 48. The energy density of a PRGO supercapacitor ionic electrolyte was approximately one order of magnitude higher than that of a PRGO supercapacitor aqueous electrolyte, which demonstrates a typical benefit of wide potential window of an ionic electrolyte supercapacitor. The power density of a PRGO supercapacitor ionic electrolyte is also one orders of magnitude higher than that of a PRGO supercapacitor aqueous electrolyte. In an organic electrolyte PRGO supercapacitor, a $TEABF_4$/AN organic electrolyte has little bit better performance than a $TEABF_4$/PC organic electrolyte. A $TEABF_4$/AN organic electrolyte has 2.75 potential window while a $TEABF_4$/PC organic electrolyte has 2.7 potential window.

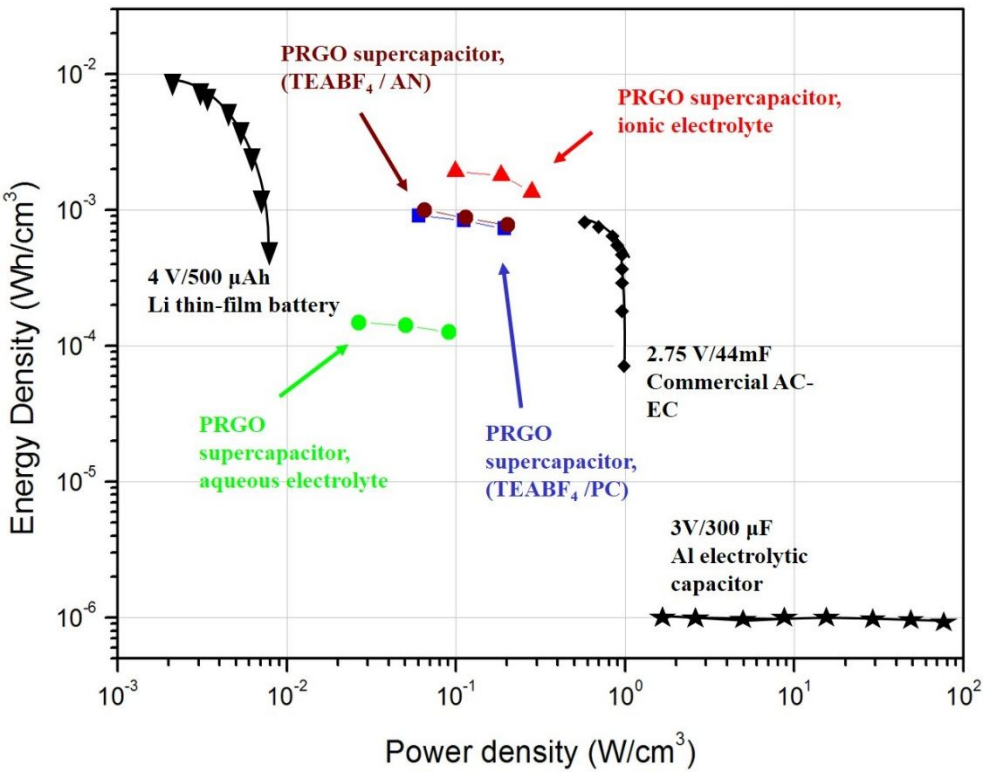

Figure 47. Energy and power density of a PRGO supercapacitor from CV test: ionic liquid, organic liquid and aqueous electrolyte. Li thin-film battery, commercial AC-EC, and AL electrolytic capacitor are from [15]

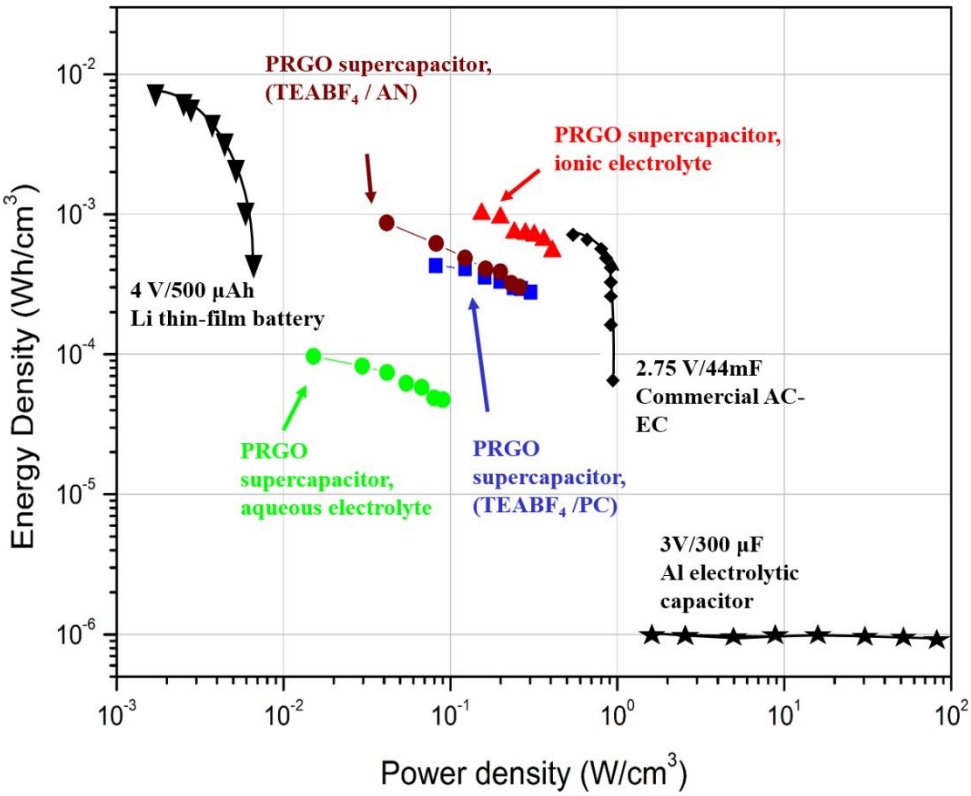

Figure 48. Energy and power density of a PRGO supercapacitor from CC test: ionic liquid, organic liquid and aqueous electrolyte. Li thin-film battery, commercial AC-EC, and AL electrolytic capacitor are from [12, 15]

The Ragone plot with mass density from CV test shows specific energy and specific power of a PRGO supercapacitor aqueous electrolyte, a PRGO supercapacitor organic electrolyte ($TEABF_4$/PC), a PRGO supercapacitor organic electrolyte ($TEABF_4$/AN), a PRGO supercapacitor ionic electrolyte, respectively shown in Figure 49. The Ragone plot with mass density from CC test shows specific energy and specific power shown in Figure 50.

A PRGO supercapacitor organic electrolyte ($TEABF_4$/PC), a PRGO supercapacitor organic electrolyte ($TEABF_4$/AN), and a PRGO supercapacitor ionic electrolyte have similar specific energy with batteries and similar specific power with capacitors.

A conventional lithium-ion battery has normally 100 Wh/kg specific energy and 100 W/kg specific power. Specific energy of an aqueous electrolyte PRGO supercapacitor is lower than that of a lithium-ion battery while specific power of a supercapacitor was higher than that of a lithium-ion battery.

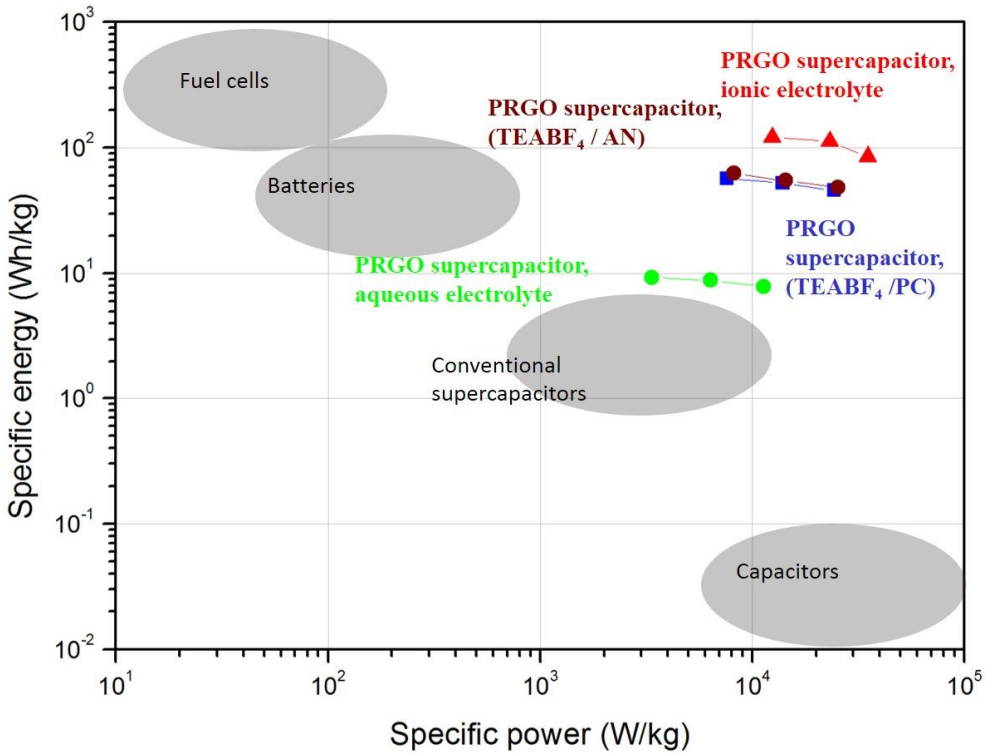

Figure 49. The Ragone plot of mass density from CV test. Specific energy and power of conventional batteries, supercapacitors and capacitors. Fuel cells, batteries, conventional supercapacitors, and capacitors are from [16]

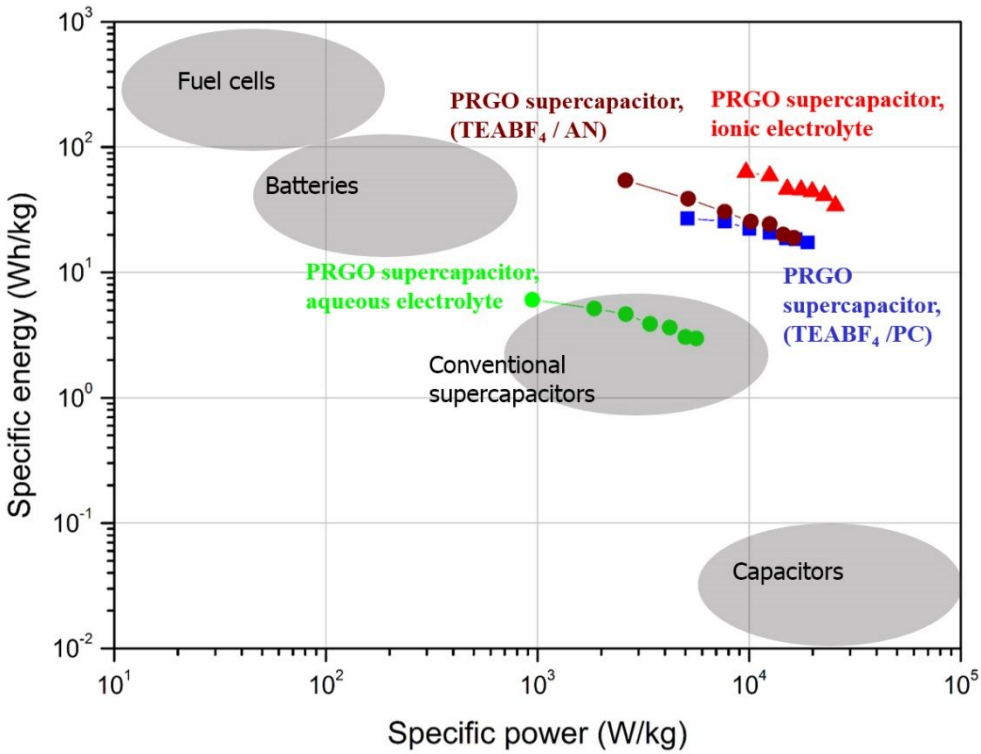

Figure 50. The Ragone plot of mass density from CC test. Specific energy and power of conventional batteries, supercapacitors and capacitors. Fuel cells, batteries, conventional supercapacitors, and capacitors are from [16]

5.3 Folding and retention test

A significant trend in electronics involves folding and stretching of devices.[17] PRGO could be coated on any substrate such as a thin film and it had high flexibility as it sustained its form without fractures even though a substrate beneath was highly deformed.[18]

A PRGO supercapacitor was bended at different angles of 0°, 45°, 90°, 135° and 180° and its performance was shown in Figure 51 Interestingly, performance of a PRGO supercapacitor at 180° folding angle was similar with that at a 0° folding angle. In Figure 51(a), conical folding fracture, a PRGO supercapacitor showed enough flexibility and adhesion to the substrate. From the result, it was observable that performance of a PRGO supercapacitor was not influenced much by the geometry of its substrate.

Folding cycle was also measured in 100 mV/s scan rate of aqueous electrolyte supercapacitor. Every 10 cycle data was in 100 times cycles of 45°, 90°, 135°, and 180° folding test. Although supercapacitor was completely folded condition, performance sustained over 80% of flat condition in Figure 52(b).

A retention test was performed to check the stability of a PRGO supercapacitor. A supercapacitor has over 10,000 cycle stability while lithium-ion battery cycle durability has normally over 1000 cycles. In common use, a supercapacitor should bear specific charge and discharge current can be exceeded at infrequent peak pulse.

In a laboratory, a retention test could show reliability enough although infrequent impulse could not estimate.

A retention test was performed to check stability of a twisted PRGO supercapacitor shown in Figure 53. A CV graph was checked to durability test in 100 mV/s scan rate for 2000 times including one day pausing. Every 100 cycle date was extracted from the whole date. After a repeated 1000 cycles test, a CV graph did not change much. After a CV test paused one day, performance was increased a little bit.

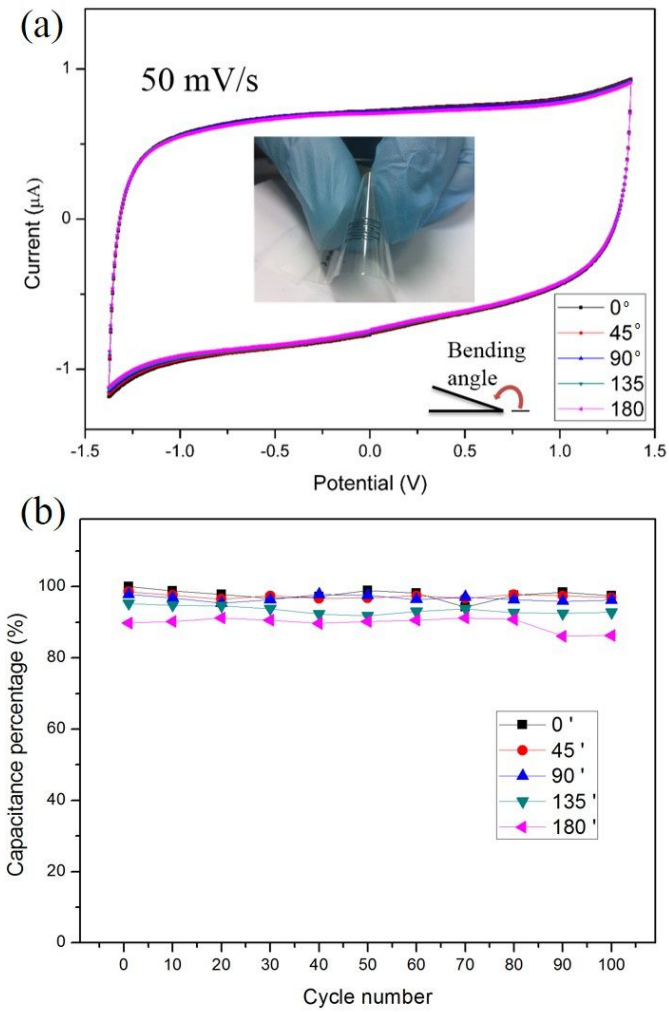

Figure 51. A CV test of (a) a folding test with organic electrolyte with 50 mV/s scan rate[12] (b) repetition of capacitance on folding test

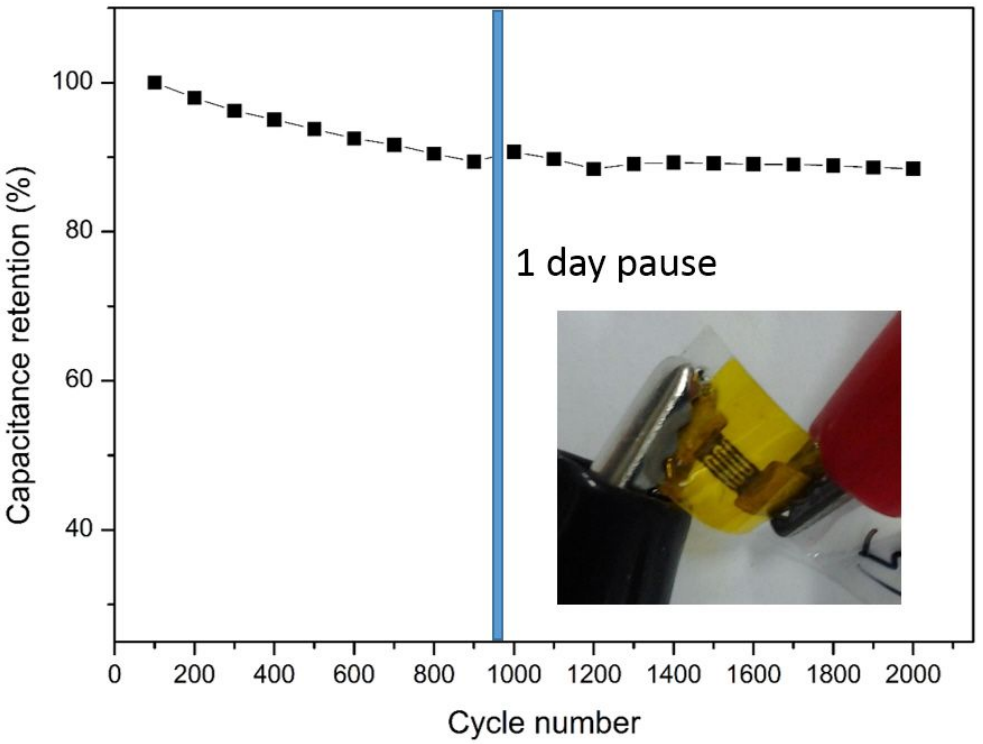

Figure 52. Retention test of a PRGO supercapacitor with one day pause

5.4 Bibliography

[1]. Du, C.S. and N. Pan, "High power density supercapacitor electrodes of carbon nanotube films by electrophoretic deposition" *Nanotechnology*, Vol. 17, No. 21, pp. 5314-5318, 2006.

[2]. Gomez, J. and E.E. Kalu, "High-performance binder-free Co-Mn composite oxide supercapacitor electrode" *Journal of Power Sources*, Vol. 230, No., pp. 218-224, 2013.

[3]. Lee, S.W., J. Kim, S. Chen, P.T. Hammond, et al., "Carbon Nanotube/Manganese Oxide Ultrathin Film Electrodes for Electrochemical Capacitors" *Acs Nano*, Vol. 4, No. 7, pp. 3889-3896, 2010.

[4]. Wang, Y.X., C. Zheng, L. Qi, M. Yoshio, et al., "Utilization of (oxalato)borate-based organic electrolytes in activated carbon/graphite capacitors" *Journal of Power Sources*, Vol. 196, No. 23, pp. 10507-10510, 2011.

[5]. Kim, T., G. Jung, S. Yoo, K.S. Suh, et al., "Activated Graphene-Based Carbons as Supercapacitor Electrodes with Macro- and Mesopores" *Acs Nano*, Vol. 7, No. 8, pp. 6899-6905, 2013.

[6]. Shi, K.Y. and I. Zhitomirsky, "Influence of current collector on capacitive behavior and cycling stability of Tiron doped polypyrrole electrodes" *Journal of Power Sources*, Vol. 240, No., pp. 42-49, 2013.

[7]. Yu, A.P., I. Roes, A. Davies, and Z.W. Chen, "Ultrathin, transparent, and flexible graphene films for supercapacitor application" *Applied Physics Letters*, Vol. 96, No. 25, 2010.

[8]. Wang, Y., Z.Q. Shi, Y. Huang, Y.F. Ma, et al., "Supercapacitor Devices

Based on Graphene Materials″ *Journal of Physical Chemistry C*, Vol. 113, No. 30, pp. 13103-13107, 2009.

[9]. Lu, Q., M.W. Lattanzi, Y.P. Chen, X.M. Kou, et al., "Supercapacitor Electrodes with High-Energy and Power Densities Prepared from Monolithic NiO/Ni Nanocomposites″ *Angewandte Chemie-International Edition*, Vol. 50, No. 30, pp. 6847-6850, 2011.

[10]. Gomez, H., M.K. Ram, F. Alvi, P. Villalba, et al., "Graphene-conducting polymer nanocomposite as novel electrode for supercapacitors″ *Journal of Power Sources*, Vol. 196, No. 8, pp. 4102-4108, 2011.

[11]. Chandrasekaran, R., Y. Soneda, J. Yamashita, M. Kodama, et al., "Preparation and electrochemical performance of activated carbon thin films with polyethylene oxide-salt addition for electrochemical capacitor applications″ *Journal of Solid State Electrochemistry*, Vol. 12, No. 10, pp. 1349-1355, 2008.

[12]. Jung, H., C.V. Cheah, N. Jeong, and J. Lee, "Direct printing and reduction of graphite oxide for flexible supercapacitors″ *Applied Physics Letters*, Vol. 105, No., 2014. [http://dx.doi.org/10.1063/1.4890840].

[13]. Zhao, X., H. Tian, M.Y. Zhu, K. Tian, et al., "Carbon nanosheets as the electrode material in supercapacitors″ *Journal of Power Sources*, Vol. 194, No. 2, pp. 1208-1212, 2009.

[14]. Pech, D., M. Brunet, H. Durou, P.H. Huang, et al., "Ultrahigh-power micrometre-sized supercapacitors based on onion-like carbon″ *Nature Nanotechnology*, Vol. 5, No. 9, pp. 651-654, 2010.

[15]. El-Kady, M.F., V. Strong, S. Dubin, and R.B. Kaner, "Laser scribing of high-performance and flexible graphene-based electrochemical capacitors″

Science, Vol. 335, No. 6074, pp. 1326-1330, 2012.

[16]. Winter, M. and R.J. Brodd, "What are batteries, fuel cells, and supercapacitors?" *Chemical Reviews*, Vol. 104, No. 10, pp. 4245-4269, 2004.

[17]. Xu, S., Y.H. Zhang, J. Cho, J. Lee, et al., "Stretchable batteries with self-similar serpentine interconnects and integrated wireless recharging systems" *Nature Communications*, Vol. 4, No., 2013.

[18]. Grantab, R., V.B. Shenoy, and R.S. Ruoff, "Anomalous Strength Characteristics of Tilt Grain Boundaries in Graphene" *Science*, Vol. 330, No. 6006, pp. 946-948, 2010.

6 Conclusion

6.1 Summary

We demonstrated that a patterning of GO using a liquid dispenser lead to a high quality supercapacitor. A direct printing of GO enabled a fabrication process without a high temperature process and chemical treatments.

Substrate material was selected by a contact angle and adhesion. A multiple dispensing printing method was used for high resolution, porosity, and reduction. Despite absence of current collectors, separator and chemical binders, Our PRGO-based supercapacitor simplified the whole structure, and improved overall performance. The stacking of GO was controlled precisely by way of using a PRGO method.

As a result, the flexibility and thickness of a supercapacitor could be customized for a specific power application, e.g., cellular phone or laptop computer surface. High energy density was obtainable without sacrificing power density in spite of a simple structure and a production process. Furthermore, combination of layer insertion like carbon nanotube, polymer and heterogeneous material is conveniently adaptable by using a direct printing. This alternating multiphase layer of various materials has huge potential of versatile application in sensor and display components.

6.2 Application

A graphene based electrode had been showed potential industrial applications.[1, 2] Application field will be in all places such as materials, display devices, electronics and biology.

An interdigitated electrode could be changed to bio sensor easily due to large surface area of graphene. Printing technology of a GO solution could replace conventional transparent indium tin oxide (ITO) conducting electrodes in various electronic devices. Graphene Field effect transistor (FET) devices with a single back gate was investigated.[3, 4] There were electronic devices such as an ultrasound generation graphene-antenna.[5, 6] Graphene double layer capacitors with ac line filtering were already developed.[7]

Our flexible thin film supercapacitor will have a potential application in Figure 53. A supercapacitor could stack in a device directly or package with stack in the semiconductor chip.

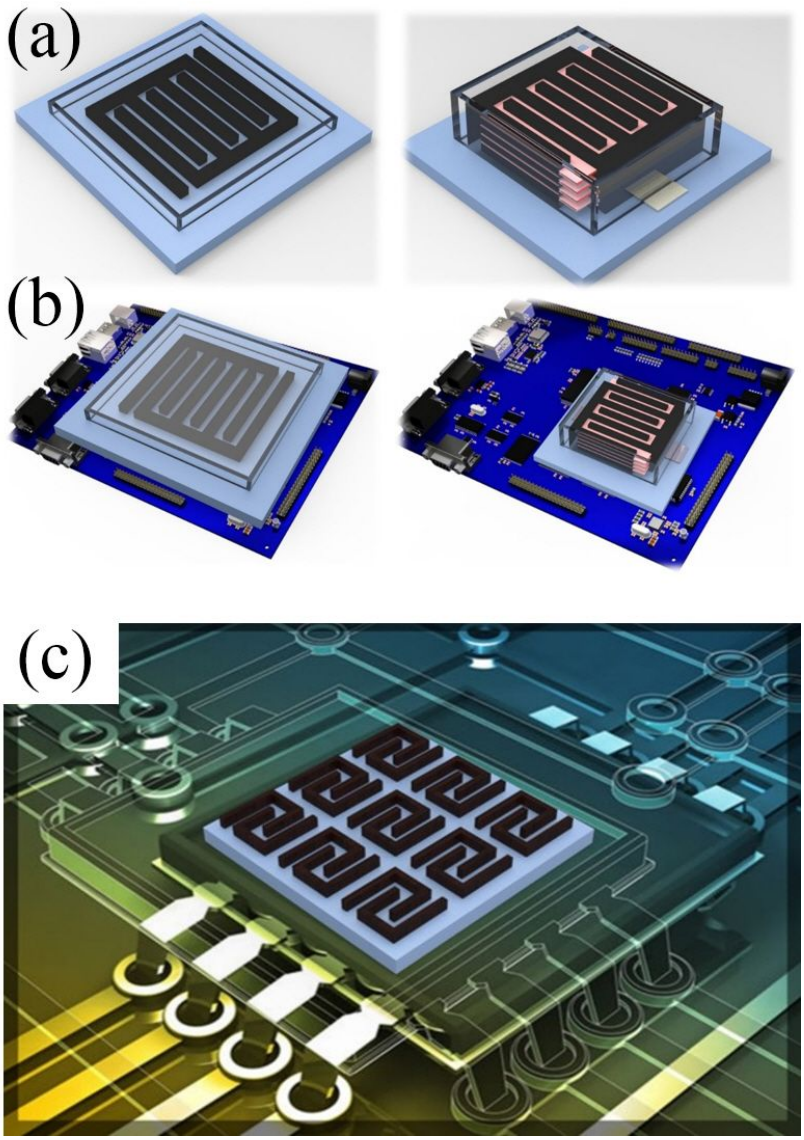

Figure 53. (a) One layer vs stacked layer type (b) Energy storage source on PCB board (c) A supercapacitor in a semiconductor package

6.3 Bibliography

[1]. Bae, S., S.J. Kim, D. Shin, J.H. Ahn, et al., "Towards industrial applications of graphene electrodes" *Physica Scripta*, Vol. T146, No., 2012.

[2]. Low, C.T.J., F.C. Walsh, M.H. Chakrabarti, M.A. Hashim, et al., "Electrochemical approaches to the production of graphene flakes and their potential applications" *Carbon*, Vol. 54, No., pp. 1-21, 2013.

[3]. Zhu, Y.W., S. Murali, W.W. Cai, X.S. Li, et al., "Graphene and Graphene Oxide: Synthesis, Properties, and Applications" *Advanced Materials*, Vol. 22, No. 35, pp. 3906-3924, 2010.

[4]. Marconcini, P., A. Cresti, F. Triozon, G. Fiori, et al., "Atomistic Boron-Doped Graphene Field-Effect Transistors: A Route toward Unipolar Characteristics" *Acs Nano*, Vol. 6, No. 9, pp. 7942-7947, 2012.

[5]. Lee, S.H., M.A. Park, J.J. Yoh, H. Song, et al., "Reduced graphene oxide coated thin aluminum film as an optoacoustic transmitter for high pressure and high frequency ultrasound generation" *Applied Physics Letters*, Vol. 101, No. 24, 2012.

[6]. Fang, Z.Y., Z. Liu, Y.M. Wang, P.M. Ajayan, et al., "Graphene-Antenna Sandwich Photodetector" *Nano Letters*, Vol. 12, No. 7, pp. 3808-3813, 2012.

[7]. Miller, J.R., R.A. Outlaw, and B.C. Holloway, "Graphene Double-Layer Capacitor with ac Line-Filtering Performance" *Science*, Vol. 329, No. 5999, pp. 1637-1639, 2010.

Appendix

A. Zeta potential of GO

Zeta potential is an electrokinetic potential with colloidal dispersions of which particle forms electric potential in the interfacial double layer.[1] Zeta potentials of commercial GO solution and GO solution made in our group were measured using electrophoretic light scattering (NanoPlus, Japan's Otsuka Electronics) in the -200 mV to 200 mV range with concentrations between 0.001% and 40%.[2, 3]

Figure 54 shows that zeta potential are a similar characteristic in commercial GO and GO made in our group. The significance of zeta potential is that its value can be related to the stability of colloidal dispersions. The degree of repulsion between adjacent, similarly charged particles in a dispersion. The functional groups at the edges of the graphene oxide sheets can weakly develop negative charges in the solution due to deprotonation, yielding a hydrophilic nature. Negatively charged graphene oxide sheets were investigated by zeta potential measurements.

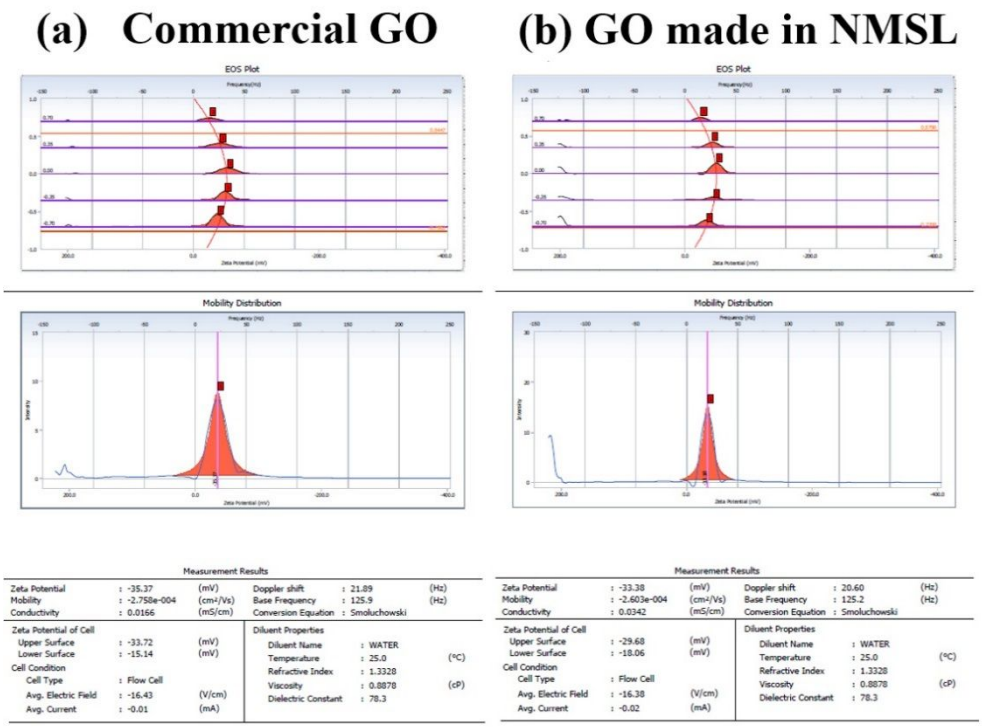

Figure 54. Zeta potential of (a) commercial GO and (b) GO made in NMSL

B. Liquid dispenser specification

A liquid dispenser was a compact automated non-contact dispensing system of ultra-low volumes. A liquid dispenser of SCIENION had many advantages of homogenous spots morphology, no damage to sensitive surfaces, dispensing into very small cavities, and drop volume control technology with vision based algorithm.

It was centered around, on the other hand not limited to, microarray based application on DNAs, oligos, peptides, antibodies, glycans, lysates as well as cells. The ultrasonic wash station eliminates cross contamination.

Table 9. sciFLEXARRAYER DW technical information

Piezo dispensing	Non-contact, drop-on-demand
Number of dispense capillaries	1
Dispense volume	300 ~ 800 pL per drop
Capillary orifice	50 ~ 100 µm
Capillary material	Borosilicate glass
Typical spot size	80 ~ 250 µm
Typical pitch (spacing)	300 µm (scaleable)
Dispense control	Integrated horizontal CCD camera
Fiducial recognition	Vertical head camera
Capacity	4 slides or twice 75 x 50 mm
Dimensions (L/W/H)	330 x 410 x 380 mm
Weight	9 kg
Voltage	VAC 100 ~ 240
Software	Window XP based

C. GO solution evaporation on different materials

A 10 nL GO solution was on several materials. Figure 55 ~ 58 show the snapshot of full movie clip. A GO solution which had a high contact angle evaporated slowly in Table 10, i.e., in case of GO on glass substrate, a GO solution was dried up in 17 minutes later and ready to a flash reduction. After a GO solution was dried up fully, remained GO would produce electrode line. A high contact angle of GO evaporated fast while a low contact angle of GO evaporated slowly.

Table 10. Contact angle and evaporation time

	Glass	*PET film*	*Paper*	*CYTOP*
Contact angle	30°	80°	90°	110°
Evaporation time	17 min	28 min	29 min	30 min

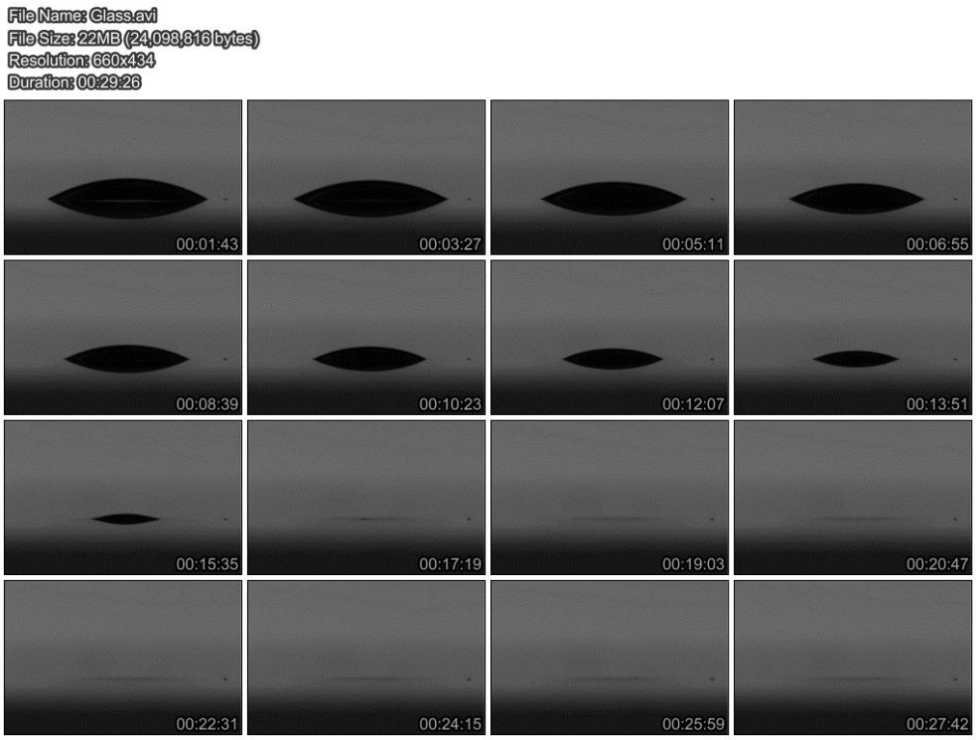

Figure 55. GO droplet on glass

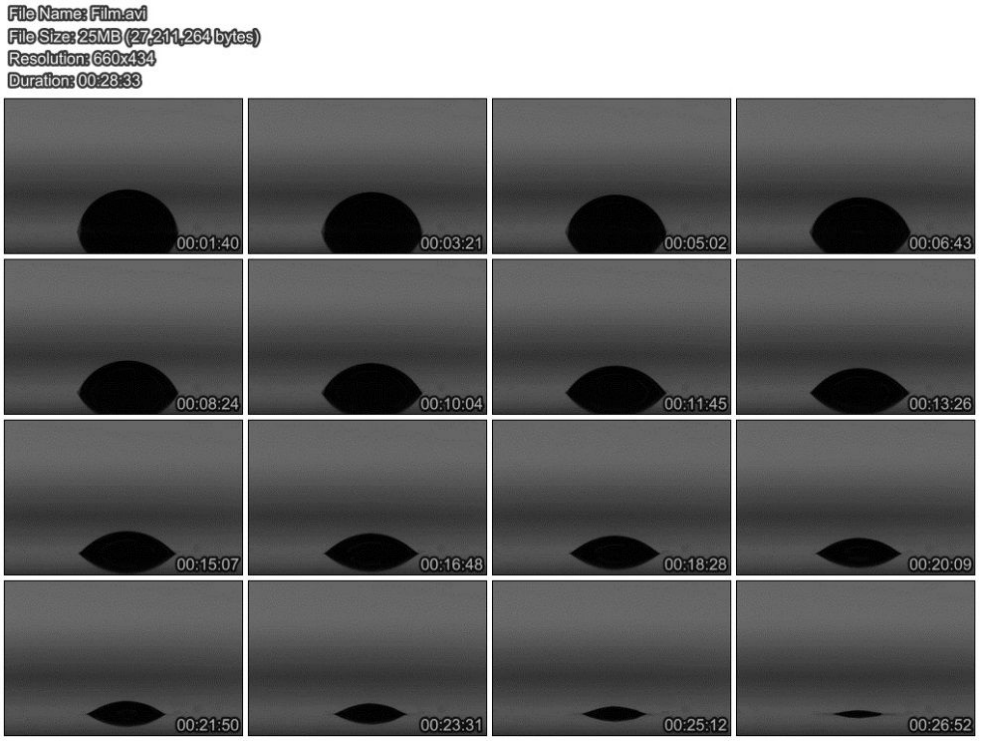

Figure 56. GO droplet on PET film

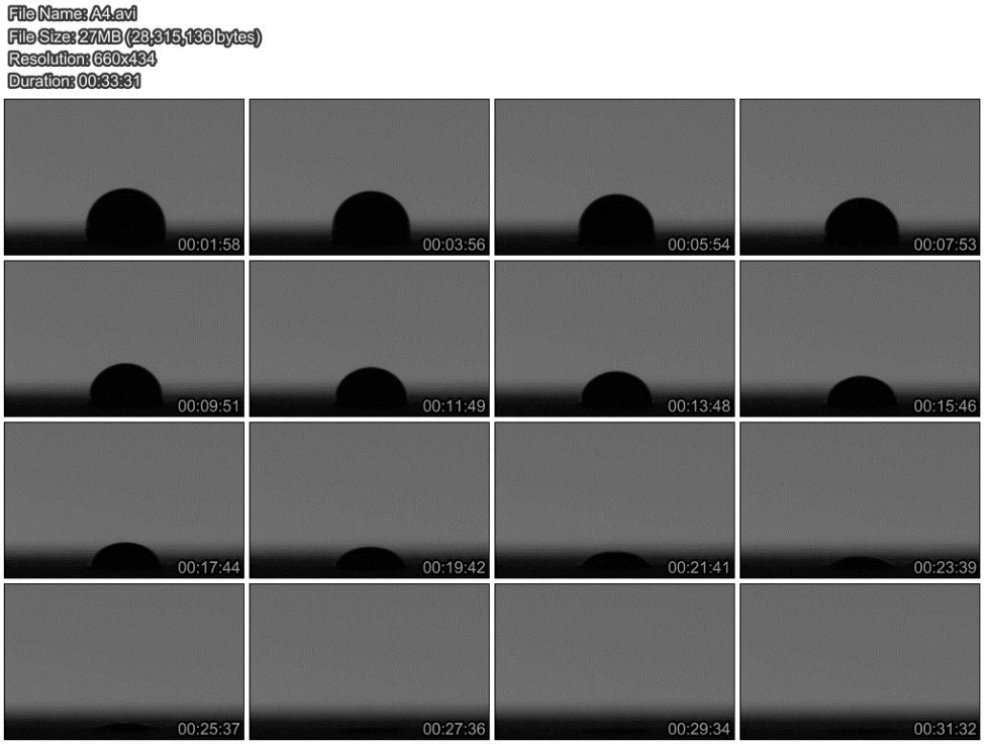

Figure 57. GO droplet on paper

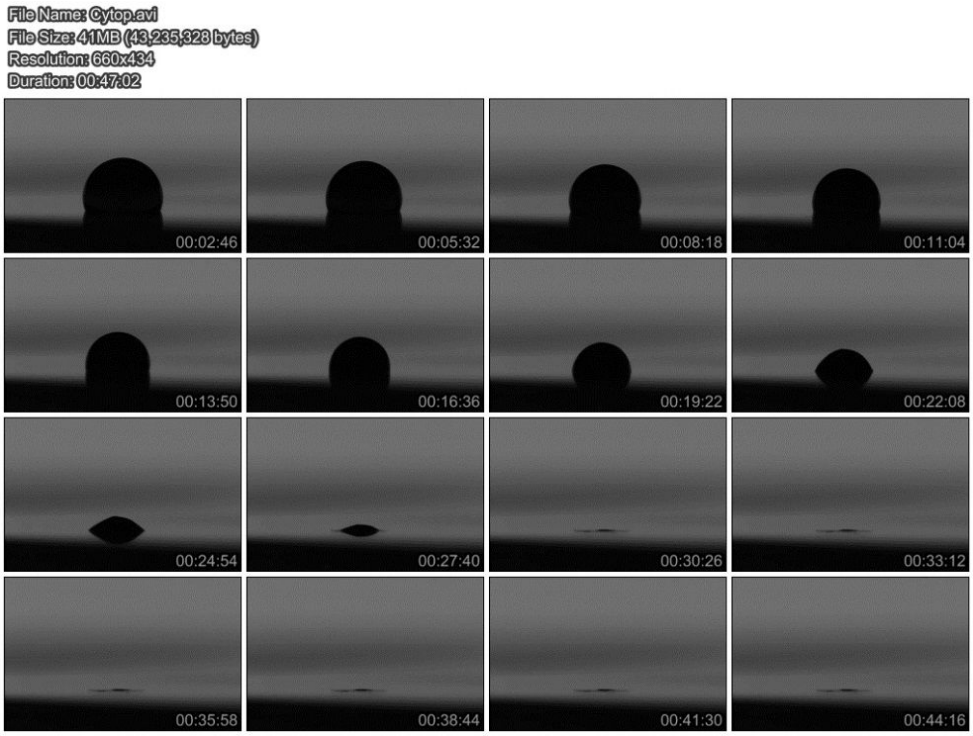

Figure 58. GO droplet on CYTOP

D. Thickness change by multiple dispensing number

Multiple dispensing printing method produced an interdigitated electrode pattern with 40 and 60 fields. In normally, 10 fields of GO solution droplet was used to produce PRGO supercapacitors. Amount of GO could be used more to increase energy capacitance. Thickness was increased and controlled by dispensing droplet number. Every 10 fields of thickness could be distinguished by bare eyes. CV test was also executed and showed different results in scan rate 1 V/s 40 and 60 fields. (Figure 59)

Design layout could be changed by re-program. Amount of droplet could be changed by changing piezo nozzle. Several piezo nozzles have several type of droplet amount per one dispensing. For example, dispense capillary is 150 pL, 300 pL, 450 pL, and so on. Inside of capillary nozzle is coated with several type for designated solution.

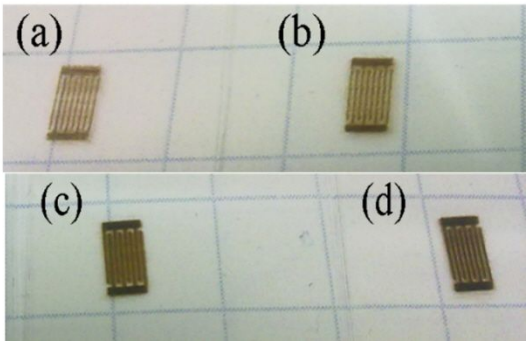

Figure 59. (a) 20 times fields (b) 30 times fields (c) 40 times fields (d) 50 times fields

E. Example of printing malfunction

Samples of printing malfunction were shown in Figure 60. When a liquid dispenser produced electrode patterns, mistake of one droplet led a defective product. Even air flowed around a liquid dispenser of disturbing droplet direction, a patterning could result in failure.

Every field also needed to align previous fields. Although electrode was well patterned in Figure 60(a), disconnection and connection to adjacent line were happened after flash reduction in Figure 60(b)-(e).

Figure 60(f) show that GO concentration was too low to produce an electrode line. This patterning happened when GO concentration was low or total amount of GO was not enough.

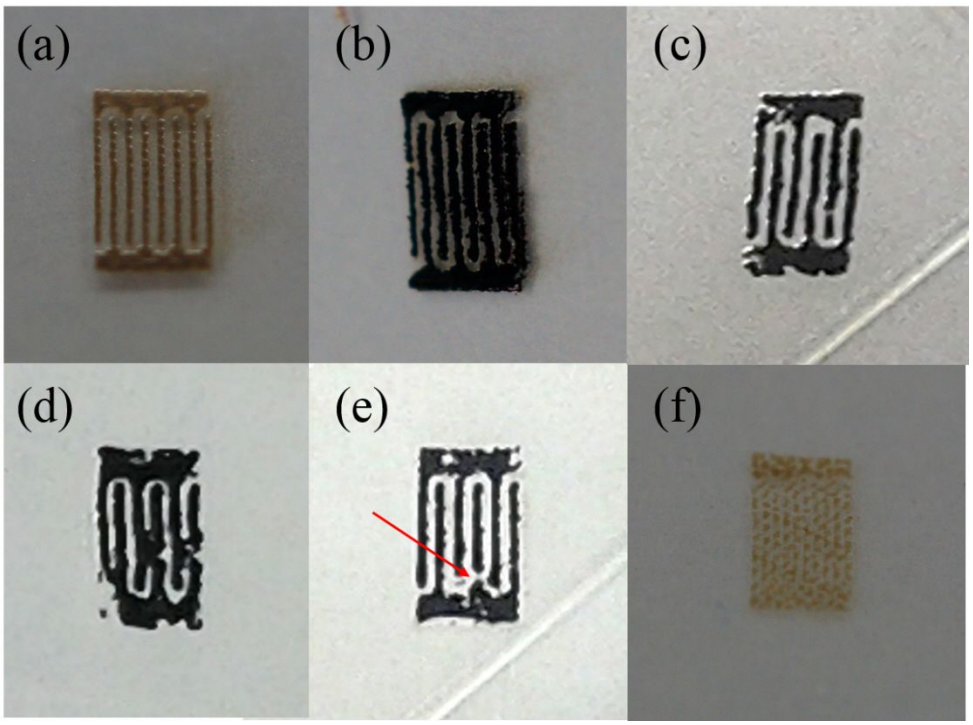

Figure 60. (a) Good alignment of 8 interdigitated electrode (b) disconnected and short electrodes (c) disconnected electrode (d) short electrode (e) disconnected electrode (f) 100 gap coalescence drying

G. Bibliography

[1]. *Zeta potential*. Available from: http://en.wikipedia.org/wiki/Zeta_potential.

[2]. Li, D., M.B. Muller, S. Gilje, R.B. Kaner, et al., "Processable aqueous dispersions of graphene nanosheets" *Nature Nanotechnology*, Vol. 3, No. 2, pp. 101-105, 2008.

[3]. Chartarrayawadee, W., S.E. Moulton, D. Li, C.O. Too, et al., "Novel composite graphene/platinum electro-catalytic electrodes prepared by electrophoretic deposition from colloidal solutions" *Electrochimica Acta*, Vol. 60, No., pp. 213-223, 2012.

초 록

그라파이트 옥사이드의 인쇄/ 환원에 의한 다공성 패터닝 및 수퍼 커패시터 응용

정 한 영
서울대학교 융합과학기술 대학원
나노융합학과

그래핀은 이차원의 크리스탈 구조로 높은 전기적 전도도, 빛 투과성, 및 다공성의 넓은 표면적으로 많은 관심을 받아오고 있는 물질이다. 그래핀의 여러 우수한 성질들로 인해 다양한 분야에서 많이 실험되며 개발되고 있다. 특히 화학적 탐지, 나노 전자, 부식방지 코팅, 고감도 광 센서, 그래핀 트랜지스터, 가스 분리 막, 및 에너지 저장분야에 큰 가능성을 보여주고 있다.

그래핀은 언급된 여러 우수한 성질을 가지고 있지만, 실질적으로는 해결되어야 할 몇 가지 문제점들이 있다. 우선, 그래핀 제작비용은 아직 대량생산을 하기에는 비용이 많이 부담스러우나, 그라파이트로부터 화학적으로 그라파이트 옥사이드를 만들고 이를 사용하여 환원시켜서 사용하면 이러한 문제점을 많이 개선할 수 있다.

그래핀 (Graphene)은 소수성 성질로 물에 녹지 않는 물질이므로, 그라파이트를 산화하여 그래핀 옥사이드 (Graphene oxide) 또는 그라파이트 옥사이드 (Graphite oxide)를 만들어 수용액 상태에서 패터닝을 가능하게 하였다. 패터닝 이후에 광에너지로 환원된 환원 그라파이트 옥사이드 (Reduced graphite oxide)는 그래핀과 유사한 성질을 가지게 된다.

그라파이트 옥사이드 용액은 분사 조건과 광열 에너지량을 조절하여 환원되어 도체를 패터닝 하게 된다. 패터닝은 평평한 표면뿐 아니라, 곡면 표면에서 직접 분사되어 그라파이트 옥사이드 라인을 구성할 수 있다. 최대 4 mm 단차가 있는 평면과, 기울어진 면에 패터닝 할 수 있는 조건을 개발하였다. 만들어진 깍지 낀 모양의 전극은 광열 에너지에 의하여 환원되어 수퍼커패시터로의 응용을 보여주고 있다.

기존 전기화학적 작용에 의한 충전배터리에 비해서 전기 이중층 (EDLC) 안에 물리적으로 직접 이온을 저장하는 수퍼커패시터는 수십 배 이상의 파워 밀도가 높고, 라이프 사이클 또한 십만 번 이상으로 뛰어난 성능을 보여준다. 또한, 동작 온도도 -40 ~ 80도에 이르러, 배터리 보다 훨씬 넓은 영역에서 동작함을 보여준다. 그럼에도 불구하고, 수퍼커패시터가 아직 널리 사용되지 못하는 있는 결정적인 이유는 기존 이차전지에 비해 에너지 밀도가 몇 배 이상 낮기 때문이다. 그러므로, 다공성의 전극물질의 개발로 에너지 밀도의 향상이 필요하며, 이에 최적화된 단위 무게당 최고의 표면적을 가지는 그래핀 전극 물질이 필요하다.

일반적으로 수퍼커패시터는 높은 파워를 필요로 하는 전자 기기에 많이 사용되어 왔다. 예를 들어, 전기 자동차에 순간 가속도를 높이는 장치와

브레이크 시스템이 동작할 때, 발생하는 전기에너지를 빠르게 받아들이는 모듈에 사용되었다. 하지만, 우리 그룹은 수퍼커패시터를 이용한 CMOS 공정이 용이하며, 휘어지는 플래폼을 가진 높은 파워와 에너지를 요구하는 마이크로 전자 기기에 중점을 두었다.
본 연구를 통해 미세 용액 분사기로 그래핀 베이스 물질인 그라파이트 옥사이드를 이용하여 수용액형태로 변환하여 잉크와 같이 직접 패턴을 만들어 내었다. 패턴을 직접 인쇄하여 만들어 낼 수 있는 조건으로서 기질 물질의 선택, 인쇄 방법, 그라파이트 옥사이드 용액 량의 조절이 필요하다.

기질 물질의 선택을 위하여 여러 물질에 인쇄하여, 유용한 매개 변수들과 기술들이 도출되었다. 유리, PET 필름, 복사 종이, PDMS, CYTOP 에 그라파이트 옥사이드 수용액을 떨어뜨려 투명하면서도 적절한 접촉각을 만들어 특성을 비교하였다. 이중에서 미세패턴 구현과 환원 효율이 우수하여 가장 패터닝하기 좋은 PET 필름이 선택되었다.

다음으로 특별한 인쇄 방법과 적절한 그라파이트 옥사이드 수용액량이 필요한 것을 보여주었다. 다분사 인쇄기술 (Multiple dispensing)은 많은 양의 용액을 일 회로 분사하지 않고, 소량의 용액을 여러 회 분사하는 기술이다. 인쇄되고 말려진 그라파이트 옥사이드는 다분사 방식으로 인해서 그라파이트 옥사이드가 적응된다. 이는 그라파이트 옥사이드가 퍼지지 않고, 높게 적층되는 패턴을 형성하게 되어서 미세선의 형성, 다공성 증가, 미세용액의 유착 감소, 환원 효율 증가의 장점이 있다. 또한 정해진 광 환원에너지의 최소 그라파이트 옥사이드의 양을 실험적으로 찾아내었다.

인쇄되고 말려진 그라파이트 옥사이드는 상용품인 카메라 플래쉬에 의한 광에너지에 의해 환원되어 전도도가 우수한 환원된 그라파이트 옥사이드가 된다. 환원의 방법으로는 고온의 열환원, 하이드라진 환원제를 이용한 화학적 방법, 광 에너지를 이용한 방법이 있다. 간편하고 빠른 광 에너지를 이용한 방법으로 제논 플래쉬와 레이저를 이용한 환원 방법을 검토해 보았다. 제논 카메라 플래쉬를 이용한 환원 방법은 짧은 시간안에 그라파이트 옥사이드 적층에 깊숙히 환원시킬 수 있는 장점이 있다.

패터닝되어 환원된 깍지 낀 모양의 수퍼커패시터는 수용액, 유기계, 이온계 전해질로 만들어져 테스트 되었다. 이온계전해질에서 4 V의 높은 전압으로 인해서 높은 성능을 보였다. 순환 전압법과 충방전 테스트에 의해 구해진 에너지밀도와 파워밀도에서 경쟁력 있는 결과들을 보여주고 있다. 또한 단위 무게당 에너지밀도와 파워밀도 및 라곤 플랏도 계산하여 비교해보았다.

얇은 표면에 인쇄된 필름 형태의 수퍼커패시터는 적층되고 연결되어 성능을 향상 시킬 수 있다. 인쇄된 깍지 낀 모양의 패턴은 전극을 연결되게 변형하여, 그래핀의 넓은 표면적을 이용한 센서로 응용될 수 있다.

그래핀 베이스 물질인 그라파이트 옥사이드의 직접 인쇄와 환원을 통해 그라파이트의 곡면 표면 프린팅에 최적 조건을 찾아내었다. 제작한 휘어지는 수퍼커패시터는 새로운 스마트 기기시대의 인쇄된 에너지 저장장치로서의 가능성을 보여준다.

주제어: 수퍼 커패시터, 그래핀, 환원 그라파이트 옥사이드, 인쇄 패터닝
학번: 2009-31185